AD-A041 971 BOEING COMMERCIAL AIRPLANE CO SEATTLE WASH F/G 17/7
AIR TRAFFIC CONTROL EXPERIMENTATION AND EVALUATION WITH THE NAS--ETC(U)
SEP 76 S G WILSON, C V PAULSON, I R REESE DOT-TSC-707-6
UNCLASSIFIED D6-44051 FAA-RD-75-173-6 NL

1 OF 2

ADA041-971

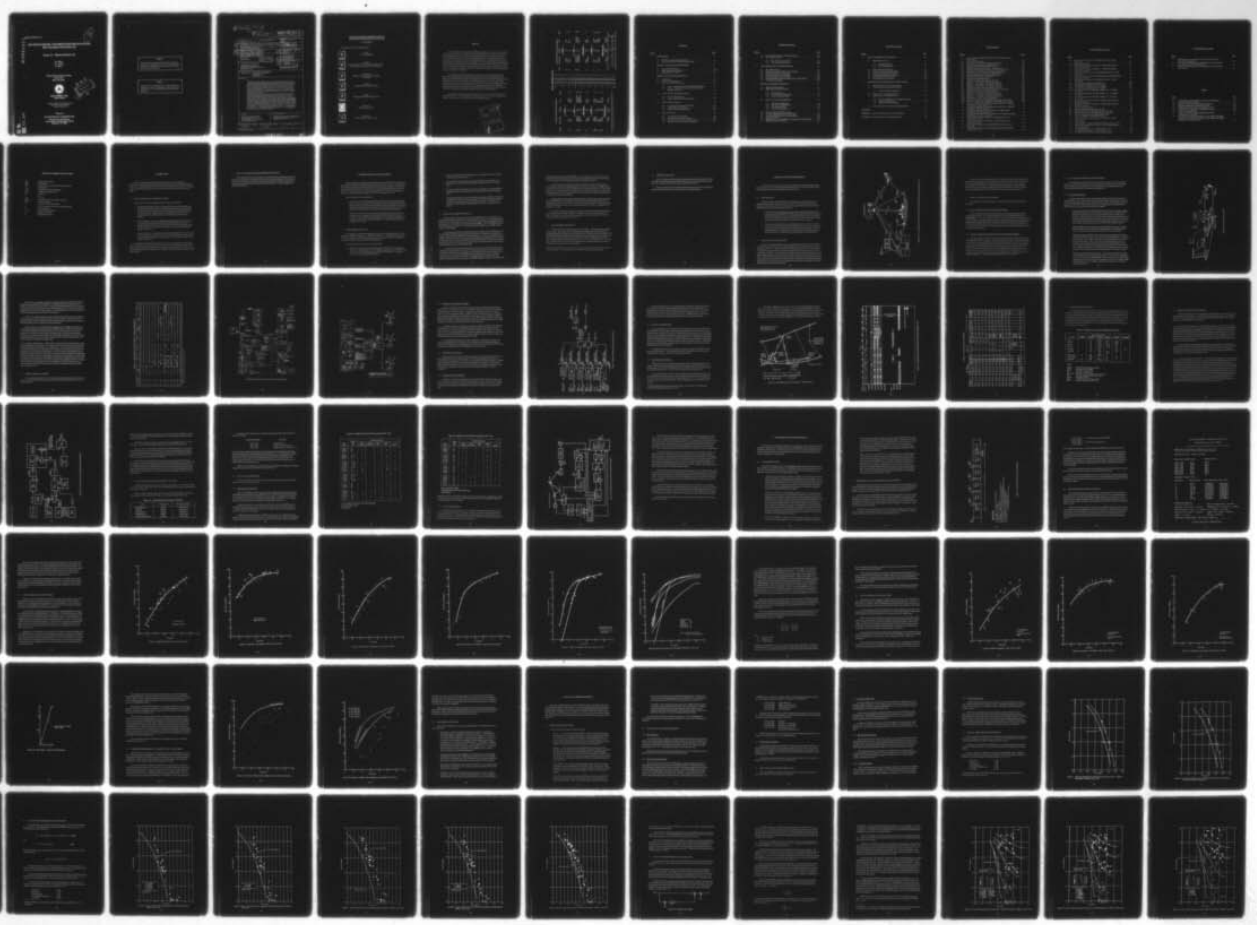

Report No. FAA-RD-75-173, VI

AIR TRAFFIC CONTROL EXPERIMENTATION AND EVALUATION WITH THE NASA ATS-6 SATELLITE

Volume VI: Modem Evaluation Test

S.G. Wilson
C.V. Paulson
I.R. Reese

Boeing Commercial Airplane Company
PO Box 3707
Seattle WA 98124

SEPTEMBER 1976
FINAL REPORT

Prepared for

U.S. DEPARTMENT OF TRANSPORTATION
Federal Aviation Administration
Systems Research and Development Service
Washington DC 20591

NOTICE

This document is disseminated under the sponsorship of the Department of Transportation in the interest of information exchange. The United States Government assumes no liability for its contents or use thereof.

NOTICE

The United States Government does not endorse products or manufacturers. Trade or manufacturers' names appear herein solely because they are considered essential to the object of this report.

(18) FAA-RD, MSC

(19) 75-173-6, FAA-76-22-6

TECHNICAL REPORT STANDARD TITLE PAGE

1. Report No. FAA-RD-75-173, VI	2. Government Accession No.	3. Recipient's Catalog No. (11)
(6) 4. Title and Subtitle AIR TRAFFIC CONTROL EXPERIMENTATION AND EVALUATION WITH THE NASA ATS-6 SATELLITE Volume VI Modem Evaluation Test		5. Report Date September 1976
		6. Performing Organization Code DOT-TSC-FAA-76-22,VI
(10) 7. Author(s) S.G. Wilson, C.V. Paulson, T.R. Reese		(14) 8. Performing Organization Report No. D6-44051
9. Performing Organization Name and Address Boeing Commercial Airplane Company* P.O. Box 3707 Seattle, WA 98124 (12) 154 p.		10. Work Unit No. FA711/R7106
		(15) 11. Contract or Grant No. DOT-TSC-707-6
12. Sponsoring Agency Name and Address U.S. Department of Transportation Federal Aviation Administration Systems Research and Development Service Washington, DC 20591		(9) 13. Type of Report and Period Covered Final Report Sep. 1973 to Dec. 1975
		14. Sponsoring Agency Code

15. Supplementary Notes U.S. Department of Transportation
*Under contract to: Transportation Systems Center
Kendall Square
Cambridge, MA 02142

16. Abstract

Results of performance evaluation of voice, digital data and ranging modems in the aeronautical satellite environment are given. Approximately 80 hours of modem performance data were acquired on board an FAA KC-135 jet aircraft operating over the North Atlantic. L-band test signals received at the aircraft were generated by ATS-6 satellite relay of transmissions from a NASA ground station. The modem evaluation tests were conducted between September 1974 and April 1975 as part of the U.S. Department of Transportation (DOT) aeronautical technology test program. The U.S. DOT tests were a component of the International ATS-6 L-Band Experiment coordinated by the NASA/Goddard Space Flight Center.

Measured modem performance includes: the word intelligibility achieved by four distinct speech transmission modems; the average bit-error probability and error patterns associated with five phase-shift-keyed 1200-bps data modems; and the rms ranging accuracy achieved with two ranging modems. In each case the performance was evaluated as a function of carrier-to-noise density ratio (C/N_0) and direct-signal-to-multipath-signal ratio (S/I). Testing was performed with representative operational-class aircraft antennas as well as with special antennas, allowing the variation of the relative multipath level.

The report consists of seven volumes: I – Executive Summary; II – Demonstration of Satellite-Supported Communications and Surveillance for Oceanic Air Traffic Control; III – Summary of U.S. Aeronautical Technology Test Program; IV – Data Reduction and Analysis Software; V – Multipath Channel Characterization Test; VI – Modem Evaluation Test; VII – Aircraft Antenna Evaluation Test.

17. Key Words	18. Distribution Statement
Speech, Data, Ranging, AEROSAT, Aircraft, L-band, Satellite, Error Rate, Intelligibility, Accuracy, Modem, Noise, Multipath, Antennas	Document is available to the U.S. public through the National Technical Information Service, Springfield, Virginia 22161

19. Security Classif. (of this report)	20. Security Classif. (of this page)	21. No. of Pages	22. Price
Unclassified	Unclassified	158	

Form DOT F 1700.7 (8-69)

390145

AIR TRAFFIC CONTROL EXPERIMENTATION AND EVALUATION WITH THE NASA ATS-6 SATELLITE

FINAL REPORT

This report consists of the following volumes.

Volume I
Executive Summary

Volume II
Demonstration of Satellite-Supported Communications and Surveillance for Oceanic Air Traffic Control

Volume III
Summary of U.S. Aeronautical Technology Test Program

Volume IV
Data Reduction and Analysis Software

Volume V
Multipath Channel Characterization Test

Volume VI
Modem Evaluation Test

Volume VII
Aircraft Antenna Evaluation Test

PREFACE

The U.S. Department of Transportation (DOT) aeronautical test program entitled "Air Traffic Control Experimentation and Evaluation with the NASA ATS-6 Satellite" was part of the Integrated ATS-6 L-Band Experiment. The overall ATS-6 L-band experiment was coordinated by the NASA/ Goddard Space Flight Center (GSFC) and was international in scope. The following agencies were participants in the experiment: NASA/Goddard Space Flight Center; DOT/Federal Aviation Administration; DOT/Transportation Systems Center; DOT/U.S. Coast Guard; DOC/Maritime Administration; European Space Agency (EAS); and the Canadian Ministry of Transport and Department of Communications. Each participant performed tests in one or more of three categories: aeronautical, maritime safety, and maritime fleet operations. All tests were conducted in accordance with an overall integrated test plan coordinated by NASA/GSFC.

The U.S. DOT Aeronautical test program was under the direction and sponsorship of the Federal Aviation Administration, Systems Research and Development Service (SRDS), Satellite Branch, with the DOT/TSC conducting the technology tests and the FAA/NAFEC conducting the ATC demonstration tests. The technology tests included multipath channel characterization, modem evaluation, and aircraft antenna evaluation. Results of these tests are presented in volumes III through VII, and the results of the ATC demonstration tests are presented in volume II. The DOT/TSC test program was supported by the Boeing Commercial Airplane Company under contract DOT-TSC-707. Mr. R. G. Bland was the TSC Project Engineer and Contract Technical Monitor.

This volume describes the modem evaluation test. All work described was performed under contract DOT-TSC-707. Most of the material contained in section 7 of this volume was prepared by CNR Inc., under subcontract to the Boeing Commercial Airplane Company.

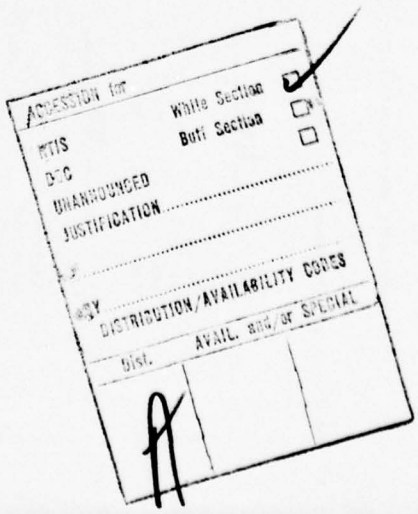

METRIC CONVERSION FACTORS

Approximate Conversions to Metric Measures

Symbol	When You Know	Multiply by	To Find	Symbol
		LENGTH		
in	inches	*2.5	centimeters	cm
ft	feet	30	centimeters	cm
yd	yards	0.9	meters	m
mi	miles	1.6	kilometers	km
		AREA		
in^2	square inches	6.5	square centimeters	cm^2
ft^2	square feet	0.09	square meters	m^2
yd^2	square yards	0.8	square meters	m^2
mi^2	square miles	2.6	square kilometers	km^2
	acres	0.4	hectares	ha
		MASS (weight)		
oz	ounces	28	grams	g
lb	pounds	0.45	kilograms	kg
	short tons (2000 lb)	0.9	tonnes	t
		VOLUME		
tsp	teaspoons	5	milliliters	ml
Tbsp	tablespoons	15	milliliters	ml
fl oz	fluid ounces	30	milliliters	ml
c	cups	0.24	liters	l
pt	pints	0.47	liters	l
qt	quarts	0.95	liters	l
gal	gallons	3.8	liters	l
ft^3	cubic feet	0.03	cubic meters	m^3
yd^3	cubic yards	0.76	cubic meters	m^3
		TEMPERATURE (exact)		
°F	Fahrenheit temperature	5/9 (after subtracting 32)	Celsius temperature	°C

*1 in = 2.54 (exactly). For other exact conversions and more detailed tables, see NBS Misc. Publ. 286, Units of Weights and Measures, Price $2.25, SD Catalog No. C13.10:286.

Approximate Conversions from Metric Measures

Symbol	When You Know	Multiply by	To Find	Symbol
		LENGTH		
mm	millimeters	0.04	inches	in
cm	centimeters	0.4	inches	in
m	meters	3.3	feet	ft
m	meters	1.1	yards	yd
km	kilometers	0.6	miles	mi
		AREA		
cm^2	square centimeters	0.16	square inches	in^2
m^2	square meters	1.2	square yards	yd^2
km^2	square kilometers	0.4	square miles	mi^2
ha	hectares (10,000 m^2)	2.5	acres	
		MASS (weight)		
g	grams	0.035	ounces	oz
kg	kilograms	2.2	pounds	lb
t	tonnes (1000 kg)	1.1	short tons	
		VOLUME		
ml	milliliters	0.03	fluid ounces	fl oz
l	liters	2.1	pints	pt
l	liters	1.06	quarts	qt
l	liters	0.26	gallons	gal
m^3	cubic meters	35	cubic feet	ft^3
m^3	cubic meters	1.3	cubic yards	yd^3
		TEMPERATURE (exact)		
°C	Celsius temperature	9/5 (then add 32)	Fahrenheit temperature	°F

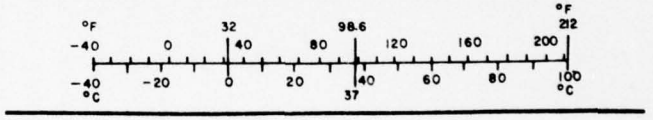

CONTENTS

CONTENTS (Continued)

CONTENTS (Concluded)

ILLUSTRATIONS

ILLUSTRATIONS (Continued)

ILLUSTRATIONS (Concluded)

TABLES

SYMBOLS AND ABBREVIATIONS

ADVM	adaptive delta voice modulation (modem)
AGC	automatic gain control
AI	articulation index
ANBFM	adaptive narrowband frequency modulation (modem)
ATC	air traffic control
ATS-6, (-5)	Applications Technology Satellite 6, (5)
AZ	azimuth
bpi	bytes per inch
bps	bits per second
BER	bit-error rate
B_F	one-sided e^{-1} Doppler bandwidth
B_L	loop bandwidth
BPF	bandpass filter
cw	continuous wave
C/N_o	ratio of unmodulated carrier power to noise power density, dB-Hz
CPSK	coherent phase-shift keying
dB	decibel(s)
D	data
DECPSK	differentially encoded, coherent phase-shift keying
DOT	Department of Transportation
DPSK	differential phase-shift keying
DR&A	data reduction and analysis
DSBSC	double-sideband-suppressed carrier
$D(\omega)$	Doppler spectrum
E_b/N_o	ratio of signal energy per bit to noise power density
FAA	Federal Aviation Administration
FDM	frequency division multiplex
FFT	fast Fourier transform
FM	frequency modulation
FMP	forward multipath antenna
FSK	frequency-shift keying
GMT	Greenwich mean time
GSFC	Goddard Space Flight Center
Hz	hertz
IF	intermediate frequency
IRIG	Inter-Range Instrumentation Group
LHC	left-hand circular polarization

SYMBOLS AND ABBREVIATIONS (Continued)

LO	local oscillator
LSD, (RSD)	left (right) slot-dipole antennas
LWSD/RWSD/TOP	left-wing-root slot-dipole/right-wing-root slot-dipole/top antenna system
m	meter(s)
MP	multipath antenna
MUX	multiplexer
NAFEC	National Aviation Facilities Experimental Center
NASA	National Aeronautics and Space Administration
NBFM	narrowband frequency modulation
PAT	patch antenna
PB	phonetically balanced
PDM	pulse-duration modulation
P_e	error probability
PGE	PLACE ground equipment
PHA	phased-array antenna
PLACE	position location and communication equipment
PLL	phase-lock loop
PM	phase modulation
PN	pseudo-noise
PSK	phase-shift keying
QH	quad-helix antenna
Q-M	quadrature modulation
$Q(\tau)$	delay spectrum
RF	radio frequency
RHC	right-hand circular polarization
R_N, (R_W)	ranging, narrowband (wideband), TSC modem format
R/T	receive/transmit
RX	receiver
sec	second(s)
S&R	surveillance and ranging (PLACE format)
SACP	satellite aeronautical channel prober
SCIM	speech communication index meter
SCPDM	suppressed-clock pulse-duration modulation
S/I	ratio of direct-path signal power to multipath signal power, dB
SMP	side-mounted multipath antenna
SMU	subcarrier multiplex unit
S/N	signal-to-noise ratio
S&R	surveillance & ranging

SYMBOLS AND ABBREVIATIONS (Concluded)

SOP	side-operational antenna
SSB	single sideband
$S(\tau,\omega)$	delay-Doppler scatter power spectral density function
T	symbol period
TDPC	Test Data Processing Center (Boeing)
TSC	Transportation Systems Center
TX	transmitter
V	voice
VU	voice units
WSSUS	wide-sense stationary uncorrelated scattering
XLT	crossed-slot antenna
γ	parameter, function of B_L and B_F
γ_s	ratio of direct-path power to total indirect-path power
σ	rms range deviation
$\sigma^2,(\sigma)$	variance, (standard deviation)
τ_s	differential path delay
ω_s	Doppler frequency shift.

1. INTRODUCTION

The U.S. aeronautical technology tests were conducted by the U.S. Department of Transportation/Transportation Systems Center (DOT/TSC) as part of the Integrated L-Band Experiment (ref. 1-1). The overall objective of these tests was to provide data for the evaluation of advanced system concepts and hardware applicable to the design of future satellite-based air traffic control systems.

1.1 DOT/TSC AERONAUTICAL TECHNOLOGY TESTS

Three types of aeronautical technology tests were conducted by DOT/TSC:

a. *Multipath Channel Characterization:* Pseudo-noise (PN) code modulated signals were transmitted from the KC-135 using several different antennas and various polarizations. After relay by ATS-6, the signals were received at Rosman, processed by satellite aeronautical channel prober (SACP) equipment, recorded, and later analyzed to obtain a characterization of the multipath channel. The multipath tests are described in volume V.

b. *Modem Evaluation:* Several voice, digital data, ranging, and hybrid voice/data modems were tested using signals transmitted from Rosman through ATS-6 to the aircraft. Modem demodulator outputs were recorded onboard the aircraft and analyzed to determine performance for various carrier-to-noise density (C/N_o) and signal-to-multipath interference (S/I) ratios.

c. *Antenna Evaluation:* A cw signal radiated by Rosman through ATS-6 was received by the various aircraft antennas under test. Data was recorded and analyzed to evaluate antenna gain and multipath rejection as a function of geometry. The antenna evaluation tests are described in volume VII.

This volume describes the modem evaluation tests. Section 2 summarizes the results and conclusions. Section 3 gives a general description of the tests, and sections 4 through 6 provide details and present experimental data obtained for voice, digital data, and ranging modems. Section 7 investigates the performance impact of multipath on the overocean aeronautical satellite communication and ranging channels.

1.2 DOT/FAA AIR TRAFFIC CONTROL DEMONSTRATION TESTS

These demonstration tests were conducted by the Federal Aviation Administration as part of the overall U.S. Department of Transportation L-band aeronautical test program. The tests demonstrated and evaluated voice and digital data communications (including full duplex operations) over L-band aeronautical satellite links in an operational-type environment. The tests are described in volume II of this report.

2. SUMMARY OF RESULTS AND CONCLUSIONS

Various modulation and demodulation techniques are being considered for the transmission of voice, digital data, and ranging/surveillance signals to and from aircraft via satellites. The performance of several voice, digital data, and ranging modems representing candidate approaches for this application were evaluated. Flight tests were conducted in the overocean multipath environment at various locations over the North Atlantic. The data acquired includes 37 hr of voice modem intelligibility tests, 34 hr of digital data modem performance, and 11 hr of ranging accuracy tests.

Tests were divided into two general types:

Type I Tests: Type I tests determined modem performance over a range of flight geometries and carrier-to-noise power density ratios (C/N_0) using candidate operational slot-dipole antennas. Several different aircraft headings relative to the satellite were employed and elevation angles ranged between 10^o and 30^o. The test range of C/N_0 was 39 to 48 dB-Hz for voice modems and 37 to 45 dB-Hz for digital data and ranging modems.

Type II Tests: Type II tests evaluated modem performance parametrically in terms of C/N_0 and S/I over a wide range of the two parameters for the overocean multipath environment. Tests spanned C/N_0 values between 38 and 52 dB-Hz in combination with S/I values ranging from heavy multipath fading (S/I = 3 dB) to essentially nonfading conditions (S/I > 20 dB).

2.1 VOICE MODEM TEST RESULTS

Four distinct voice modulation techniques were tested: (1) adaptive narrowband frequency modulation (ANBFM), (2) Hybrid No. 1 (Q-M/PSK), (3) Hybrid No. 2 (PDM/PSK), and (4) adaptive delta voice modulation (ADVM). Performance was measured primarily by the word intelligibility scores achieved with lists of phonetically balanced (PB) words.

The major findings of the voice tests were the following.

a. Over the C/N_0 range of 40 to 48 dB-Hz, the relative ranking of the four modems was Hybrid No. 1, ADVM, Hybrid No. 2, and ANBFM. All modems except ANBFM achieved in excess of 70% PB word intelligibility at 43 dB-Hz, with Hybrid No. 1 achieving in excess of 70% word intelligibility at 40 dB-Hz.

b. No detectable degradation in the intelligibility due to multipath was observed for any of the modems for S/I as poor as 3 dB.

c. In the combined voice and data mode, both hybrid modems required roughly 3 dB additional C/N_0 to achieve PB word intelligibility equivalent to that of the voice-only mode.

d. For the limited speaker population tested, the two male speakers were consistently more intelligible than the two female speakers. This is probably due to audio band limiting effects.

e. The relationship between the speech communication index meter (SCIM) score and word intelligibility was found to be modem dependent. Thus, SCIM evaluations do not appear to offer a universal modem performance evaluation technique. As a minimum, the relation between the SCIM score and psychometric scores must be calibrated for each modem.

2.2 DIGITAL DATA MODEM TEST RESULTS

Digital data modem tests evaluated the bit-error-rate (BER) and error burst behavior of five digital modems operating at 1200 bps on the L-band aeronautical channel. The modems included four implementations of differentially encoded, coherently detected phase-shift keying (DECPSK) and one implementation of differentially coherent phase-shift keying (DPSK). The four DECPSK modems are designated Hybrid No. 1, Hybrid No. 2, FAA CPSK, and NASA DECPSK, and the DPSK modem is referred to as FAA DPSK.

For Type I tests the modems exhibited inefficiencies that ranged from 0.9 dB (Hybrid No. 1) to 1.9 dB (NASA DECPSK) relative to theoretical performance on the additive white Gaussian noise channel. All modems met the AEROSAT system specification of 1×10^{-5} error probability at C/N_0 = 43 dB-Hz. There was no visible evidence of bit-error-rate performance degradation due to multipath, thus indicating that S/I exceeded 15 dB when tested with the three-element slot-dipole antenna system during the Type I tests. This observation is consistent with the S/I values measured for the wing-root slot-dipole antennas during antenna evaluation tests.

Type II tests evaluated modem error performance for various combinations of S/I and C/N_0. Experimental performance data was compared with theoretical predictions of performance derived from analytical models used in conjunction with the multipath channel parameters measured by the multipath tests. The Type II measured DPSK error-rate performance was in close accord with theoretical prediction, whereas the performance of DECPSK modems was slightly poorer than modeled. Comparing the relative performance of DECPSK and DPSK revealed that for S/I larger than

about 10 dB, DECPSK outperforms DPSK slightly in error probability; for poorer S/I (less than 10 dB), DPSK exhibits a slight superiority. In both cases, the performance advantage was not dramatic and no clear preference for either DPSK or DECPSK was indicated by the data.

In contrast with voice modem results, the BER performance of all data modems degraded severely whenever appreciable multipath interference was present. For instance, for DPSK and an S/I of 10 dB, C/N_0 must be increased from 43 dB-Hz to about 51 dB-Hz to maintain 1×10^{-5} error probability. Since a channel power increase of 8 dB appears to be prohibitively large, error-control coding or multipath-tolerant waveform design appears to be a necessary adjunct to existing modem designs if S/I values as low as 10 dB are anticipated.

Error groupings were analyzed to determine the effective memory length of the error patterns. When multipath interference was negligible, error patterns were correlated only over two bits. As multipath interference increased, obvious error bunching occurred as a result of the multipath fading. The effective memory time of the error process was found to be 7 bits for S/I = 6 dB and about 14 bits for S/I = 2.5 dB.

Testing in the hybrid voice/data mode for the two hybrid modems showed that the Hybrid No. 2 modem required an additional 3.5 dB C/N_0 to maintain the same error rate as in the data-only mode. The Hybrid No. 1 modem needed only an additional 1 dB at high error rates (10^{-2}) while requiring an additional 4 dB at low error rates (10^{-5}).

2.3 RANGING MODEM TEST RESULTS

The performance of two distinct ranging modem techniques – TSC digital ranging and NASA PLACE ranging – was evaluated on the L-band aeronautical satellite channel. Results of the TSC ranging test showed that rms range error was typically 100 m at 43 dB-Hz carrier-to-noise density ratio in the narrowband mode (19.53-kHz clock) and roughly 30 m in the wideband mode (156.25-kHz clock). These errors are somewhat larger than laboratory-measured values, particularly for the wideband mode. NASA ranging tests exhibited a typical rms error of 276 m for a forward-link C/N_0 in the vicinity of 43 dB-Hz. This measure is in reasonable agreement with expectation, taking into account the maximum tone frequency of 8575 Hz for this system.

Both modems exhibited rather frequent occurrences of gross range errors due to incorrect resolution of range ambiguity. These ambiguity errors were censored from the rms error calculations.

2.4 ADDITIONAL ANALYSES

Section 7 provides theoretical aeronautical satellite channel performance data for various narrowband and wideband data transmission techniques plus cw tone and pseudo-noise ranging approaches. The major portion of this section was provided by CNR, Inc.

Appendix A gives results of the SCIM measurements that were analyzed by NASA/GSFC. Appendix B includes analysis of rms range errors for the TSC ranging modem.

3. MODEM EVALUATION TEST DESCRIPTION

This section provides an overall description of the modem evaluation tests, emphasizing test aspects common to the voice, digital data, and ranging tests performed. Details and features specific to testing of particular modems are included in section 4 through 6.

3.1 TEST OBJECTIVES

Various techniques are being considered for the transmission of voice, digital data, and ranging/surveillance signals to and from aircraft via satellites. The objective of these tests was to evaluate the performance of several voice, digital data, and ranging modems representing candidate approaches for this application. Specific objectives were:

a. To evaluate modem performance over a range of flight geometries and C/N_0 using the candidate operational LWSD/RWSD/TOP (left-wing slot dipole/right-wing slot dipole/top) switchable slot-dipole antenna system. Experimental performance data was compared with theoretical and laboratory baseline data to assess the effects of the overocean flight environment on modem performance for a representative set of conditions.

b. To evaluate modem performance parametrically in terms of C/N_0 and S/I over a wide range of the two parameters for the overocean flight environment, thus providing quantitative measurement of modem performance degradation for various degrees of oceanic multipath interference. Experimental data were compared with theoretical prediction and with performance measurements made using a laboratory multipath simulator.

3.2 SATELLITE LINK CONFIGURATION

All U.S. aeronautical technology tests were conducted between the FAA KC-135 airplane and the NASA/Rosman ground station via the NASA geostationary ATS-6 satellite using the basic link configuration of figure 3-1. With the exception of the PLACE ranging tests, which used a round-trip configuration for range measurements, all modem evaluation tests were performed with a one-way forward-link configuration. The test signals were transmitted from the Rosman ground station to the ATS-6 satellite for relay to the aircraft. The forward-link configuration was very efficient in the utilization of ATS-6 satellite test time since it allowed several L-band experiment participants to conduct tests simultaneously at their respective mobile (or fixed) L-band terminals. Return-link transmissions from the KC-135 were used only for test coordination purposes and for the surveillance and ranging (S&R) responses during PLACE ranging tests.

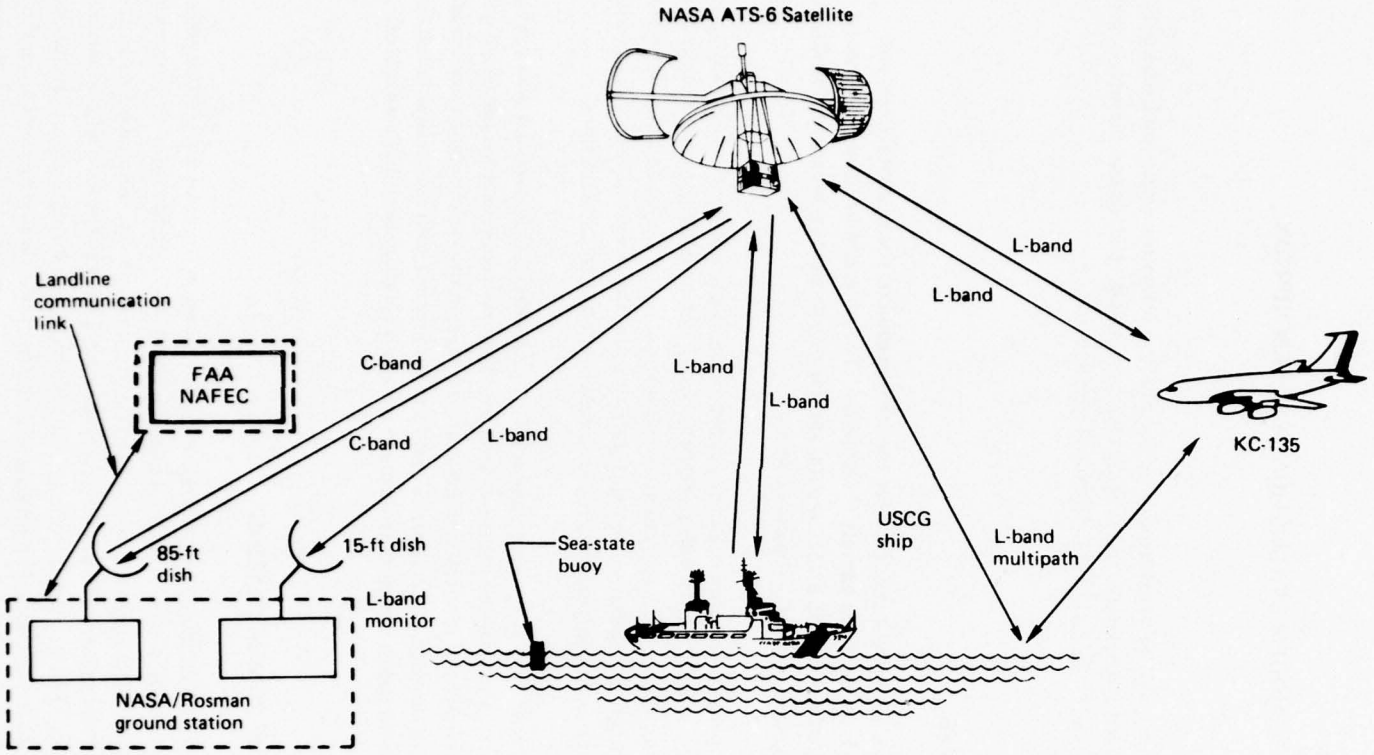

Figure 3-1. Link Configuration for DOT ATS-6 L-Band ATC Experimentation and Evaluation Tests

Except for a few of the initial tests of the 1974 fall series, the ATS-6 satellite transponder was operated in the coherent mode. The forward-link reference carrier needed for coherent mode operation was normally transmitted from the NASA/Mojave ground station. This mode of operation referenced the L-band frequencies to a highly stable ground-based standard, thus eliminating any forward-link frequency uncertainty and drift associated with the satellite internal master oscillator. For modem evaluation tests, the ATS-6 L-band antenna was operated in the fan-beam mode.

3.3 TYPE I AND TYPE II TEST CATEGORIES

In accordance with the test objectives, the modem evaluation tests were divided into two general types.

3.3.1 Type I – Performance With Aircraft Operational Antennas

These tests acquired modem performance with operational antennas at satellite elevation angles ranging from 10^{o} to 30^{o}. Bearing angles relative to the ATS-6 subsatellite direction were approximately 45^{o}, 135^{o}, 225^{o}, and 315^{o}. About 65% of the acquired modem evaluation data was of the Type I variety. The signal-to-multipath interference ratio (S/I) for these tests was dependent upon the polarization and gain characteristics of the airborne operational antenna and the magnitude and polarization characteristics of the sea-reflected signals. Type I tests evaluated modem performance over a range of C/N_0 values and with the S/I values inherent to the antenna system at the relative bearings and elevation angles tested.

3.3.2 Type II – Performance with Various Levels of Oceanic Multipath Interference

Type II tests used the quad-helix antenna for reception of the direct-path signal and the side multipath (SMP) antenna for reception of the sea-reflected multipath signals. After preamplification, these signals were combined at RF in the desired power ratio to simulate an antenna with a specified S/I ratio. The quad-helix and SMP antennas are both directive and thus do not have any significant spatial pattern overlap. All flights were approximately broadside to the satellite at an elevation angle of 15^{o}. This constant orientation was used since the SMP antenna pointing was fixed. The test parameters varied were the direct path C/N_0 and the combining ratio that determines S/I. Tests spanned C/N_0 values between 38 and 52 dB-Hz in combination with S/I values ranging from heavy multipath fading (S/I = 3 dB) to essentially nonfading conditions (S/I > 20 dB).

3.4 KC-135 AIRCRAFT TERMINAL INSTRUMENTATION

Test instrumentation was installed in 19-in. racks to allow convenient access for equipment calibration, operation, and maintenance. Seven racks located aft housed most of the equipment for modem evaluation, antenna evaluation, and system calibration. Three additional racks located forward contained equipment associated with the multipath tests.

3.4.1 KC-135 L-Band Antennas

The approximate locations of the L-band antennas installed on the KC-135 test aircraft are shown in figure 3-2. The principal antennas used for modem evaluation data acquisition were (1) the three-element slot-dipole system for Type I tests and (2) the quad-helix and side-mounted multipath antennas for Type II tests. Major features of the aircraft L-band antennas are summarized below. Unless otherwise noted, polarization is right-hand circular (RHC).

Three-Antenna Slot-Dipole (LWSD/RWSD/TOP) Antenna System: This system consists of three flush-mounted antennas. Side coverage is provided by the left (LWSD) and right (RWSD) side antennas mounted in the upper wing/body (wing-root) fairing areas at station 766. This location was chosen because of the excellent multipath rejection due to the shielding effect of the wing. High-elevation angle and fore/aft coverage is provided by a third antenna (TOP) mounted near the top centerline at station 805. Nearly all of the Type I modem evaluation data was acquired with the LWSD and RWSD antennas.

Quad-Helix (QH) Antenna: This antenna is mechanically steerable and can be pointed anywhere within the forward region of the upper hemisphere. The antenna provides about 15.5-dB gain toward the satellite for reception of the direct-path signal.

Side-Mounted Multipath (SMP) Antenna: This antenna, located below the left wing at station 804 and waterline 150, has a fixed beam that points approximately 15^{o} below the horizon and 10^{o} aft of broadside. Gain is about 13 dB and polarization is selectable between dual linear, RHC, or LHC. For these tests, horizontal polarization was used exclusively. This antenna received the ocean-reflected multipath signals for Type II tests. Reception is maximized for flights approximately broadside to the satellite direction at elevation angles near 15^{o}. Reception of the direct-path signal is held to an acceptable low level by the shielding effect of the wing under which the antenna is installed.

Right/Left Slot-Dipole (RSD/LSD) Antennas: These antennas are mounted at station 1135 approximately 35^{o} down from the top centerline. Due to the more favorable location of the three-element LWSD/RWSD/TOP slot-dipole antenna system, the RSD/LSD antennas were used only (1) as backups for acquiring data in the event of LWSD or RWSD antenna failure and (2) for transmission and reception of auxiliary test coordination communication signals.

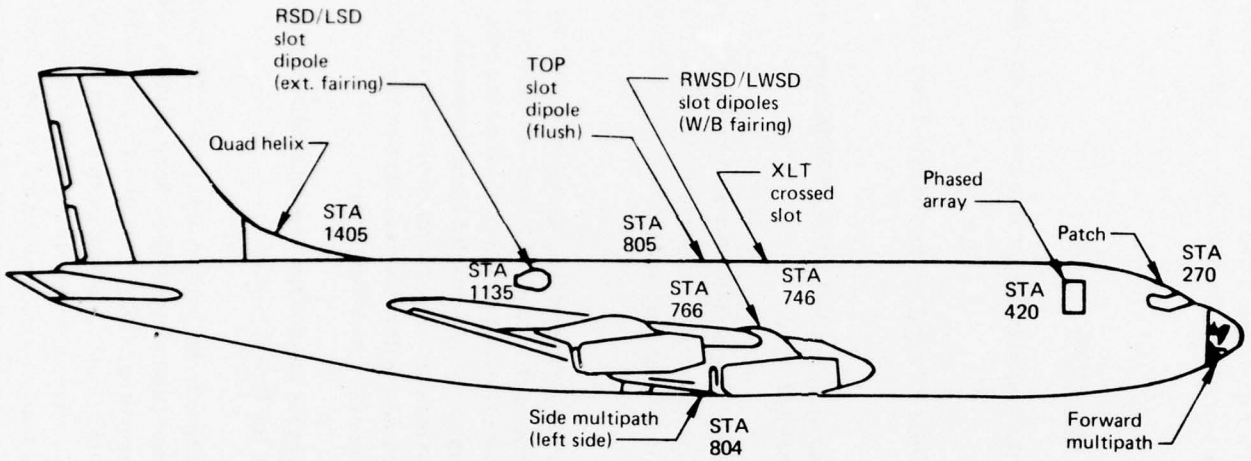

Figure 3-2. KC-135 Antenna Locations

The LWSD/RWSD/TOP slot dipoles were furnished by Boeing and installed specifically for this test program. The side multipath, RSD/LSD slot-dipole, and quad-helix antennas were developed and installed by Boeing for the earlier FAA ATS-5 tests (ref 3-1). Other antennas shown in figure 3-2 were not used during modem evaluation tests; descriptions of antennas are given in volume III.

3.4.2 Airborne Terminal Functional Description

A simplified block diagram of the modem evaluation instrumentation is shown in figure 3-3.

3.4.2.1 RF Signal Routing – The normal RF signal routing for Type I data acquisition was as follows.

a. Depending on aircraft heading, either the LWSD or RWSD antenna was selected for reception of the L-band downlink test signal.

b. Other RF switches preceding the preamplifier were set as shown in figure 3-3 to bypass the PLACE diplexer, thus reducing receive-channel insertion loss. The variable-step attenuator preceding the preamplifier allowed the C/N_o of the received signal to be set at the desired value.

c. The antenna port of the PLACE diplexer was connected to either the LSD or RSD antenna to permit transmission of a voice link for test coordination purposes. The use of separate antennas for transmission and reception functions not only allowed receive-channel losses to be minimized but also guarded aginst the possiblity of interference in the receive channel due to diplexer leakage during transmitter operation. Extensive testing showed that receive-channel performance was immune to simultaneous transmission of test coordination signals with this configuration.[1]

d. Two RF switches following the preamplifier were set as shown in figure 3-3 to bypass the RF power combiner used for Type II tests.

---

[1] The PLACE diplexer was part of the equipment configurations used for the FAA ATC demonstration tests and the NASA two-satellite position-determination tests. Some mild degradation of receive-channel performance, attributed to intermittent faulty operation of either the diplexer or transmitter, was observed on occasion when the diplexer and a common antenna were used for transmission and reception. These observed degradations were neither severe enough nor frequent enough to warrant a system configuration change for these tests. The observations did, however, provide motivation for developing the standard approach of using a separate antenna if transmission of return-link coordination signals was required during modem evaluation tests.

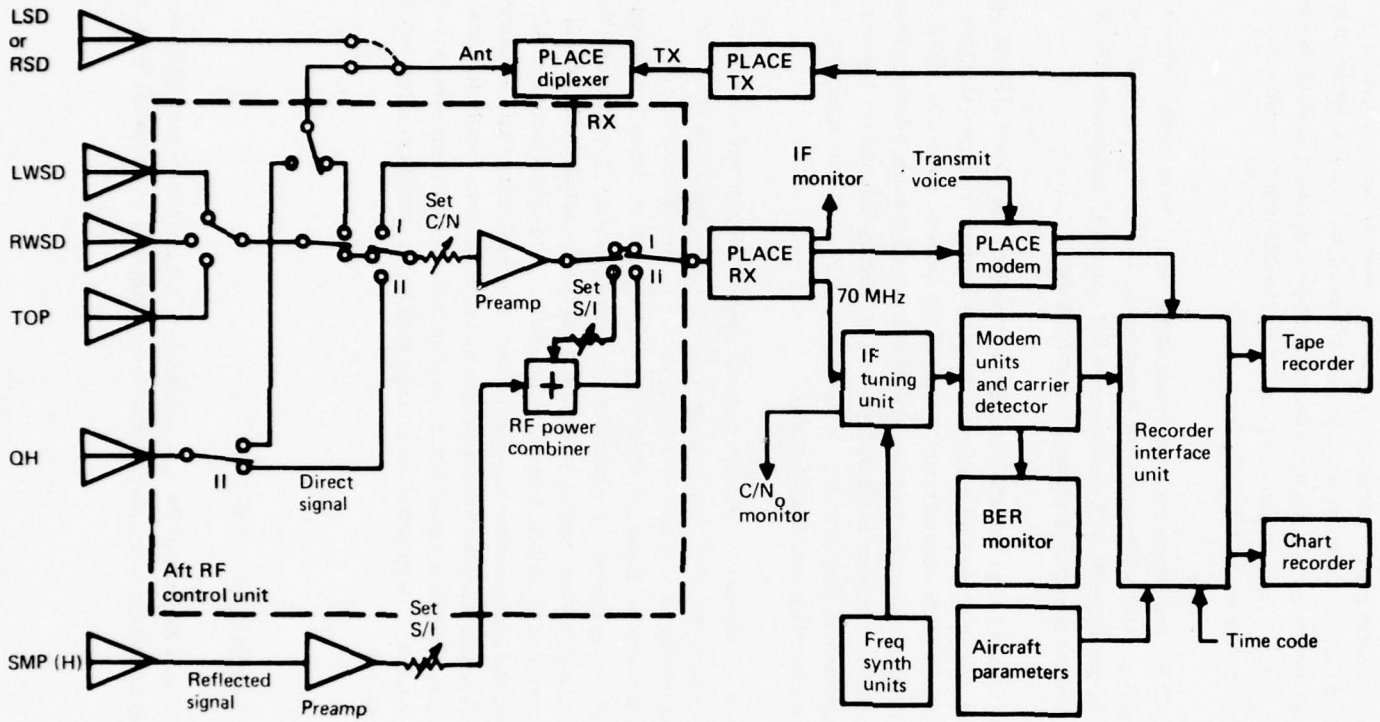

Figure 3-3. Simplified KC-135 Terminal for Modem Evaluation Test

For Type II data acquisition, the quad-helix antenna was selected for reception of the direct-path signal, again bypassing the PLACE diplexer. The variable-step attenuator preceding the pre-amplifier set the desired C/N_0 value as before. The side-mounted multipath antenna, in its horizontal polarization mode, was used to receive the sea-reflected multipath signal. The outputs from the pre-amplifier were routed to the RF power combiner. The two variable-step attenuators preceding the RF power combiner adjusted the ratio of S/I to the desired value.

The Type I or II RF test signals processed as described above were further linearly amplified, without automatic gain control (AGC), and down-converted to 70 MHz by the PLACE receiver. A multi-output power divider in the PLACE receiver provided isolated IF outputs for the IF tuning unit, the PLACE modem, and for monitoring and calibration purposes.

The IF tuning unit (1) provided additional amplification of the 70-MHz IF test signals and (2) demultiplexed the frequency-division-multiplex (FDM) downlink test signal spectrum to provide correctly tuned test signals at the desired level for each of the modems under test. Each tuning channel used a combination of internal fixed local oscillators and a tunable reference frequency derived from an external synthesizer. Outputs at 70 and 10 MHz as required for the various modems and monitoring functions were thus provided. Isolated outputs for test and monitor purposes were available at selected intermediate and output points.

3.4.2.2 Data Recording Subsystem – Modem outputs, carrier detector unit data, time code, and aircraft flight parameters were recorded by a 14-track instrumentation magnetic tape recorder. Modem tests were subdivided into types such as voice, digital data, etc. For each type, several modems were normally tested simultaneously. Rapid selection of the signals to be recorded and the recorder track assignments were made using the recorder interface unit. This unit also (1) performed Manchester encoding of clock and data modem outputs prior to recording, (2) provided other signal conditioning such as level adjustment, and (3) selected signals to be applied to the chart recorder. Aircraft heading, roll angle, pitch angle, and altitude were multiplexed onto one track using IRIG subcarrier FM recording techniques. All channels being recorded were also played back concurrently to allow monitoring of the recording process. Signals recorded for the modem tests, as well as for other tests such as antenna evaluation, FAA ATC demonstration, and the NASA two-satellite position-determination tests, are given in table 3-1.

3.5 ROSMAN TERMINAL EQUIPMENT

A functional block diagram of the U.S. aeronautical L-band experiment equipment is shown in figure 3-4. This diagram indicates equipment, functions, signal flow paths, signal types, and equipment rack locations.

TABLE 3-1. INSTRUMENTATION RECORDER CHANNEL ASSIGNMENTS

TEST TRACK NO.	VOICE ONLY	DATA[a] ONLY	VOICE & DATA	RANGING	ANTENNA EVALUATION	ATC DEMO	TWO-SAT
1. FM	Time Code (5B)	→	→	→	→	→	→
2. DIRECT[b]	IRIG FDM/FM (5C)	→	→	→	→	→	→
3. FM	CARR. DET C/N_o (5D)	→	→	→	→	→	→
4. DIRECT	NBFM VOICE (5E)	→	→	→	→	→	→
5. FM	HYB #1 C/N_o (1A)	→	→	CARR. DET MUX →	→	→	→
6. DIRECT	OPEN	(1C) HYB #2 DATA & CLOCK (1D) →	→	OPEN →	→	→	→
7. FM	HYB #2 C/N_o (1F)	→	→	TSC DIG. MODEM (6A)	OPEN →	→	→
8. DIRECT	OPEN	(2A) HYB #1 DATA & CLOCK (2B) →	→	OPEN →	→	(2C) FAA TRANSMIT DATA & CLOCK (2D)	OPEN
9. FM	OPEN →	→	→	→	→	→	→
10. DIRECT	HYB #1 VOICE (2E)	(2F) FAA CPSK DATA & CLOCK (3A)	HYB #1 VOICE (2E)	OPEN →	→	→	(3B) S&R 600 BPS DATA & CLOCK (3C)
11. FM	ADVM C/N_o (3D)	CARRIER DET. 1.25 KHZ IF (3E)	OPEN	TONE DEMOD. (3F)	OPEN →	→	→
12. DIRECT	ADVM VOICE (4A)	(4B) PLACE 1200 BPS DATA & CLOCK (4C) →	→	OPEN →	→	(4B) FAA RECEIVE DATA & CLOCK (4C) →	→
13. DIRECT	VOICE TO PLACE (1E)	→	→	→	→	→	→
14. DIRECT	HYB #2 VOICE (4D)	(4E) FAA DPSK DATA & CLOCK (4F)	HYB #2 VOICE (4D)	OPEN →	→	→	→
A. DIRECT	VOICE ANNOTATION	→	→	→	→	→	→

[a]Tape speed 7-1/2 ips for data only mode; 3-3/4 ips for all other modes.

[b]Track 2 recorded using IRIG 7-1/2% proportional subcarrier channels.

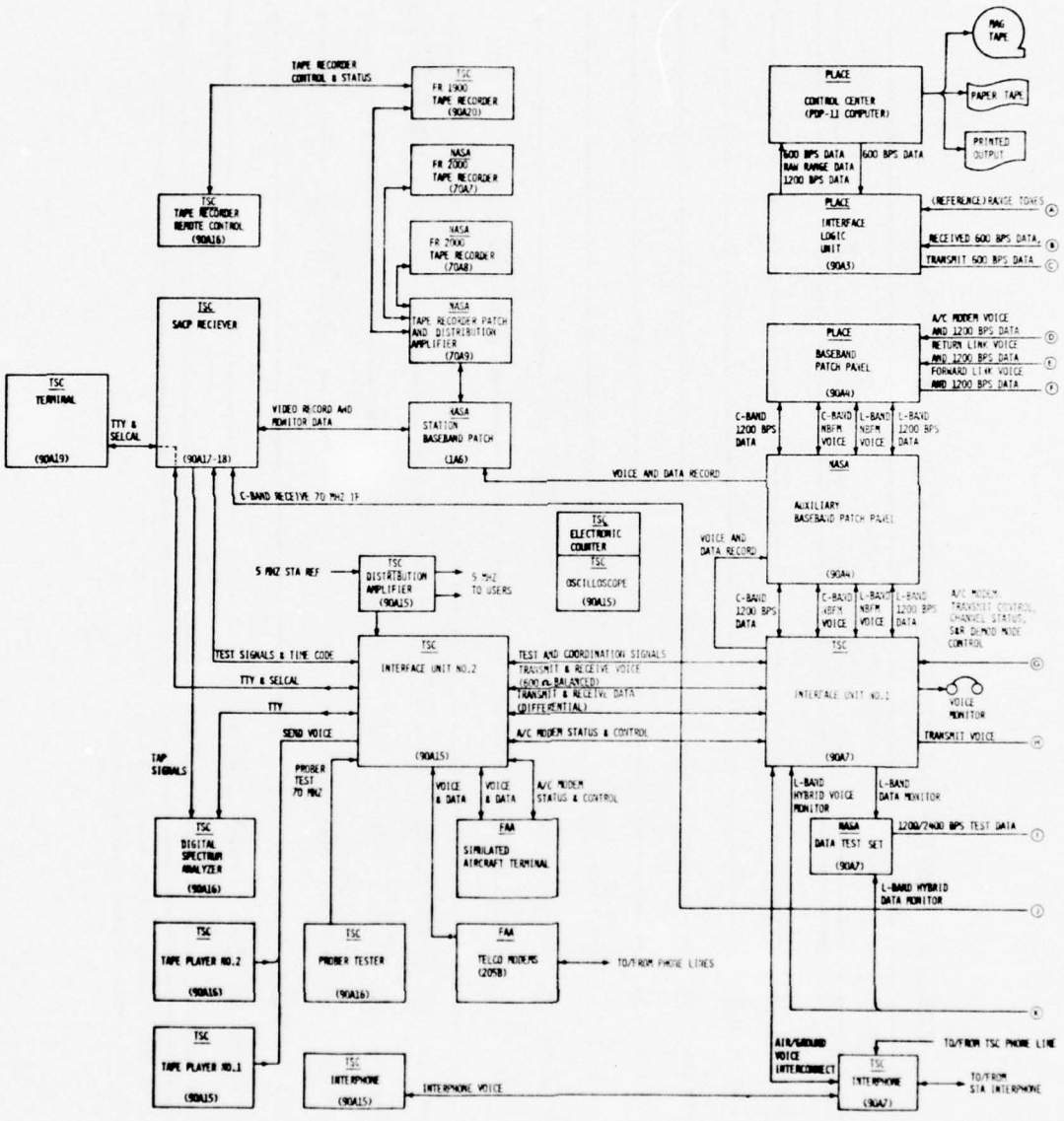

Figure 3-4. Rosman U.S. Aeronautical Terminal Block Diagram

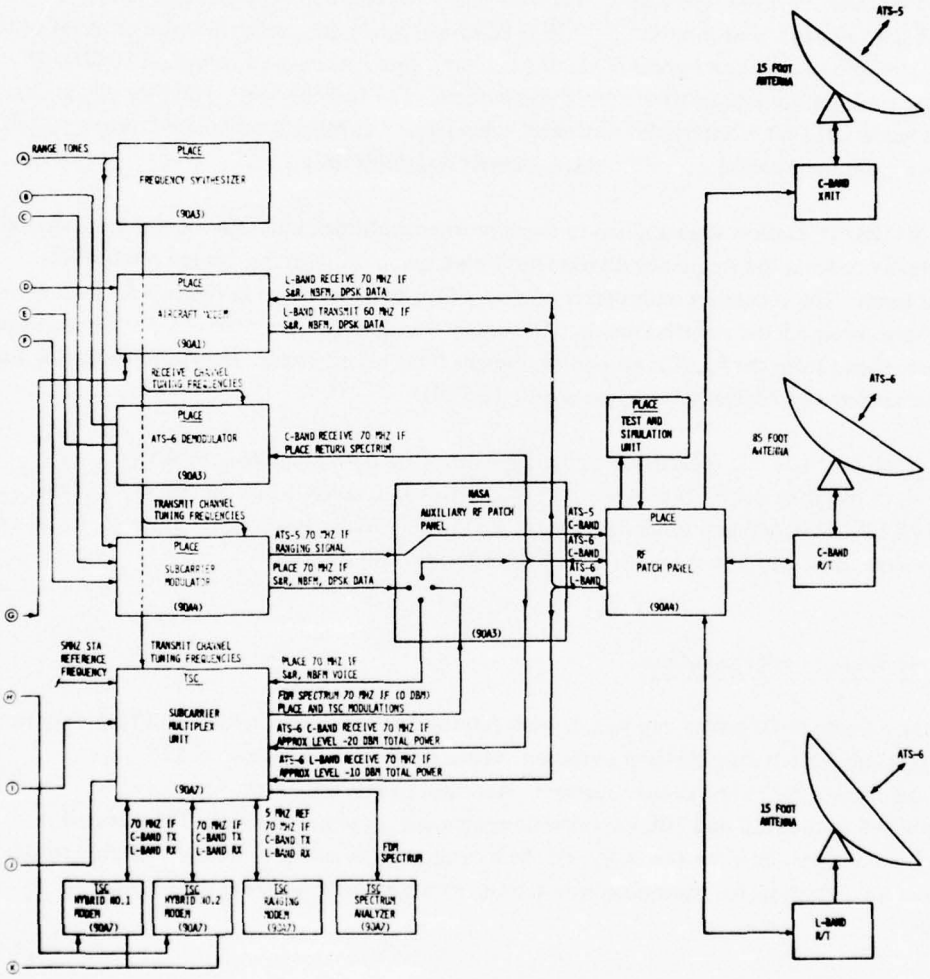

FUNCTIONAL BLOCK DIAGRAM
ROSMAN U.S. AERONAUTICAL TERMINAL

3.5.1 Generation of Forward-Link Test Signals

Baseband test signals for the modem evaluation tests were generated locally at the Rosman ground station. For voice modem tests, voice and SCIM test signals were obtained by reproducing pre-recorded test tapes on an audio tape player. This test signal was distributed to all voice modems under test. Each voice modulator output a 70-MHz IF carrier modulated with the voice or SCIM test signal. Similarly, the ranging and hybrid modems (voice and data), when used, provided 70-MHz IF carriers having modulations unique to the particular modem. The baseband test signal for digital data modem tests was a 2047-bit 1200-bps PN sequence. This signal was biphase modulated onto a 70-MHz IF carrier by a modulator contained within the subcarrier multiplex unit.

The 70-MHz IF carriers were applied to the subcarrier multiplex unit (SMU), which translated them individually to form the frequency division multiplex spectrum with the desired relative frequencies and levels. The subcarrier multiplexer portion of the SMU is shown in figure 3-5. Five subcarriers can be accommodated simultaneously. Frequency translations were normally performed using reference frequencies from the PLACE ground equipment (PGE) synthesizer. Frequency selection for individual subcarriers was normally in increments of 12.5 kHz.

The resultant FDM test spectrum was then up-converted for transmission to ATS-6 via the station C-band transmitter and 85-ft antenna. For the NASA two-satellite position-determination tests, the PLACE S&R signals and similar signals for the ATS-5 link were generated in the PGE. These modulations were transmitted to ATS-5 and ATS-6 for relay to the aircraft.

3.5.2 C-Band Return-Link Reception

During modem tests, return-link signals were transmitted from the aircraft via ATS-6 only for PLACE ranging and for test coordination purposes. These return-link signals from ATS-6 were received by the 85-ft antenna and C-band receiver. Received signals were down-translated to a 70-MHz IF and distributed to the PGE and TSC experiment equipment for demodulation. The return-link S&R channel was demodulated by the PGE, and the baseband voice and data were distributed to the experimenters for recording, for transmission to remote locations via telephone, or for test coordination.

3.5.3 L-Band Operations and Monitoring

In addition to the C-band operations described, transmission and reception of forward- and return-link signals at L-band to/from ATS-6 were provided by the station L-band receiver/transmitter and a 15-ft antenna. The PGE also contained a PLACE aircraft modem that was used as a simulated aircraft terminal during FAA ATC demonstration and NASA two-satellite position-determination tests.

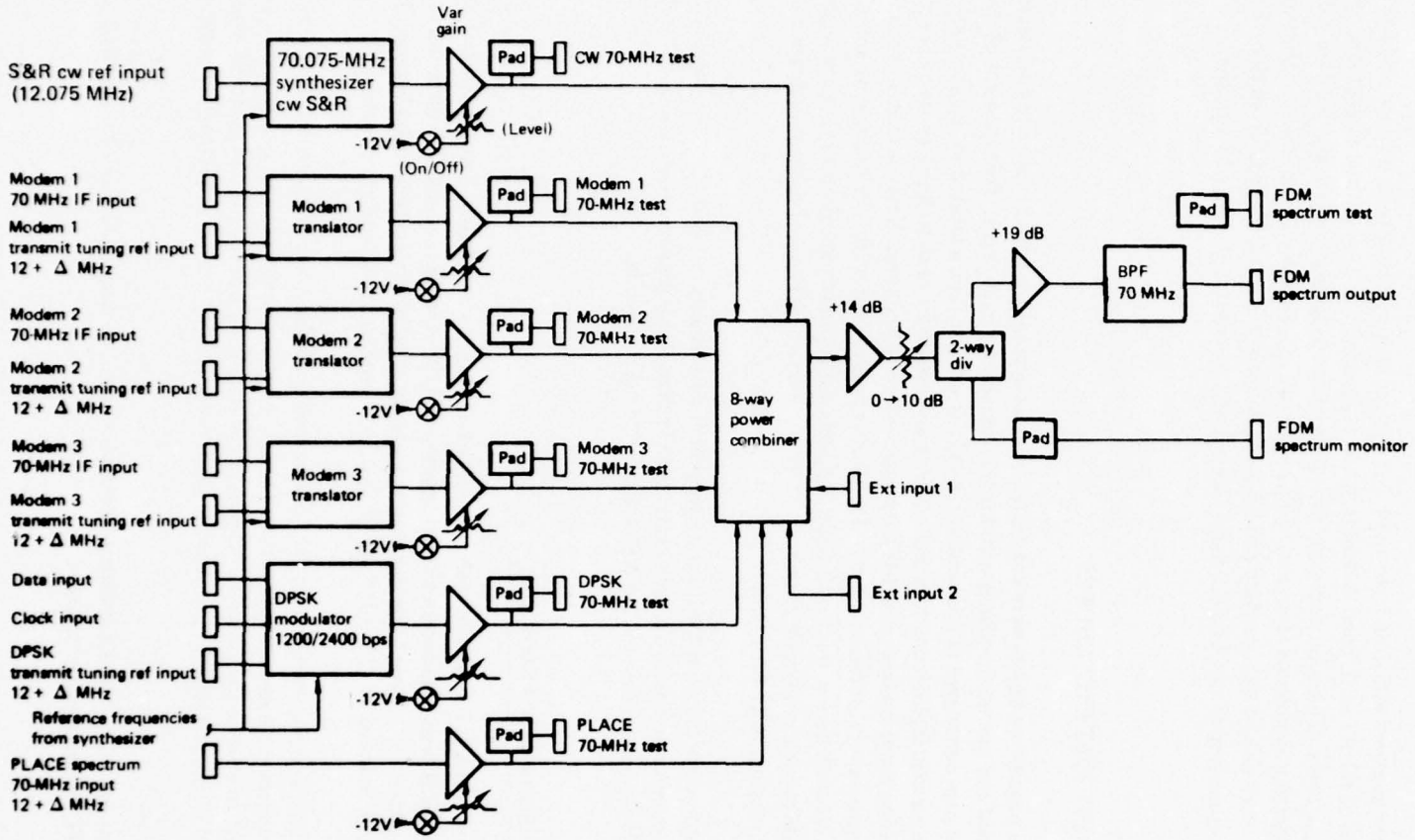

Figure 3-5. Subcarrier Multiplexer (Subcarrier MUX Unit)

During modem evaluation tests, the L-band transmission capability at Rosman was not used, but reception of the ATS-6 L-band downlink signal at Rosman was of particular importance for monitoring purposes. This reception capability allowed observation of the relative levels of L-band downlink spectral components after processing by the satellite transponder limiter. A spectrum analyzer was used as part of a standard procedure to monitor a 70-MHz IF signal from the L-band receiver corresponding to the ATS-6 L-band forward link received at the KC-135 airplane.

3.6 FLIGHT TEST PROCEDURES

Data acquisition flights were conducted in strict accordance with a master test schedule and with a detailed test operations plan specifying the scenario for each flight. Development of the overall flight test plan considered (1) the amount of ATS-6 satellite time allocated for L-band experimentation, (2) the specific flight geometries and other requirements for each technology test, (3) the ATS-6 satellite antenna beam coverage, and (4) the constraints resulting from the simultaneous requirements of other L-band experiment participants. The above requirements were best fulfilled by spreading the tests over a 7-month period, with each flight involving a mix of technology test types. A single flight might provide oceanic multipath, antenna evaluation, and several types of modem evaluation (voice, digital data, ranging) tests, for example.

Coordination between the L-band experiment participants resulted in an integrated L-band experiment operations plan.[2] This plan specified the master test schedule (date and time) and the signal transmission sequences for the ATS-6 forward and return links.

3.6.1 Test Scenarios and Geometries

Flight test legs for modem evaluation data acquisition were straight-line segments of 23 min duration. Type II tests required an aircraft heading of 110^{o} relative to the ATS-6 direction at an elevation angle of 15^{o}. Type I test legs spanned a range of satellite elevation angles between 10^{o} and 30^{o} at aircraft headings of 45^{o}, 135^{o}, 225^{o}, and 315^{o} relative to the satellite direction.

Geometrical requirements for the oceanic multipath and antenna evaluation tests also influenced the modem evaluation test scenarios. Oceanic multipath tests required aircraft headings of 0^{o}, 45^{o}, and 90^{o} relative to the satellite at elevation angles ranging from 3^{o} to 30^{o}. Antenna tests used both orbital flights and straight-line segments at various headings and elevation angles between 10^{o} and 45^{o}.

---

[2] "ATS-6 Integrated L-Band Experiment Operations Plan," contract NAS5-21789, prepared for NASA/GSFC, Westinghouse Electric Corp., 1974.

Twelve different flightpaths were needed to satisfy the combined data acquisition requirements of the modem, multipath, and antenna tests. An example of a typical flightpath is shown in figure 3-6. The associated test signal transmission sequence and detailed test operations plan are given in figure 3-7 and table 3-2. The test operations plan specifies all flight waypoints, aircraft tracks, C/N_O and S/I conditions, detailed timing of significant events, antenna selection, and any other parameters needed for test conduct. This particular flightpath was scheduled on four different occasions.

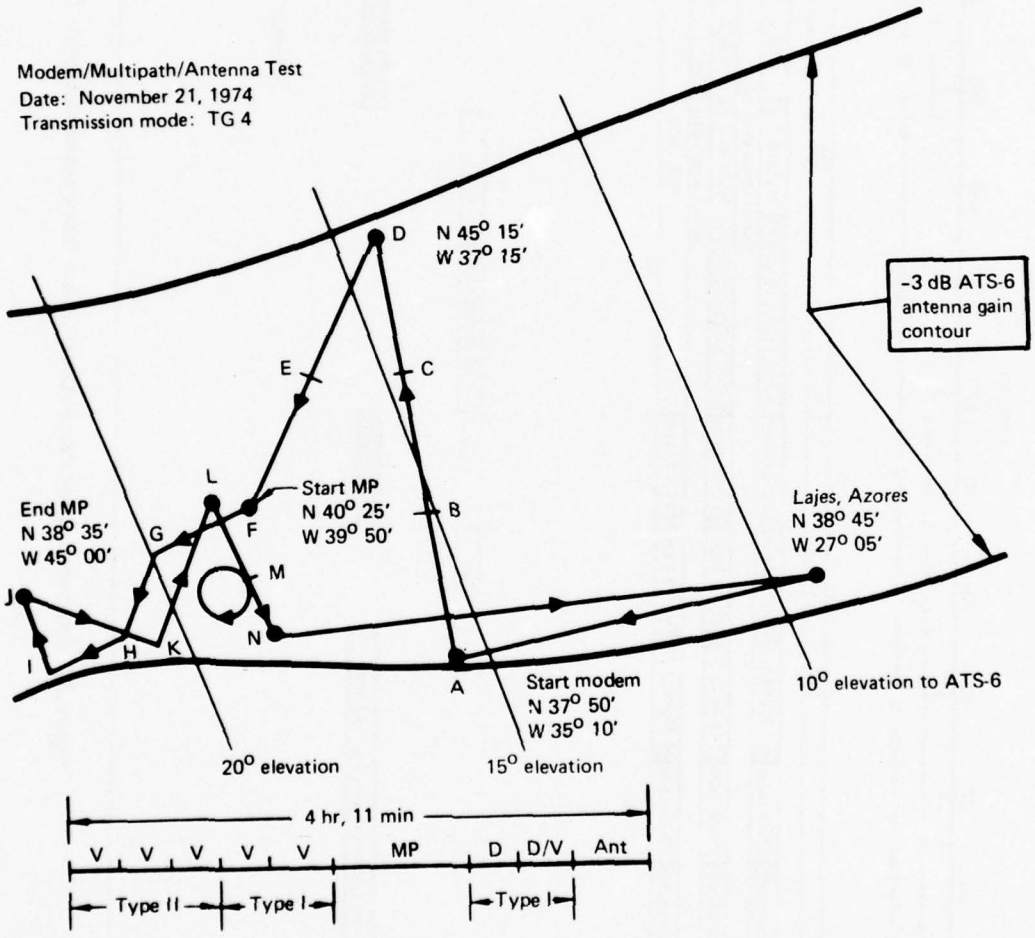

Figure 3-6. Modem/Multipath Antenna Evaluation – Flightpath No. 4

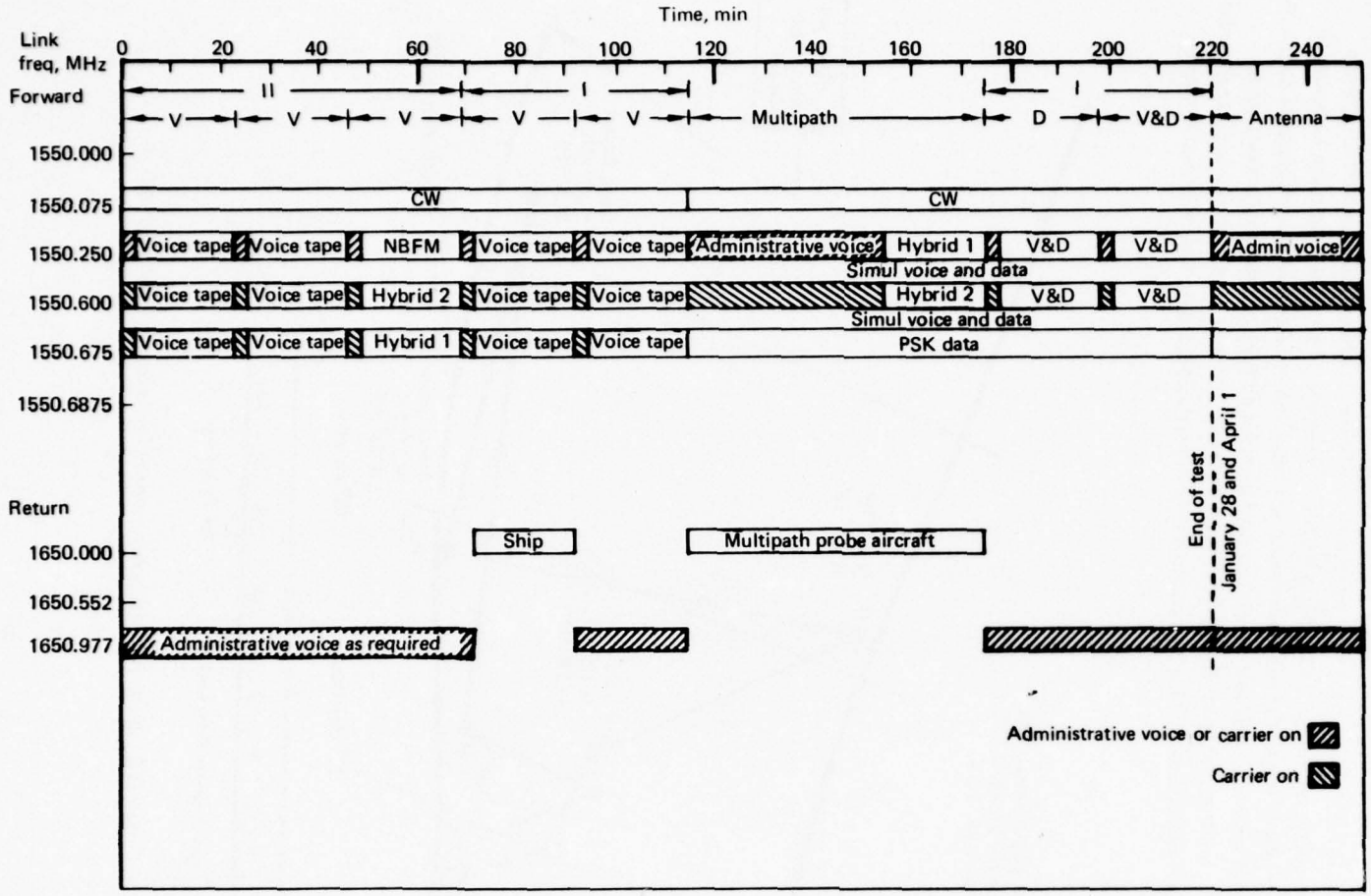

Figure 3-7. Integrated Aeronautical/Coast Guard Transmission Sequence TG 4

TABLE 3-2. DETAILED TEST SCENARIOS

Date: 1-28-75 Sequence: TG 4 Start Location: N 37° 50', W 35° 10'

Type: Modem/MP/ANT Base : AZ

TIME REL	TIME GMT	PILOT	TRACK °T	WAYPOINT	MAG VAR	TIME REL	TIME GMT	TEST TYPE	C/N$_o$	S/I	ROSMAN TRANS.	ANT USED	QH AZ, ELEV	MP POLAR	FMP AZ	FMP ELEV		DIG REC	REC INT	TAPE SPEED
0+00		Leg AB	349.6	(A) N 37 50 W 35 10	19°W	0+00		V, II	46	6	CW	QH,SMP	260, 15	LIN	--	--			V	3.75
0+23						+03					Tapes ON									
						+23														
0+23		Leg BC	348.2	(B) N 40 21 W 35 46	20°W	0+23		V, II	46	20	CW	QH,SMP	260, 15	LIN	--	--			V	3.75
						+26					Tapes ON									
0+46						+46														
0+46		Leg CD	346.6	(C) N 42 52 W 36 30	22°W	0+46		V, II	46	13	CW	QH,SMP	260, 15	LIN	--	--			V	3.75
						+49					Tapes ON									
1+09		Turn				1+09														
1+09		Leg DE	200.0	(D) N 45 21 W 37 20	22°W	1+09		V, I	37	--	CW	RWSD	(45, 16)						V	3.75
						+12					Tapes ON									
1+32						+32														
1+32		Leg EF	199.9	(E) N 42 56 W 38 32	22°W	1+32		V, I	39	--	CW	RWSD	(45, 18)						V	3.75
						+35					Tapes ON									
1+55		Turn				+55														
1+55		Leg FG	245.0	(F) N 40 31 W 39 41	22°W	1+55		MP, FMP	D_1 = 127			QH,FMP	0, 19	LIN	0	-35		ON		OFF
						2+07		TOP	D_2 = 490			QH,TOP		---	--	--				
2+13		Turn				+13														
2+13		Leg GH	198.5	(G) N 39 39 W 42 02	22°W	2+13		MP, FMP	C.R.= 5 MHz			QH,FMP	45, 20	LIN	45	-35				
						+22		SOP	C.L.= 1023			QH,RWSD	45, 20	---	--	--				
2+27		Turn				+27														
2+27		Leg HI	243.7	(H) N 38 10 W 42 40	22°W	2+27		MP, FMP				QH,FMP	0, 21	LIN	0	0				
						+36										-35				
2+41		Turn				+41														
2+41		Leg IJ	332.6	(I) N 37 27 W 44 26	22°W	2+41		MP, SOP				QH,LWSD	270, 23	---	--	--				
						+51		FMP				QH,FMP		LIN	270	-35				
2+55		Turn				+55												OFF		
2+55		Leg JK	106.1	(J) N 38 50 W 45 21	22°W	2+55		D, I	43	--	1200,PSK	RWSD	(135, 21)						D	7.5
						3+08														
3+18		Turn				+18														
3+18		Leg KL	19.1	(K) N 38 05 W 42 13	22°W	3+18		V&D, I	40	--	CW	LWSD	(225, 20)						V&D	3.75
						+21					Tapes ON									
3+41						+41														
3+41		Leg LM	153.8	(L) N 40 31 W 41 07	21°W	3+41		ANT	Best Hdg	175°M	(Nom)	QH,PHA,RW	90, 19						ANT	3.75
3+47						+47														
3+47		Start Circle to Right at 18° per min (360° in 20 minutes)			21°W	3+47			Hdg	175°M 255°M 295°M 55°M 95°M	(Nom)	RWSD,PHA TOP,PAT LWSD,PAT TOP, PAT RWSD,PHA									
4+07		Stop Turn				4+07														
4+07		Leg MN	154.5	(M) N 39 55 W 40 45	21°W	4+07						QH,PHA	90, 19							
4+11		End										RWSD								
				(N) N 39 27 W 40 27																

3.6.2 Forward-Link Transmission Formats

The principal forward-link transmission formats used for the modem evaluation tests are given in table 3-3. Four uplink signals were transmitted from Rosman at relative power levels that caused the L-band downlink channel powers received at the airplane (with modulations applied) to be equal. Special precautions and monitoring techniques ensured this equalization. If adjustment of the transmitted relative channel power was required at Rosman, such adjustment was made during the 3-min time intervals between test legs indicated in figure 3-7. Onboard the aircraft, these 3-min time intervals allowed for turns and readjustment of received C/N_0 and S/I for the next test leg in accordance with the test operations plan.

TABLE 3-3. MODEM EVALUATION TRANSMISSION FORMATS

Test mode	Channel frequency, MHz					
	1550.000	1550.075	1550.250	1550.600	1550.675	1550.6875
Voice (1)	–	CW	ANBFM	Hyb 2	Hyb 1	–
Voice (2)	–	CW	ADVM	Hyb 2	ANBFM	–
Voice (3)	–	CW	ANBFM	ADVM	Hyb 1	–
Voice (4)	–	CW	Hyb 2	ADVM	Hyb 1	–
Digital data	–	CW	NBFM	–	PSK	CW
Voice/data	–	CW	Hyb 1 V/D	Hyb 2 V/D	PSK	–
Ranging, NB (1)	CW	S&R	ANBFM	R_N	–	–
Ranging, NB (2)	–	S&R	CW	R_N	PSK	–
Ranging, WB	CW	S&R	ANBFM	R_W	–	–

Legend:

ANBFM	Adaptive narrowband frequency modulation
ADVM	Adaptive delta voice modulation
Hyb 1	Hybrid No. 1, voice-only mode
Hyb 2	Hybrid No. 2, voice-only mode
Hyb 1 (V/D)	Hybrid No. 1 modem, simultaneous voice and data mode
PSK	Digital data 1200-bps phase-shift-keyed test signal
NB, WB	Narrowband, wideband
R_N, R_W	TSC digital ranging: narrowband, wideband
S&R	Surveillance and ranging (NASA PLACE).

3.6.3 Aircraft C/N_0 and S/I Setup and Measurement

For all modem evaluation tests, the transmission format included a cw carrier at a power level equal to that of other test channels. C/N_0 measurements could therefore be made on this channel to infer the C/N_0 on other channels. The cw signal was normally at 1550.6875 MHz for data modem tests and at 1550.075 MHz for other modem tests.

3.6.3.1 Direct-Path C/N_0 Measurement – The desired direct-path C/N_0 for a test leg was set up by measuring the received C/N_0 on the cw channel using an HP 141T spectrum analyzer and adjusting the variable attenuator preceding the preamplifier (fig. 3-3) until the desired value was obtained. During the test, frequent C/N_0 measurements were made independently by separate operators at 70- and 10-MHz IF points using an HP 141T spectrum analyzer and HP 312A wave analyzer. These measurements were used to monitor the C/N_0 test parameter during test progress on each flight leg. C/N_0 measurements made internally within the two hybrid modems and displayed on these units were also useful for monitoring during the test.

The cw channel was also envelope detected within the carrier detector unit. This envelope-detected output was FM recorded for off-line computer analysis to determine C/N_0 and S/I on a more continuous basis in support of the detailed data analysis as described in section 3.8. Subsequent analysis showed excellent agreement between the computer-analyzed C/N_0 values and the real-time spectrum analyzer measurements made during the tests.

3.6.3.2 S/I Setup Procedure for Type II Tests – No direct method was available for real-time measurement of the received signal S/I ratio. The proper relative settings of the attenuators preceding the RF combiner (shown in fig. 3-8) for Type II tests were therefore determined from a combination of a priori knowledge and calibration measurement. The gain of the direct-path quad-helix antenna to the ATS-6 RHC forward-link signal is known to be approximately 15.5 dB. The gain of the side-mounted multipath antenna in its horizontal polarization mode as used for Type II tests is known to be about 12.0 dB. The reflection loss at the sea surface for incident horizontally polarized waves is known to be on the order of 1 dB at 15° elevation angles; this is consistent with theoretical prediction and has been verified experimentally both during this test program (vol. V) and during previous ATS-5 tests (ref. 3-2). Assuming that half of the energy in the ATS-6 downlink signal incident upon the sea surface is contained in the horizontally polarized component, the received direct-path signal power (P_D) relative to the indirect-path signal power (P_I) at the antenna terminals is

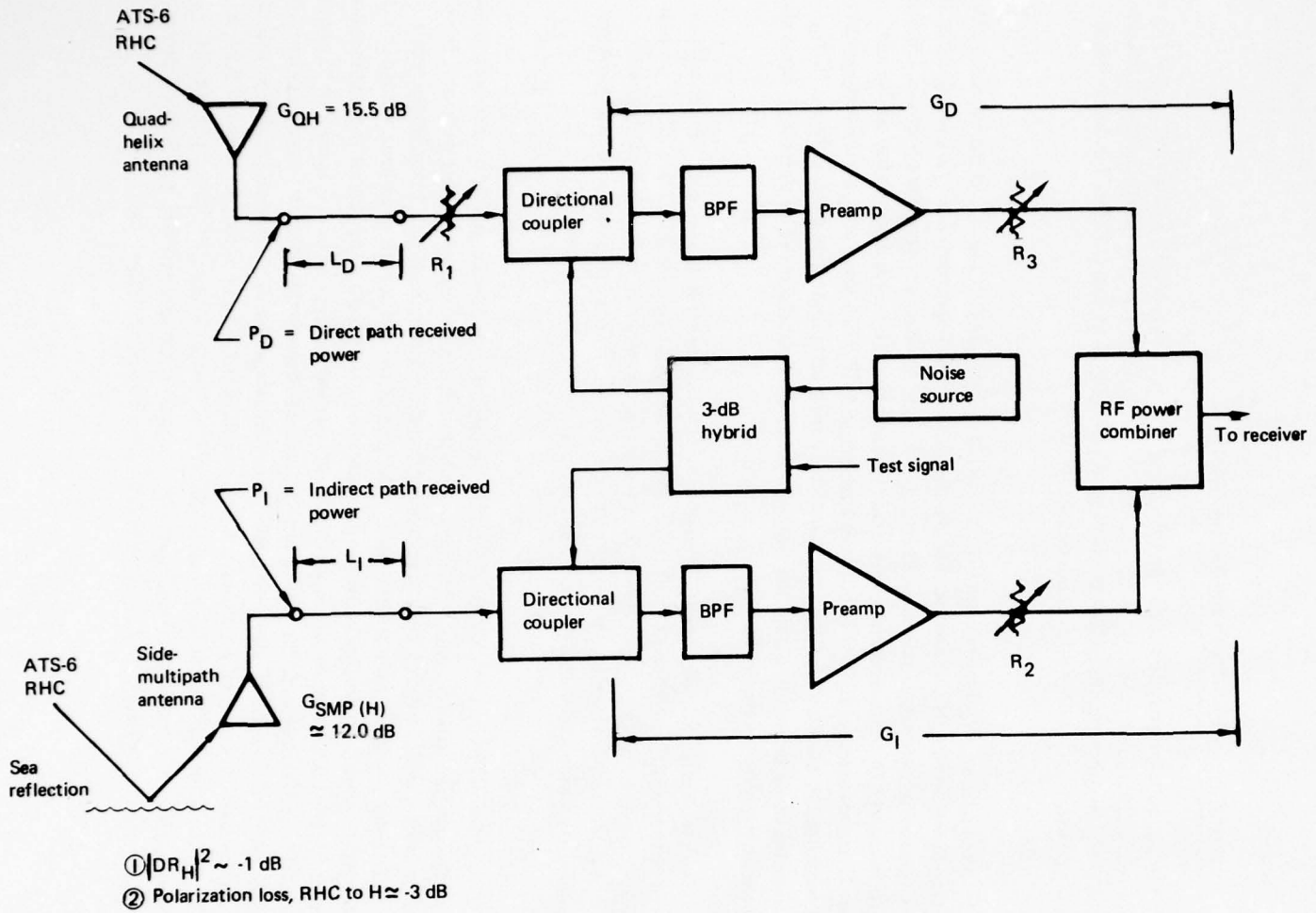

Figure 3-8. Estimation of S/I for Setup of Type II Modem Evaluation Test

$$(P_D/P_I)_{\text{at antenna}} \simeq 3\text{ dB} + 3\text{ dB} + 1\text{ dB} = 7\text{ dB}$$

G_{QH}/G_{SMP} — Polarization loss — Reflection loss for horizontal polarization

where G_{QH}/G_{SMP} is the relative gain of the QH and SMP antennas. On one occasion, measurements of P_D and P_I were made during a Type II test leg to verify that use of the above relationship was a satisfactory approximation for test setup purposes.

The above estimate of P_D/P_I was used in conjunction with RF system calibration data to set up the desired S/I value in the combined receiving channel. The RF cable losses between the antennas and their respective preamplifiers were known from measurements. The relative gains of the direct and indirect RF channels between the preamplifier inputs and the combiner output could be readily measured by injecting test signals into the two channels via directional couplers permanently installed for this purpose at the receiving channel inputs. Comparison of the signal levels at the combined output then yields the relative RF gain value of the two channels between these points. By this means the RF values were determined for Type II tests.

The above procedure for real-time estimation of S/I was used only for setting up the planned S/I test conditions for test conduct purposes. The actual value of S/I achieved during a given test run was determined by the off-line computer analysis of the cw-channel-detected envelope signal.

3.6.4 Functional Checkout and Calibration Provisions

The terminal design incorporated a sophisticated test and calibration capability designed to perform (1) functional checkout and adjustment, (2) calibration prior to data acquisition, (3) monitoring during test conduct, (4) acquisition of real-time measurement data, and (5) troubleshooting and fault correction. A calibrated noise source allowed the operating noise figure of all receiving systems to be measured. A composite L-band test signal simulating the ATS-6 and ATS-5 downlinks with appropriate 1200-bps digital data, ranging, NBFM voice, and PLACE S&R modulations could be generated and injected into the receiving system inputs for test and calibration purposes.

A block diagram of the channel calibrator is shown in figure 3-9. Modulated subcarriers corresponding to an NBFM voice channel and a 1200-bps data channel were obtained from the PLACE modem. These, together with an S&R subcarrier, were frequency multiplexed to the desired relative frequencies in the PLACE test set. A TSC digital ranging subcarrier, after translation to the correct frequency, was also added. The resultant spectrum was translated to 1650 MHz by the PLACE R/T unit. After a further 100-MHz translation in the L-band test set, this signal represented a four-channel

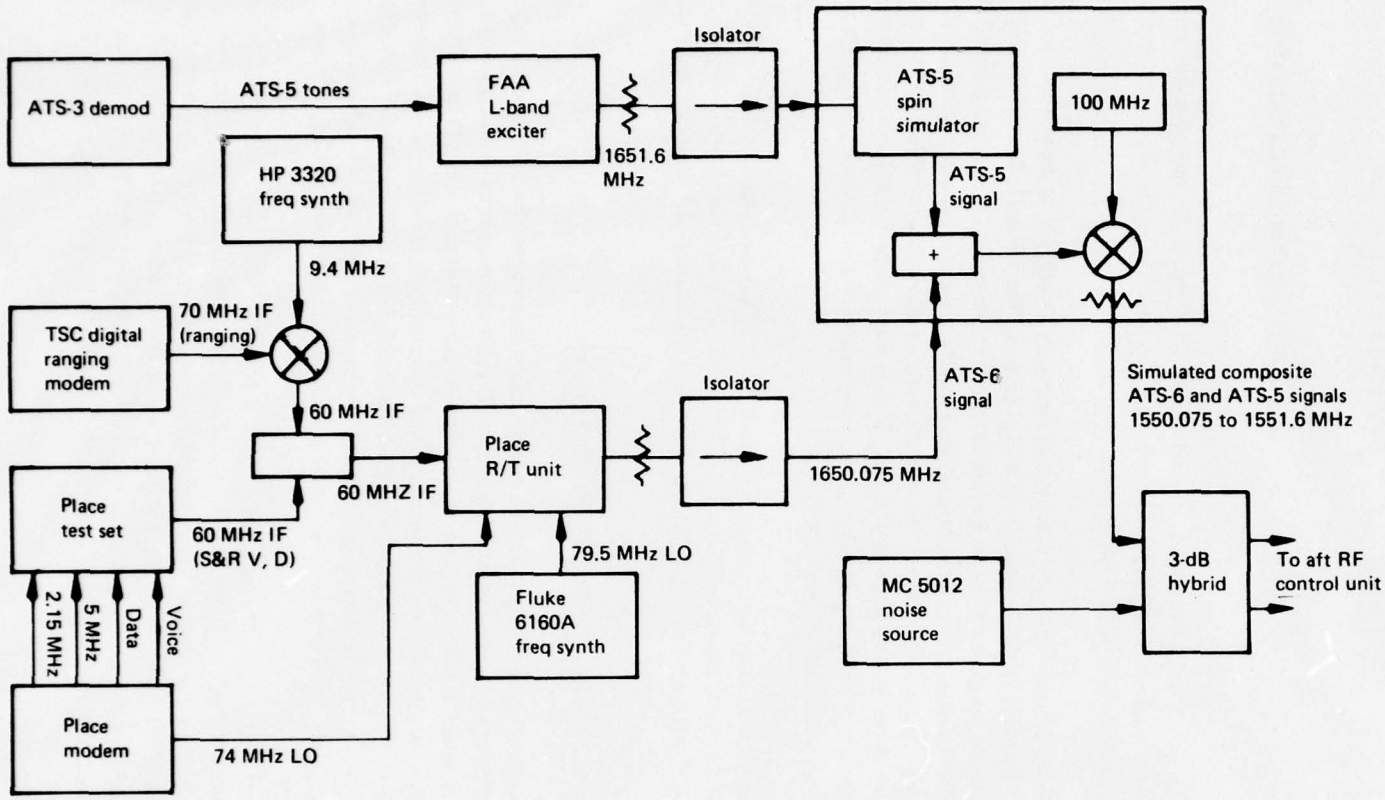

Figure 3-9. KC-135 Terminal Test and Calibration Signal Generation

ATS-6 L-band downlink test signal. The signals received from ATS-5 during the NASA two-satellite tests could also be simulated, including ATS-5 spin effects. The final composite L-band test signal was as shown in table 3-4.

These signals, either with or without the white noise from the calibrated noise source, can be injected into each receiving system input using permanently installed directional couplers.

The types of test and calibration performed using this channel calibrator were (1) operating noise-figure measurement for each receiving system, (2) receiving channel relative-gain calibration, (3) data acquisition channel checkout for continuity and adjustment, (4) PLACE S&R and NBFM channel functional checkout, (5) TSC digital ranging modem performance calibration, and (6) performance measurements on all digital data demodulators.

During test conduct, channel C/N_0 could be monitored as previously described, all voice modem outputs could be aurally monitored, all digital data modem bit-stream outputs could be viewed on a multitrace oscilloscope for rapid identification of erratic operations, BER measurements could be made both with internal error detectors or with an HP 1645A data error analyzer, all data signals being recorded could be monitored on playback, and various other RF and IF monitor points were available for performance monitoring. An eight-track chart recorder provided a hard-copy record of selected signals.

3.7 DATA ACQUISITION SUMMARY FOR MODEM EVALUATION

The DOT/TSC aeronautical technology tests acquired approximately 135 hr of flight test data over a 7-month period ending April 3, 1975. Of this, approximately 82 hr was modem evaluation data (65% Type I, 35% Type II).

Testing at satellite elevation angles in the 30^{O} range used Loring AFB, Maine, as the base for flight operations. Tests at lower elevation angles were conducted from Lajes AFB, Azores.

TABLE 3-4. L-BAND COMPOSITE CHECKOUT SPECTRUM

Signal	Frequency, MHz	Satellite signal simulated
PLACE S&R (or cw)	1550.075	ATS-6 downlink
NBFM voice	1550.250	ATS-6 downlink
TSC digital ranging	1550.600	ATS-6 downlink
1200-bps PSK data	1550.675	ATS-6 downlink
PLACE ranging tones (PM)	1551.600	ATS-5 downlink

During the modem evaluation tests, the ATS-6 fan beam antenna pierce-point locations normally were as follows:

Pierce-point location	Test series
45°N, 45°W	September 1974
40°N, 45°W	October and November 1974
40°N, 54°W	January, February, and March 1975.

The first two beam pointings described above were the nominal pierce-point locations agreed upon during the planning phase of the Integrated L-Band Experiment (ref. 1-1). Field experience obtained during the 1974 fall test series showed that uniformity of the ATS-6 antenna illumination was improved for the overocean region between satellite elevation angles of 15° and 35° with a more westerly pierce-point location. Thus the third beam pointing was used as the nominal pierce-point location during the 1975 spring test series.

Tables 3-5 and 3-6 summarize the Type I and II modem evaluation tests conducted. The tables identify the number of 23-min test legs flown for each type of test.

3.8 DATA ANALYSIS PROCEDURES

This section provides a brief description of the data reduction and analysis procedures applicable to the various modem evluation tests.

3.8.1 Data Analysis Functional Flow

Figure 3-10 illustrates the various machine and human judgment processes that constitute the total modem data reduction and analysis (DRandA) system. Time periods for which valid voice data were acquired are identified from the airborne logs and strip charts. Corresponding voice channels were transcribed to 1/4-in. tapes for intelligibility scoring by CBS Laboratories (ref. 3-3). A limited quantity of transcribed SCIM data was submitted to NASA/GSFC for processing.

Analog source tapes were sent to the Boeing Test Data Processing Center (TDPC) where (1) specified time segments and tape tracks were digitized to provide seven-track, 800-bpi digital tapes compatible with the CDC 6600 computer and (2) aircraft heading, pitch, roll, and modem monitor signals were stripped out on chart paper.

Airplane logs, onboard strip charts, and TDPC strip charts were used to identify which time segments of the digital tapes were to be analyzed. These time segments were subjected to detailed CDC 6600 processing using the applicable analysis program (vol. IV of this report). Output from the CDC

TABLE 3-5. MODEM EVALUATION DATA ACQUISITION, TYPE I

Date, mo-day-yr	Elevation angle, deg	Number of 20-min runs				
		Voice (no ADVM)	Voice (with ADVM)	Hybrid V/D	Digital data	Ranging[a]
9-24-74	30	1	-	1	1	2
9-26-74	30	5	-	-	5	-
9-30-74	30	4	-	2	2	2
10-24-74	15 - 22	2	-	1	1	-
10-25-74	15	-	-	-	5	1
10-28-74	15 - 17	2	-	-	2	1
11-13-74	12 - 15	-	-	3	1	2
11-14-74	9 - 16	4	-	-	3	-
11-15-74	15 - 17	2	-	-	2	1
11-16-74	9 - 15	4	-	-	1	2
11-19-74	15 - 17	-	-	-	4	-
11-20-74	9	5[b]	-	-	4[b]	2[b]
11-21-74	15 - 17	3	-	1	1	-
1-23-75	8 - 15	4	-	-	1	2
1-24-75	15 - 18	-	-	-	4	-
1-27-75	15	-	-	-	-	1
1-28-75	15 - 22	2	-	1	1	-
1-30-75	8 - 15	4	-	-	1	2
2-24-75	30	-	7	-	3	-
2-26-75	30	-	7	-	1	2
2-27-75	30	-	-	3	-	2
3-25-75	15	-	-	-	1	2
3-27-75	15	-	3[c]	-	-	-
3-28-75	10 - 15	3	-	-	2	-
3-31-75	15	3	-	-	-	-
4-1-75	10 - 17	-	3	1	-	-
4-2-75	10	-	-	-	1	2

[a]Low percentage of success due to erratic modem performance.

[b]Ground test parked at Azores.

[c]No ADVM data.

TABLE 3-6. MODEM EVALUATION DATA ACQUISITION, TYPE II

Date, mo-day-yr	Elevation angle, deg	Number of 20-min runs				
		Voice (no ADVM)	Voice (with ADVM)	Hybrid V/D	Digital data	Ranging[a]
10-24-74	15	3[b]	-	-	-	-
10-25-74	15	-	-	-	3[b]	1[b]
10-28-74	15	3	-	-	-	-
11-13-74	15	-	-	-	4	-
11-14-74	15	-	-	-	3	-
11-15-74	15	3	-	-	-	-
11-16-74	15	-	-	-	3	-
11-19-74	15	-	-	-	4	2
11-21-74	15	2	-	-	-	-
1-23-75	15	-	-	-	2	-
1-24-75	15	-	-	-	4	2
1-27-75	15	3	-	-	-	-
1-28-75	15	3	-	-	-	-
1-30-75	15	-	-	-	3	-
3-25-75	15	-	-	3	3	-
3-27-75	15	-	2[c]	-	1	1
3-28-75	15	1	-	-	2	1
3-31-75	15	2	-	-	2	1
4-1-75	15	-	3	-	-	-
4-2-75	15	1	-	1	1	-

[a]Erratic performance of modem.

[b]Questionable data due to RF power combiner fault.

[c]No ADVM data.

6600 included C/N_0 and S/I statistics, bit-error rates, error pattern statistics, and ranging data analysis. The above information was manually merged with other data such as voice intelligibility scores and aircraft parameters to give final outputs.

3.8.2 C/N_0 and S/I Determination

The calculation of C/N_0 and S/I is basic to all modem and antenna evaluation tests. The cw carrier transmitted from Rosman to the aircraft via ATS-6 was processed by an envelope detector in the carrier detector unit. The detected envelope output was FM recorded and computer analyzed to determine C/N_0 and S/I. The algorithm made it possible to obtain these estimates as often as every 15 sec for modem evalutaion and every 3 sec for antenna tests.

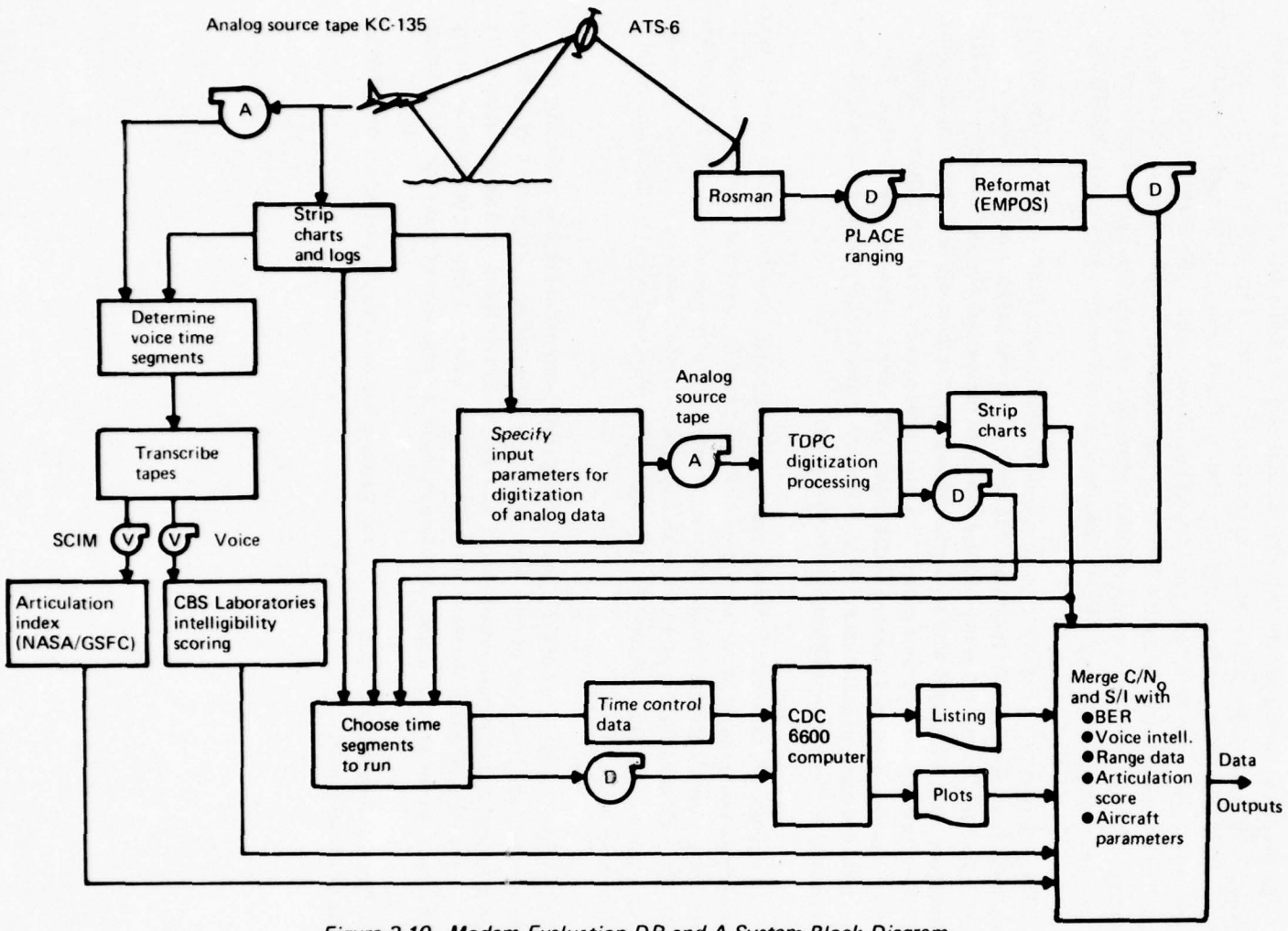

Figure 3-10. Modem Evaluation DR and A System Block Diagram

Specifically, the envelope-detected signal was digitized at a 2-kHz rate using 10-bit quantization to obtain 1025 signal strength samples in approximately 0.5 sec. The 1025 samples were processed to remove sample bias and linear drift components. The sample mean, $(\overline{S})$, mean squared values $(\overline{S^2})$, and variance (σ^2) were then determined. After the time-domain samples were tapered to minimize spectral window side-lobe peaks, the discrete Fourier transform was performed on the time-domain data. The discrete Fourier transform was implemented using the fast Fourier transform (FFT), whose output provided the power spectral density versus frequency for the 0- to 800-Hz range.

The output spectrum can be expanded as a mathematical series involving direct signal power, multipath spectrum, and the noise spectrum. The spectral data was used to calculate a quantity termed "noise floor," computed as the weighted average of the spectral density from 250 to 800 Hz. This frequency range was chosen with the a priori knowledge that there will be little multipath power above 250 Hz in comparison to noise power. The ratio of the squared mean signal strength to the noise floor value was calculated and used to determine C/N_0 using a computer look-up table. The look-up table was based on analytical modeling of the carrier detector output. The modeling has been experimentally verified for the additive noise environment.

To estimate S/I, the spectral data was numerically integrated from 2 to 250 Hz to yield a band-limited variance figure caused by the combined effects of multipath power and noise. This calculation uses the a priori knowledge that virtually all multipath-related energy will fall within the range of 0 to 250 Hz. The ratio of squared mean to the above band-limited variance was calculated and used with C/N_0 to estimate S/I by graphical methods. These graphical relationships are also based on careful analytical modeling.

Typically, several values of C/N_0 and the S/I statistic were calculated over a time segment: the mean and standard deviation of these parameters were also calculated. The mean C/N_0 is the value used in plotting data in the final output format, and the standard deviation gives an indication of the constancy of C/N_0. Similarly, the mean of the S/I statistic is used to determine the mean S/I during the data time segment and the standard deviation indicates the constancy of that parameter estimate.

The envelope detector algorithm and the mathematical basis for the analysis are described in volume IV of this report.

4. VOICE MODEM EVALUATION TEST RESULTS

Four distinct voice modulation techniques were evaluated for a variety of aeronautical channel conditions. Performance was measured primarily by word intelligibility scores achieved using lists of phonetically balanced words. Variables in the tests included C/N_0, the ratio of unmodulated carrier power to noise power density measured in dB-Hz, and S/I, the ratio of direct signal power to total scattered multipath power measured in dB.

4.1 VOICE MODEMS TESTED

The modems tested are referred to as NASA ANBFM (adaptive narrowband frequency modulation), Hybrid No. 1 (Q-M/PSK), Hybrid No. 2 (PDM/PSK), and ADVM (adaptive delta voice modulation). The two hybrid modems may operate in either voice only, data-only, or simultaneous voice/data modes. Characteristics of each are briefly described below.

Adaptive Narrowband Frequency Modulation (ANBFM) – This modem uses narrowband frequency modulation in conjunction with a wideband phase-lock demodulator. Use of a bandpass limiter prior to the demodulator PLL provides the usual loop adaptivity to C/N_0 (loop bandwidth diminishing with C/N_0) and this somewhat ameliorates the FM demodulator threshold effect. Audio processing consists of speech preemphasis, peak clipping prior to modulation, and deemphasis after demodulation. The modem was originally developed for NASA by Bell Aerospace Company.

Hybrid No. 1 (Q-M/PSK) – This unit employs quadrature carriers to convey speech and data information in a manner such that all transmitter power reverts to the data channel in the absence of audio inputs. The processed speech double-sideband-suppressed carrier (DSBSC) modulates a carrier, while data (if present) PSK modulates the quadrature carrier. The analog sum is limited to provide a constant envelope signal. This process induces time-varying power sharing between the voice and data channels since the speech waveform is random. Demodulation of the signal is accomplished with a synchronous demodulator and low-pass filter. When the modem is operating in the voice mode, the coherent reference is extracted with a second-order phase-lock loop. A Costas loop is used when the modem is operating in the data mode or combined voice/data mode. The modem was developed for TSC by Bell Aerospace Company.

Hybrid No. 2 (PDM/PSK) – Again, voice and data, if both are present, are conveyed on carriers that are in phase quadrature. The voice intelligence is impressed with suppressed-

clock pulse-duration modulation (SCPDM). The pulse waveform PSK modulates a carrier in constant-envelope fashion. The data signal PSK modulates a quadrature carrier and the linear sum of the two modulated carriers is transmitted. In the voice/data mode, a 50-50 power split is in effect whether speech is present or absent. Audio demodulation is accomplished with coherent carrier-tracking loops, a clock extraction loop, and reconversion of the PDM waveform to analog speech. This modem was developed for TSC by Magnavox Research Laboratories.

Adaptive Delta Voice Modulation (ADVM) – The ADVM modem is an implementation of delta modulation in which the step size is dynamically adjusted to operate in high-signal dynamics with minimal slope overload, yet maintain small quantizing noise when the waveform is being adequately tracked. The speech sampling rate, and hence the channel bit rate, is 19.2 kbps. Two detection options are available. One, referred to as digital, uses coherent integrate-and-dump decisions on each bit whereas the second, referenced to as analog, simply uses the filtered low-pass output of the coherent demodulator. The latter mode is superior at low C/N_o where the digital error rate becomes large. This modem, developed for TSC by Bell Aerospace Company, entered the flight test program in time for the February 1975 tests.

4.2 PERFORMANCE EVALUATION METHOD AND TEST CONDUCT

The preferred measure of performance in speech communication for aeronautical systems is the achieved intelligibility, as opposed to mean square error or test-tone-to-noise ratio. Although the latter are easier to analyze or measure, intelligibility tests incorporate all the aural perception phenomena implicitly and thus provide a proper ranking on the basis of usefulness to the human listener.

To perform these tests, phonetically balanced word lists were recorded on 1/4-in. tape by CBS Laboratories using alternate male and female speakers. A single intelligibility test involved four separate speakers, each reading two 50-word lists, making a 400-word test. List scrambling minimized learning by the listener panel. The words were spoken at approximately 2.5-sec intervals, and the total test duration, over which conditions were maintained constant, was roughly 22 min. Figure 4-1 illustrates the tape format for all sessions.

These source tapes were played as audio inputs to all modulators under test at NASA/Rosman. Three voice signals were transmitted along with a cw carrier in a four-channel FDM format. In terms of ATS-6 L-band forward-link frequencies, the frequency assignments were:

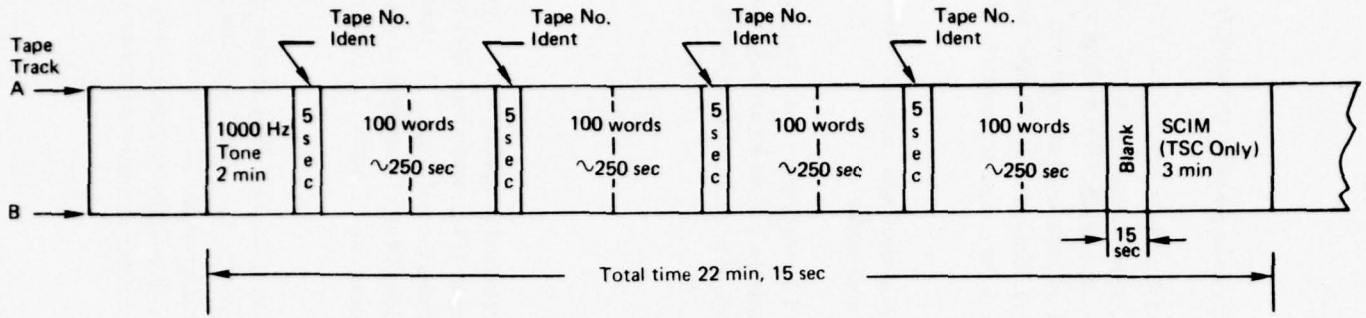

Major Parameters

1) Record Speed: 7 1/2 ips (2 tracks, forward direction)
2) Record Level: 0 VU, average
3) Tape Type: 1/4 - inch, Scotch 260
4) Tape Capacity: 1200 feet, 30 min at 7 1/2 ips, 2 tracks one direction
5) Interpause Period: 2.5 sec (time between start of each word)
6) No. of words per track: 400 uniquely scrambled PB words (8 PB 50-word lists)
7) No. of speakers per track: 4 speakers (100 words each)
8) Total record time: (a) Without SCIM: 19.0 min
   (b) With SCIM (TSC Only): 22 min, 15 sec.

Figure 4-1. DOT/TSC ATS-6 Voice Tape Composition

1550.075 MHz	CW carrier (also used for PLACE S&R)
1550.250 MHz	Up to three modems under test.
1550.600 MHz	
1550.675 MHz	

This frequency plan was chosen to minimize inband intermodulation noise arising in the satellite.

One aspect of the test setup was preleveling of the signals at Rosman to ensure equal power per channel at the aircraft. Preleveling was mandatory since C/N_o measurements were performed only on the cw carrier, and the C/N_o was assumed as identical for all channels. This leveling was accomplished by viewing the L-band satellite-to-Rosman downlink on a spectrum analyzer with no modulation applied. Resolution of 2 dB/cm was used on the display. Equalization of amplitudes on this basis thus compensated for any unequal gain versus frequency in the ground transmitter and satellite transponder.

The 1-kHz tone preamble was used to set the modulator audio levels and recorder levels on the aircraft. Once the word list was initiated, no further adjustments were made.

Aircraft crew operations involved setting the C/N_o and S/I to near the desired values, tuning the receiver frequency, and adjusting the gain to ensure nominal operating levels for each demodulator. Periodically, C/N_o measurements on the cw carrier were made with a spectrum analyzer or wave analyzer and were logged.

4.3 REDUCTION AND ANALYSIS OF VOICE DATA

The instrumentation tapes recorded on the KC-135 were returned to Seattle, and the three separate voice tracks were transcribed, along with identification, onto 1/4-in. audio high-fidelity tape using a Revox deck. These tapes were forwarded to CBS Laboratories for evaluation. The carrier detector signal was subsequently digitized at the Test Data Processing Center for analysis of channel conditions. This procedure is common to all experiments and is described in section 3.8 (and, in more detail, in vol. IV).

CBS used a trained listener panel of 10 persons. For each 400-word list, the statistics for each listener and for the panel average were provided, as shown in figure 4-2. The primary measure used in data evaluation was the mean PB word score; the 95% confidence interval provides a measure of the statistical confidence in the estimate using t-distribution tables. This assumes the actual scores are normally distributed with unknown mean and variance; thus the number of degrees of freedom is 10-2-1 = 7.

CBS LABORATORIES, STAMFORD, CONNECTICUT

INTELLIGIBILITY TEST REPORT

* *

STATISTICS FOR BOEING AIRPLANE TEST NO. 147

SESSION NO. B49 DATE: 3/11/75

TEST MEAN SCORES (%):		ORDERED ARRAY
LIST 901	82.4	79.8
LIST 902	79.8	81.6
LIST 2603	89.8	82.4
LIST 2604	90.2	83.2
LIST 4305	83.2	85.4
LIST 4306	81.6	89.8
LIST 6007	91.4	90.2
LIST 6008	85.4	91.4

LISTENER RESULTS (%):

LISTENER	MEAN SCORES	STD. DEVIATION	STD. ERROR
1	80.5	6.5683222	2.3222526
2	96	2.3904572	.84515425
3	91.75	4.5903626	1.6229363
4	85.75	5.8002463	2.0506957
5	77.5	8.1940745	2.8970428
6	84.25	5.1754917	1.8298126
7	93.75	5.3917927	1.9062863
8	85	6.8452277	2.4201535
9	80	10.69045	3.7796447
10	80.25	7.8148211	2.7629565

CONDITION RESULTS:

MEAN PB WORD SCORE = 85.4750

STANDARD DEVIATION = 4.4400 STANDARD ERROR OF MEAN = 1.5698

95% CONFIDENCE LIMITS (7 DEGREES OF FREEDOM) = 3.71252

HIGHEST TEST SCORE = 91.4000 LOWEST TEST SCORE = 79.8000

RANGE = 11.6000 MEDIAN = 84.3000

FREQUENCY DISTRIBUTION (TEN EQUAL CLASSES):

1	1	2	0	1	0	0	0	2	1

Figure 4-2. Sample Voice Intelligibility Report

CBS LABORATORIES, STAMFORD, CONNECTICUT

INTELLIGIBILITY TEST REPORT

* *

TALKER STATISTICS FOR BOEING AIRPLANE TEST NO. 147

SESSION NO. 849 DATE: 3/11/75

FEMALE TALKERS:

TEST MEAN SCORES (%):

LIST 901	82.4
LIST 902	79.8
LIST 4305	83.2
LIST 4306	81.6

MEAN PB WORD SCORE = 81.75

STANDARD DEVIATION = 1.4548769

STD. ERROR OF MEAN = .72743843

MALE TALKERS:

TEST MEAN SCORES (%):

LIST 2603	89.8
LIST 2604	90.2
LIST 6007	91.4
LIST 6008	85.4

MEAN PB WORD SCORE = 89.2

STANDARD DEVIATION = 2.6229754

STD. ERROR OF MEAN = 1.3114877

T-TEST STATISTIC =-4.3020563 FOR 6 DEG.OF FREEDOM

Figure 4-2. (Continued)

-3-

CBS LABORATORIES, STAMFORD, CONNECTICUT

INTELLIGIBILITY TEST REPORT

* *

DATA SUMMARY FOR BOEING AIRPLANE TEST NO. 147

SESSION NO. 849 DATE: 3/11/75

LISTENERS

	1	2	3	4	5	6	7	8	9	10
LIST 901	70	98	92	84	70	78	94	84	80	74
LIST 902	80	94	90	76	62	82	98	76	64	76
LIST 2603	86	94	90	90	86	90	94	92	86	90
LIST 2604	92	98	94	88	84	84	100	92	84	86
LIST 4305	76	94	82	82	80	80	92	78	86	82
LIST 4306	78	96	96	90	74	80	82	82	64	74
LIST 6007	82	94	96	94	82	92	96	94	94	90
LIST 6008	80	100	94	82	82	88	94	82	82	70

Figure 4-2. (Concluded)

The two key experiment variables were the signal-to-noise density ratio, C/N_o, and the direct-to-indirect signal power ratio, S/I. A technique of estimating these parameters was developed using samples of the detected envelope of a cw carrier multiplexed with the modulated voice carriers. This technique and underlying theory are described fully in volume IV of this report. Basically, the method utilizes moments of the envelope process and smoothed spectral estimates to determine statistical quantities that are uniquely related to C/N_o and S/I. This method provides a direct isolation of multipath and additive noise contributions to the total detector output fluctuations.

A single set of channel parameter estimates is provided every 15 sec, and the values reported here are averages over a 20-min interval of these individual estimates. The absolute accuracy that may be attached to these smoothed estimates is ± 0.5 dB for C/N_o and ± 1.0 dB for S/I. Note that since the same estimates are used for presenting the various modem results, the differential error between modems is zero.

4.4 TYPE I TEST RESULTS, VOICE-ONLY MODE

Type I voice tests were performed in the September, October, and November test series in 1974 and during January, February, and March/April in 1975. The ADVM modem became available in February 1975. All data acquired have been analyzed to obtain intelligibility scores except those of January 1975 and non-ADVM tests in March 1975. Since the other test series provided an adequate Type I data base, intelligibility scoring of these tests was deferred.

Test results for the voice-only mode are summarized for each modem in figures 4-3 through 4-7. Respectively shown are ANBFM, Hybrid No. 1, Hybrid No. 2, and ADVM performance. (Hybrid No. 2 modem results are presented separately for fall and spring series for reasons described below.) In figures 4-3 and 4-4, each point is identified as to the period of testing, i.e., fall or spring series. The ADVM modem results were obtained exclusively during the spring 1975 test series. For each modem, a best-fit curve has been drawn within the data set. These curves have been simultaneously plotted in figure 4-8 and serve as an experiment summary for Type I tests. The independent variable in each figure is the C/N_o estimate derived from the carrier detector unit. Averaging of C/N_o over a 20-min run has been used.

Modifications to the Hybrid No. 2 modem were made by Magnavox personnel during December 1974. Both Hybrid No. 1 and 2 modems were returned to manufacturers at that time for realignment and calibration. The modifications consisted of changing the preemphasis schedule from 12 to 6 dB/octave and the deemphasis schedule from 6 dB/octave to none. Also, an audio AGC prior to the modulator was included to accommodate dynamic level changes at Rosman. Because these changes apparently improved the voice intelligibility scores by 5 to 15 percentage points, the spring test results have been separately plotted.

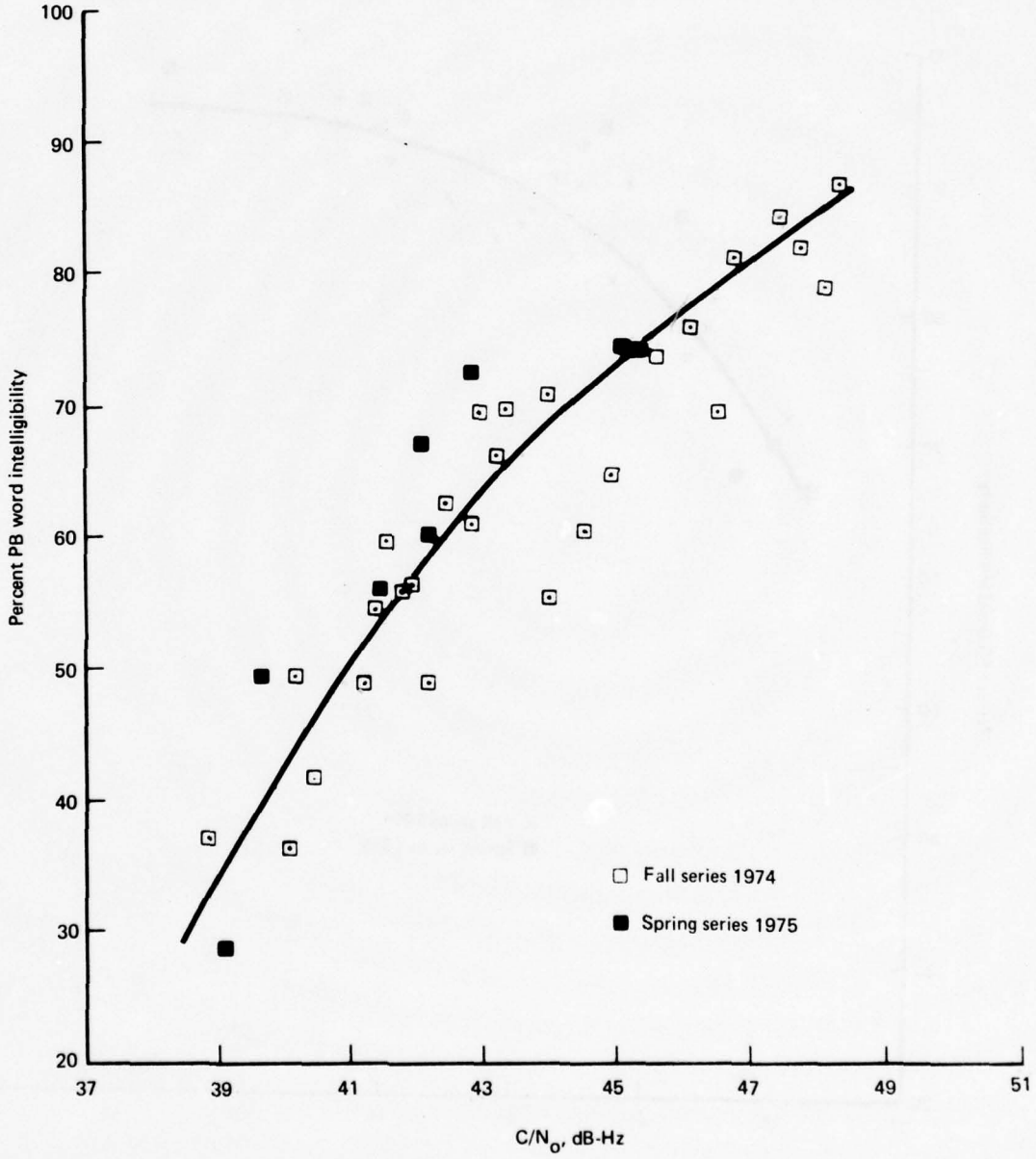

Figure 4-3. ANBFM Voice Modem, Type I Results, All Series

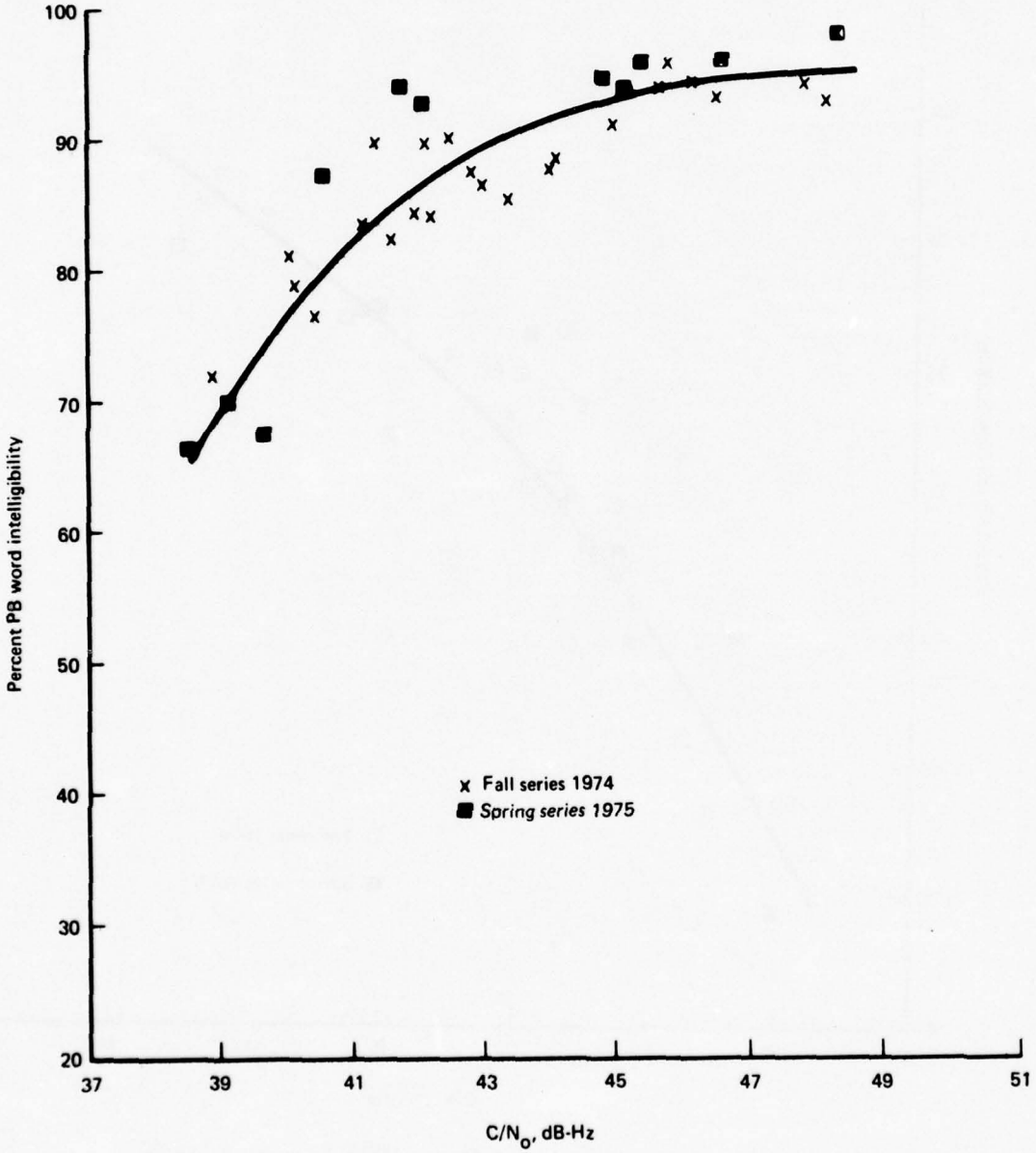

Figure 4-4. Hybrid No. 1 Voice Modem, Type I Results, All Series

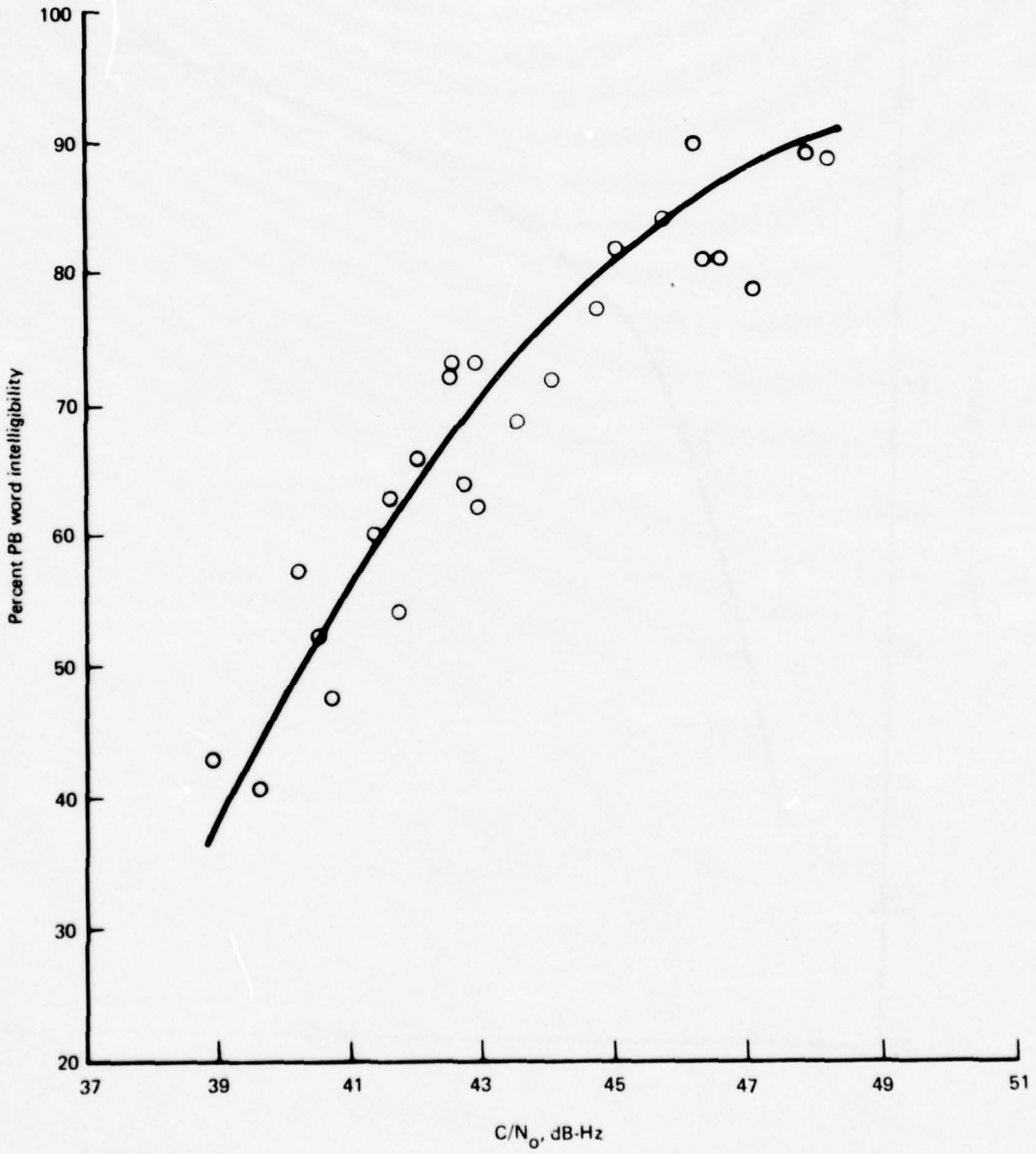

Figure 4-5. Hybrid No. 2 Voice Modem, Type I Results, Fall 1974

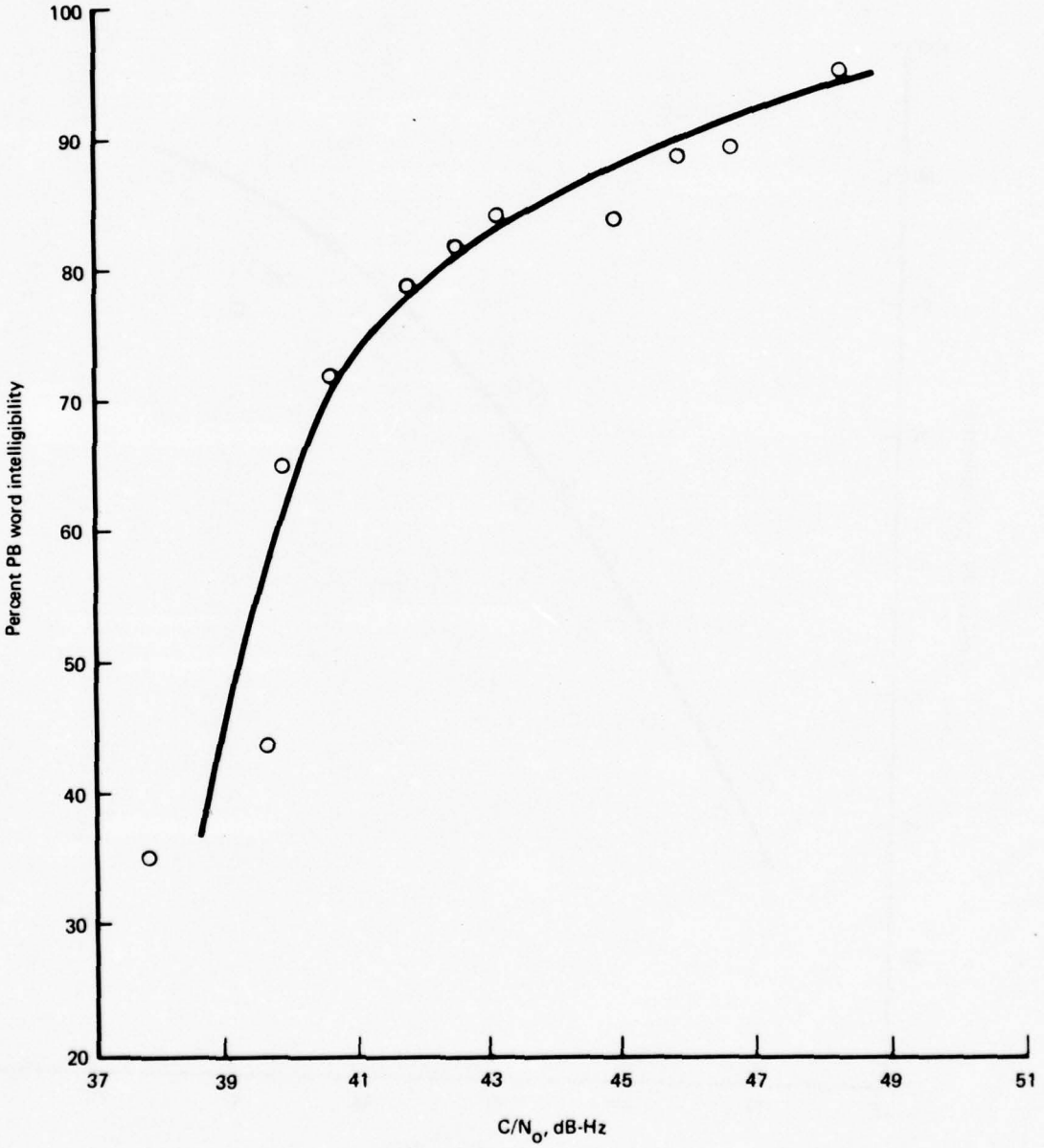

Figure 4-6. Hybrid No. 2 Voice Modem, Type I Results, Spring 1975

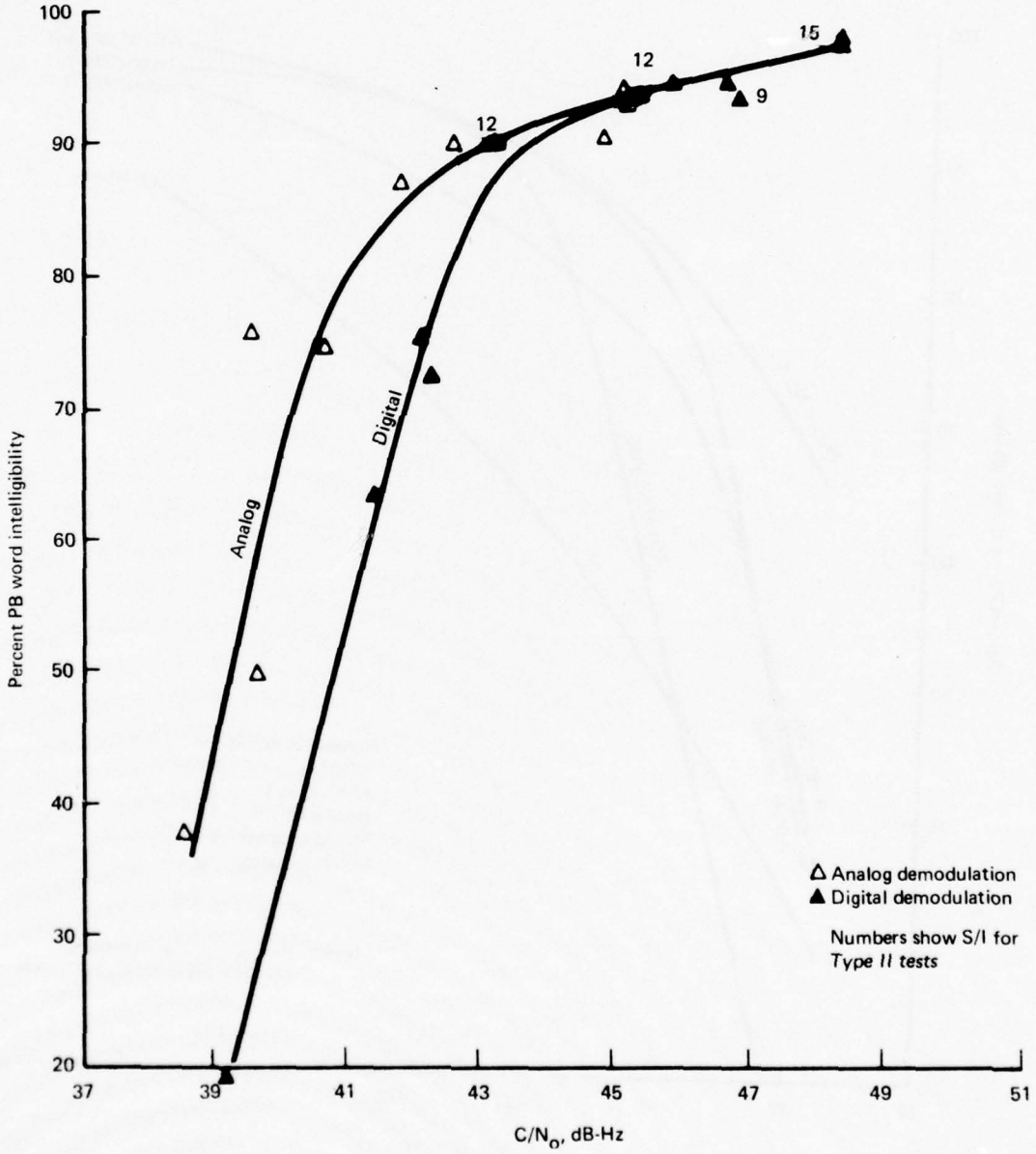

Figure 4-7. ADVM Voice Modem, Type I and II Results, All Series

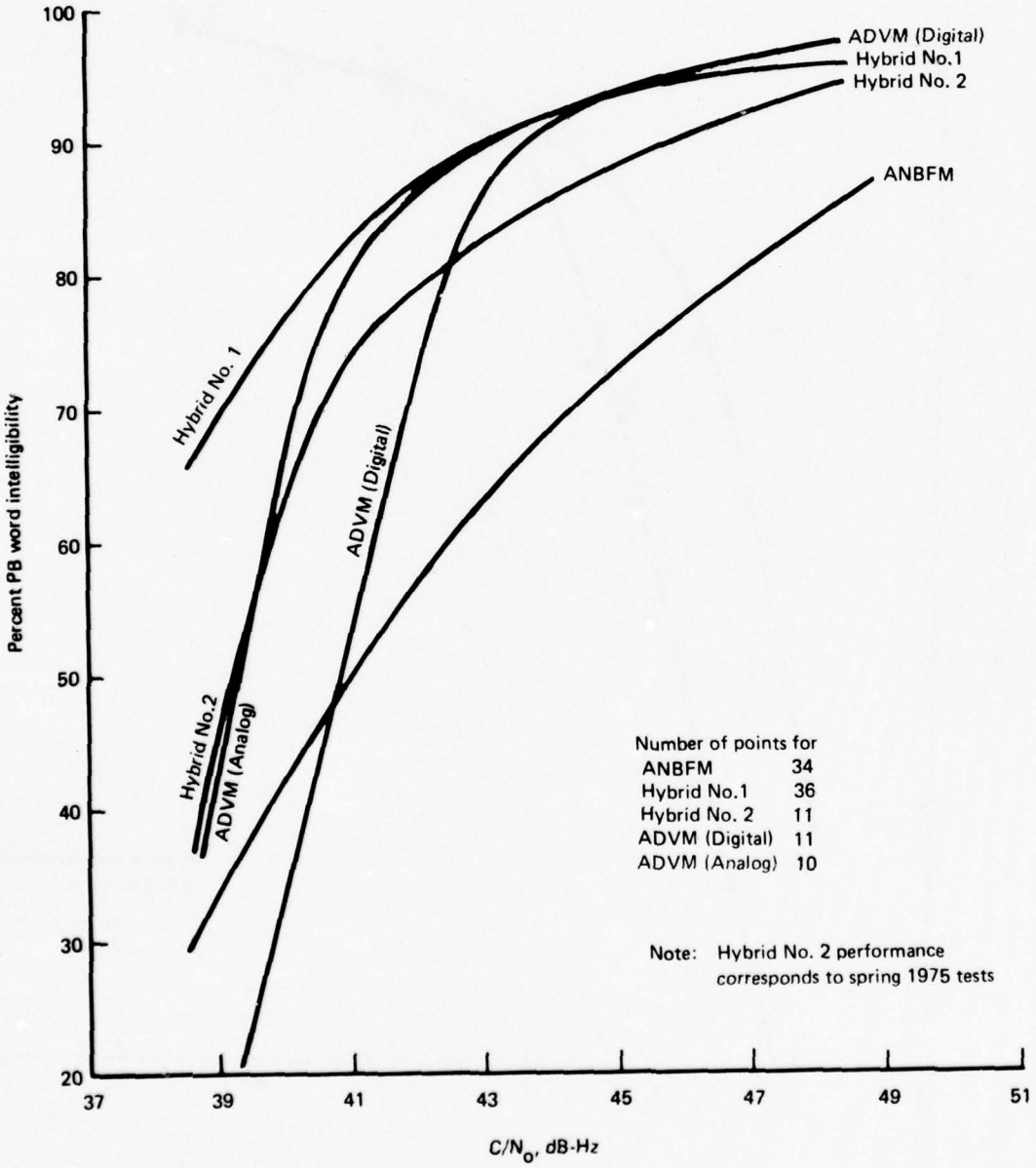

Figure 4-8. Summary Comparison of Voice Modem Performance, Type I Tests

It is observed that at low C/N_0 values, e.g., 40 to 43 dB-Hz, the Hybrid No. 1 modem performs consistently best, followed by ADVM (analog), Hybrid No. 2, and ANBFM. The latter three exhibit a rather dramatic decrease in intelligibility with decreasing C/N_0 whereas the Hybrid No. 1 modem degradation is "softer." This relative ranking is preserved at higher signal-to-noise ratios (up to 49 dB-Hz) except that ADVM seems to outperform Hybrid No. 1 slightly at these higher C/N_0 values. This might be expected since the Hybrid No. 1 modem has residual intermodulation distortion due to slight nonlinearities in modulation and demodulation, independent of C/N_0, which limits the achievable intelligibility. On the other hand, the delta modulation technique is limited primarily by the quantizing distortion at high C/N_0 where the channel error rate may be ignored. Studies have shown that 19.2-kbps adaptive delta modulation can provide extremely intelligible speech (96% on modified rhyme tests; see ref. 4-1), so the ADVM technique could be expected to have superior performance for high C/N_0. In any case the relative difference, if any, between these two methods at high C/N_0 is small relative to the sampling uncertainty, and both provide high-quality speech in this range.

An observation not apparent in the plots of PB word score is the relative intelligibility of male and female speakers. CBS results are segregated to show scores for both sexes, and it is readily apparent from a cursory look at the results that male speakers were more easily understood. Relative scores were a few percent better on the average at high C/N_0 values and typically 6% to 10% better for poorer signal-to-noise ratios.

The above conclusion may be quantitatively assessed by treating the four female and four male list scores for each test as normal random variables with unknown mean and common variance. In testing the hypothesis that the male-speaker mean is greater than the female-speaker mean, the one-sided t-test is used. The statistic t is computed:

$$t = \frac{\hat{\mu}_1 - \hat{\mu}_2}{S\left(\frac{1}{n_1} + \frac{1}{n_2}\right)^{1/2}} = \frac{\hat{\mu}_1 - \hat{\mu}_2}{S\left(\frac{1}{4} + \frac{1}{4}\right)^{1/2}},$$

where:

μ_1 = population means
n_1 = population sizes
S^2 = pooled variance.

Comparing t to a critical value t_{crit} gives a decision to accept or reject the hypothesis. In so doing, we have found that of 248 tests scored, the t-statistic exceeded the 0.05 significance value 146 times. Thus there is very strong evidence for concluding that the male speakers had a larger average intelligi-

bility. It should be said this holds for a sample of two females and two males, and care should be taken in generalizing to larger populations.

The most plausible explanation for this result is the audio band-limiting included in each modem. Typically, the cutoff frequency was 3000 to 3500 Hz. Since it is well known that the high-frequency spectrum of a female ensemble is greater than that of males, and since intelligibility is strongly influenced by high-frequency masking, female speakers could be expected to be less intelligibile relative to male speakers.

No strong relationship was found to indicate that the higher intelligibility for male speakers was modem dependent; i.e., the relative performance seemed to hold for all four modems tested.

4.5 TYPE II TEST RESULTS, VOICE-ONLY MODE

Type II voice tests were conducted during the October and November 1974 and January and March/April 1975 test series. Intelligibility scoring has been completed for all tests – a total of 13 20-min runs (39 evaluations). Since the ADVM entered testing in February, only a few data were collected in the Type II mode; these have been plotted with the Type I results in figure 4-7 and so noted.

Test setup, conduct, and data reduction procedure is exactly as for Type I tests, except that a higher level of scattered signal is injected into the receiver. The measured S/I (direct-to-indirect power ratio) ranged from 3 to about 15 dB, while C/N_0 was varied over the 40-50 dB-Hz range.

Figures 4-9 through 4-12 compile the mean PB word scores achieved by each of the modems versus C/N_0, with the number associated with each point denoting the measured S/I to the nearest decibel. The Type II scores agree well, both in absolute and relative performance, with the Type I scores for all values of S/I. Certainly no statistically significant effect of S/I is detectable for any of the modems. To emphasize the relatively large insensitivity to multipath level, the best-fit Type I performance curves for each modem are overlaid on figures 4-9 through 4-12.

Thus, whereas the performance of digital data and ranging systems can be dramatically reduced by relative multipath levels of say -6 dB, it is observed that the intelligibility of analog voice techniques is not visibly degraded for S/I as low as 3 dB. Intuitive explanations are now offered for this phenomenon.

First, recall that the L-band multipath channel is known to have a Doppler spectrum width on the order of 100 Hz, two-sided, at low angles where multipath levels are typically highest. Also, measured delay spreads imply that the channel may be modeled as "frequency flat" for the typical voice

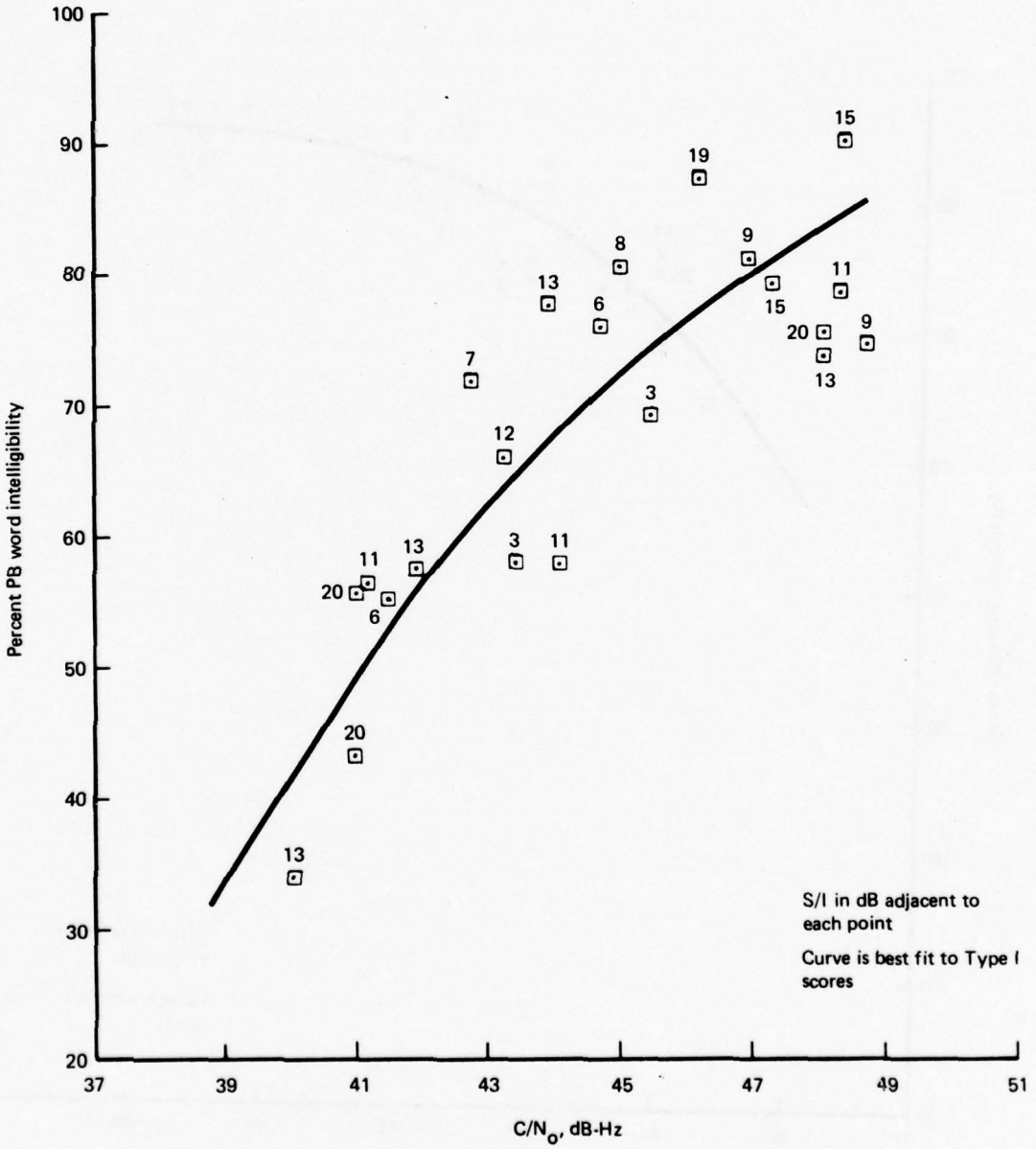

Figure 4-9. ANBFM Voice Modem, Type II Tests, All Series

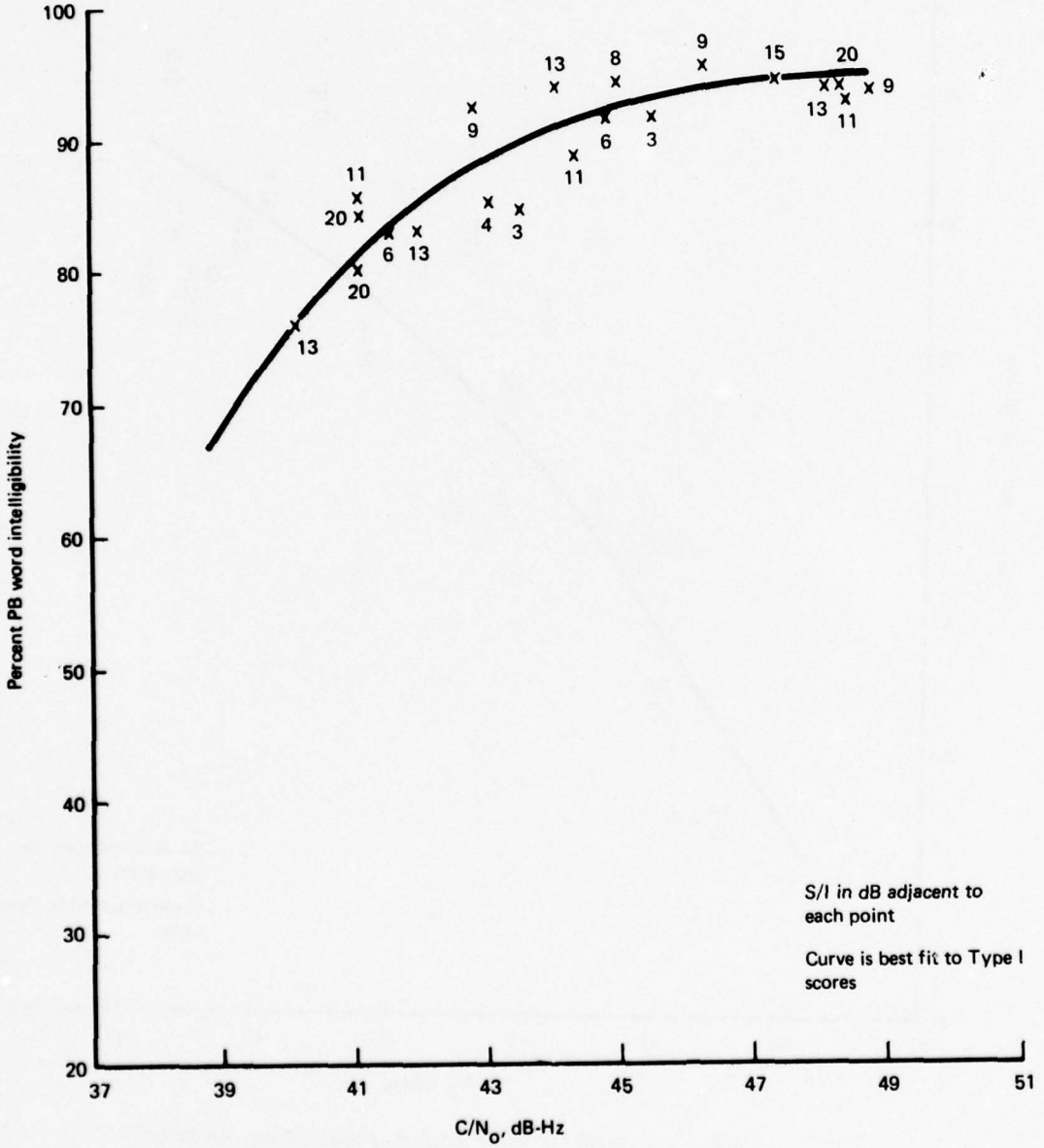

Figure 4-10. Hybrid No. 1 Voice Modem, Type II Tests, All Series

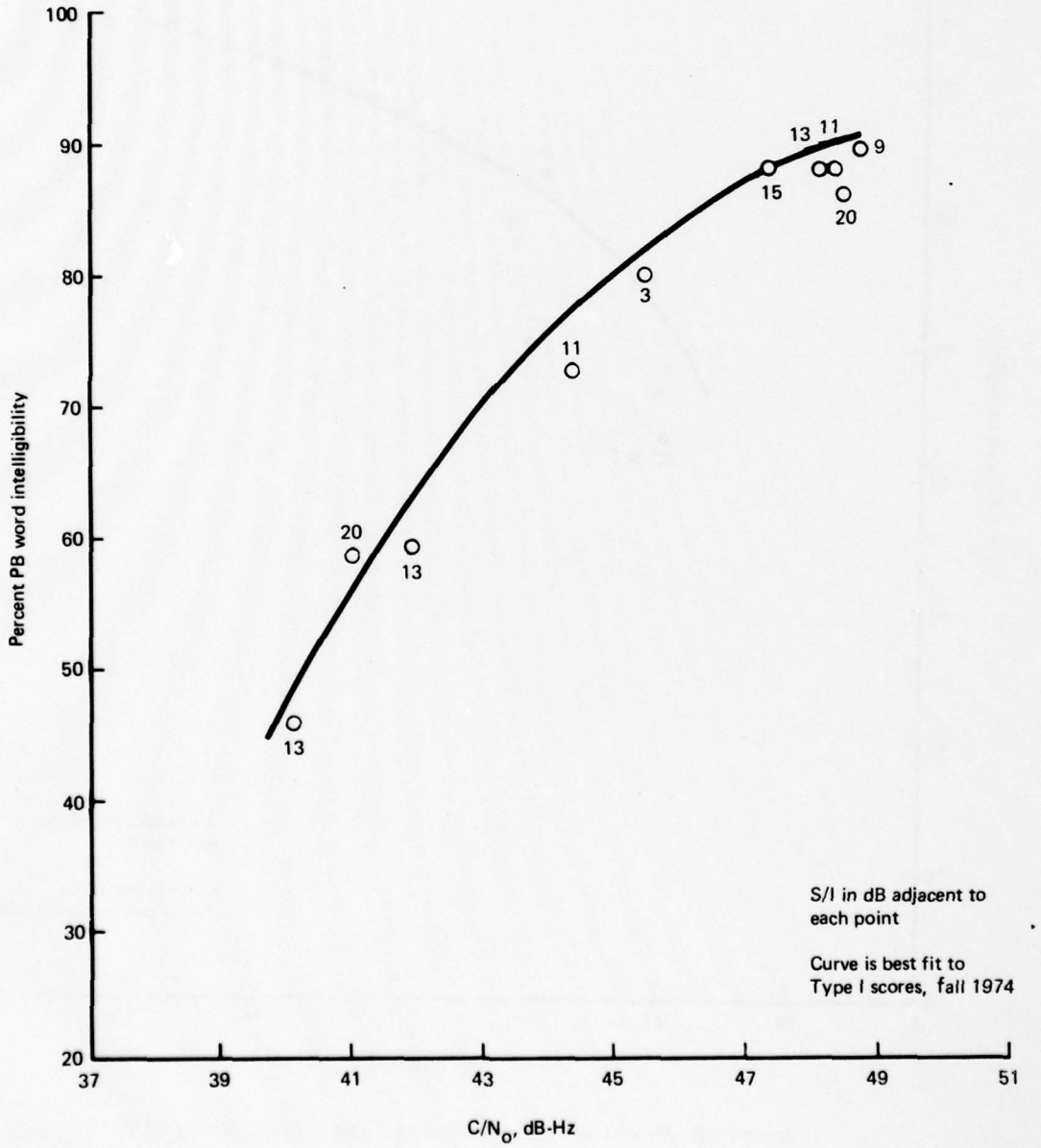

Figure 4-11. Hybrid No. 2 Voice Modem, Type II Results, Fall 1974

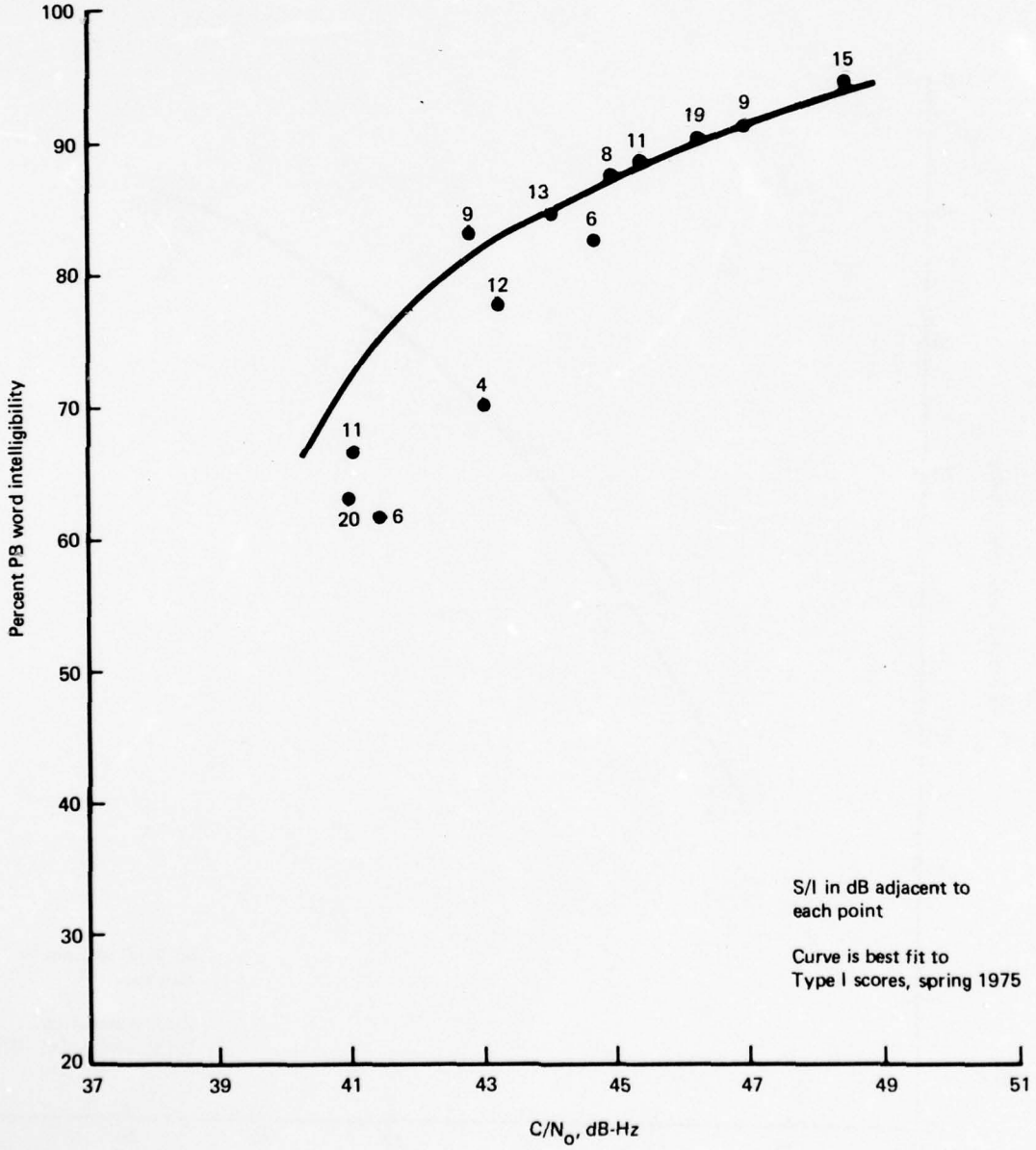

Figure 4-12. Hybrid No. 2 Voice Modem, Type II Tests, Spring 1975

channel bandwidths of 10 to 20 kHz. Thus, when excited with an unmodulated L-band carrier, the received signal in the absence of noise is

$$r(t) = \sqrt{2C}\cos\omega_c t + m_c(t)\cos\omega_c t + m_s(t)\sin\omega_c t$$

where m_c and m_s are independent Gaussian low-pass modulations, each of bandwidth roughly 50 Hz and variance I, with I being the total multipath power.

Although the signal processing pertinent to each modem needs to be examined in an exhaustive treatment, the necessary insight may be gained by considering the NBFM case, with a phase-lock demodulator preceded by a bandpass limiter. The received signal, including additive noise, is

$$r(t)_{NBFM} = \sqrt{2C}\cos[\omega_c t + \phi_m(t)] + m_c(t)\cos[\omega_c t + \phi_m(t)] + m_s(t)\sin[\omega_c t + \phi_m(t)] + n_c(t)\cos[\omega_c t + \phi_m(t)] + n_s(t)\sin[\omega_c t + \phi_m(t)] .$$

Here $\phi_m(t)$ is the angle modulation corresponding to preemphasized FM, and we have placed ourselves in a coordinate reference whose rotational phase is $\omega_{ct} + \phi_m(t)$. Thus the signal may be represented in terms of the vector diagram of figure 4-13.

The limiter removes envelope fluctuation and the phase-lock loop attempts to track the composite signal phase of those signals within the loop bandwidth. For $\sqrt{2C}$ stochastically large relative to multipath and noise, the estimated phase angle is approximately

$$\phi = \tan^{-1}\left\{\frac{m_s + n_s'}{\sqrt{2C} + m_c + n_c'}\right\}$$

$$\simeq \frac{m_s + n_s'}{\sqrt{2C}} ,$$

where the primes indicate the additive noise has been reduced by action of the PLL.

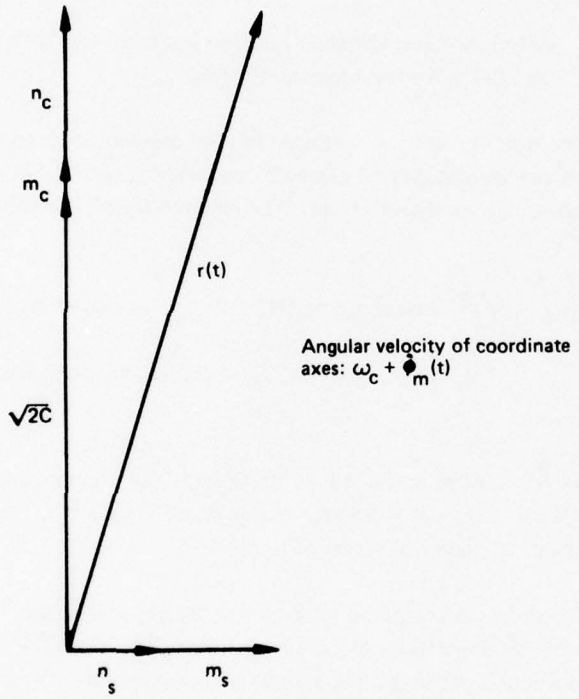

Figure 4-13. Phasor Diagram – Signal, Noise, and Multipath

Thus in addition to the usual noise contribution to phase error, we now have the multipath component appearing linearly. It is noted, however, that the spectral extent of this additional noise source is roughly 0 to 50 Hz. Audio postdemodulation filtering typically removes the near dc response; even if this explicit filtering is absent, the response of the ear is low in this region and no signals necessary for intelligibility are masked.

This argument is an above-threshold treatment. As the threshold is approached, the linear analysis breaks down, but it is clear that the spectral extent of demodulated multipath noise is still roughly the same. The addition of multipath will induce an earlier loop thresholding due to signal fading and concomitant increase in so-called click noise.

The second protection against multipath effects for analog speech is one of psychoacoustics. Namely, due to the natural waveform redundancy, portions of phonemes may be entirely masked by noise of various types and the intelligibility is still preserved. Viewed in another way, the multipath may induce audio fading that effectively eliminates audio for a time equal to the fade duration. For a fading bandwidth of 50 Hz, it could be crudely assumed that the average frequency of interruption was 50 times per second. Miller and Licklider (ref. 4-2) found that speech could be randomly interrupted in this manner up to 50% of the time while still maintaining 90% intelligibility. At lesser fading rates, as expected, the speech on-time must be larger to achieve the same score, since whole phonemes then begin to be obliterated. On the other hand, interruptions of more than 3000 times per second on the average do not affect intelligibility at all.

These two plausibility arguments lend support to the finding that S/I as low as 3 dB seems insignificant in the test scores.

4.6 HYBRID MODEM PERFORMANCE IN COMBINED VOICE AND DATA MODE

Figures 4-14 and 4-15 show voice channel performance measured for the Hybrid No. 1 and 2 modems when operated in the hybrid mode, i.e., speech simultaneous with 1200-bps data. (Results for data channel performance in the combined mode are presented in section 5.8.) In this presentation, the Hybrid No. 2 modem results for fall and spring have been plotted together and are identified according to the legend. Again, an improvement for spring tests is observed.

The solid curves show the performance obtained in the voice-only mode for the respective modems, as extracted from figures 4-4, 4-5, and 4-6. It is observed that the presence of data modulation degrades performance at least 3 dB. Since the data and speech carriers are in phase quadrature for each modem, the potential for cochannel crosstalk exists if carrier phase tracking is imperfect. If this factor is ignored, however, a 3-dB degradation can be predicted for Hybrid No. 2 since 50-50 voice/data power sharing is in effect in the hybrid mode. For Hybrid No. 1, the relative difference to

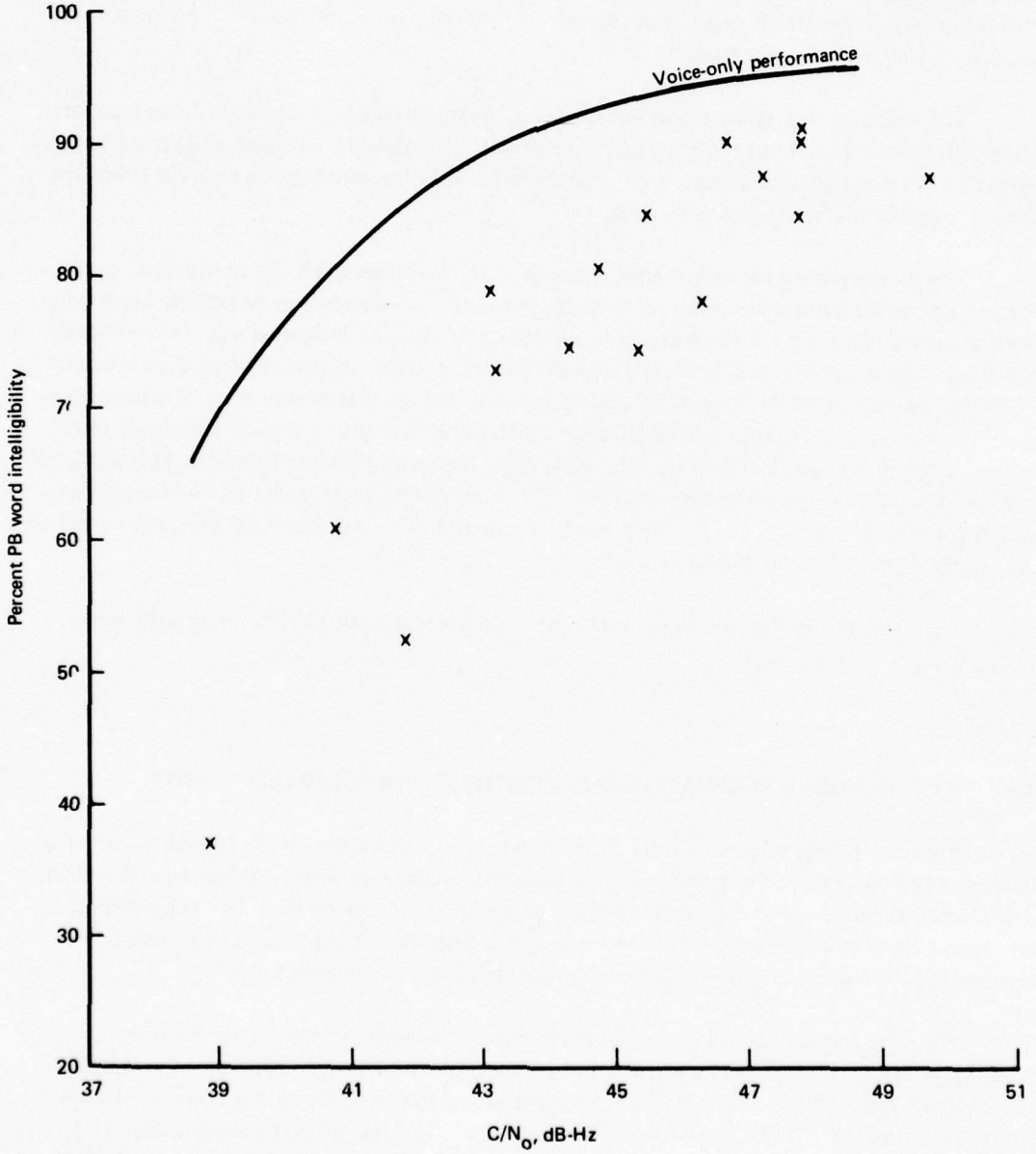

Figure 4-14. Hybrid No. 1 Modem Voice Intelligibility, Hybrid Mode, All Test Series

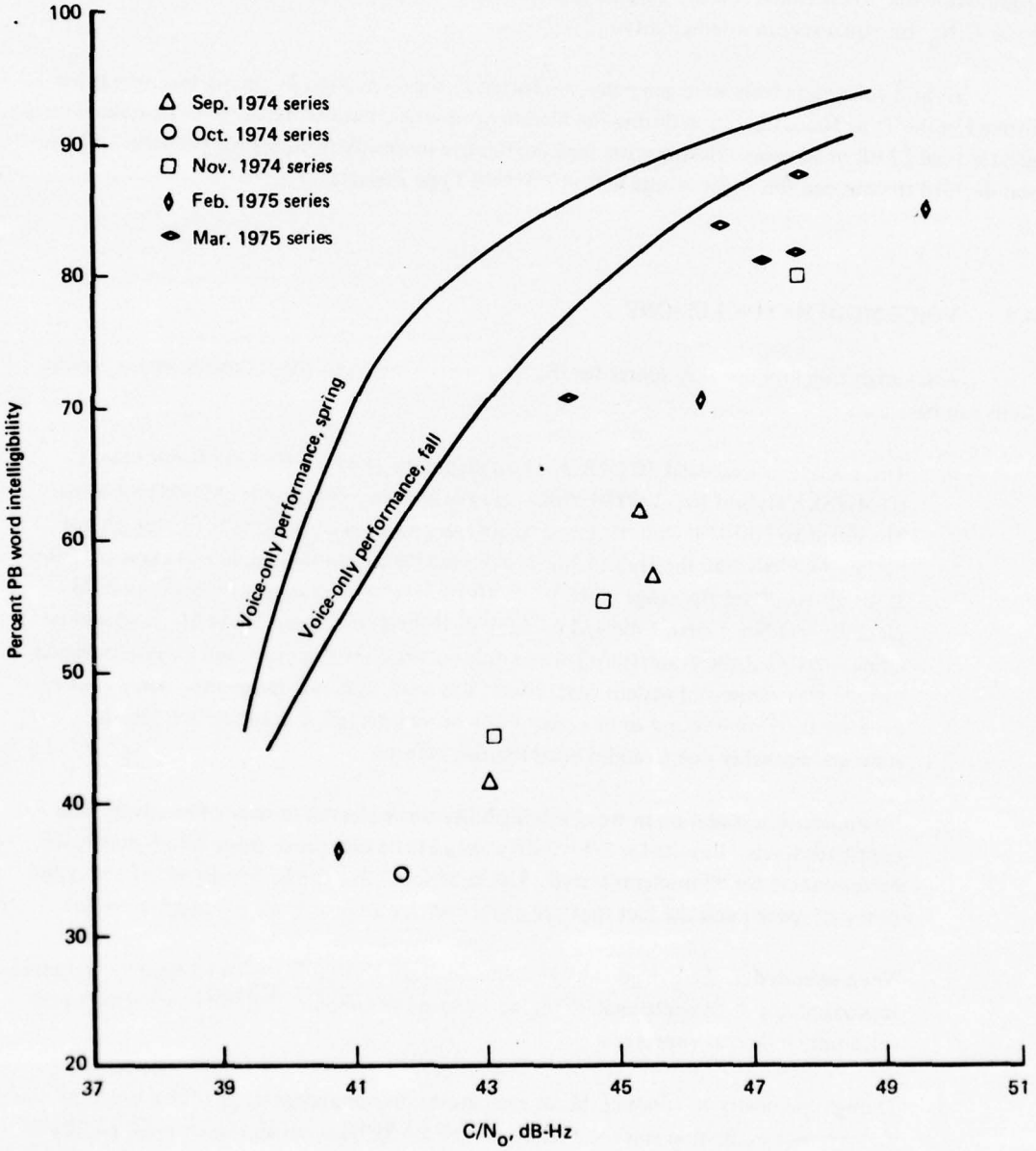

Figure 4-15. Hybrid No. 2 Modem Voice Intelligibility, Hybrid Mode, All Test Series

be expected is less clear. An approximation may be gained by noting the rms phase modulation in voice-only cases is 58^{o}, whereas it is set at about 40^{o} for the voice/data mode. In terms of demodulated speech power, the relative difference is then about 2.4 dB. Since both modems have additional degradation due to crosstalk, it is not surprising to find the hybrid mode requiring at least 3 dB greater *total* C/N_o for equal speech intelligibility.

Hybrid voice/data tests were generally conducted in the Type I mode. Some testing was performed in the Type II configuration during the March/April series, but the measured S/I parameter was greater than 12 dB in all cases. Having witnessed the relative insensitivity to S/I for the voice only, it was decided to combine these test results with the hybrid Type I results.

4.7 VOICE MODEM CONCLUSIONS

After analyzing intelligibility scores for the four speech modems, the following major conclusions can be drawn.

a. Three modems exceeded 70% PB word intelligibility at 43 dB-Hz: the Hybrid No. 1 (Q-M/PSK), Hybrid No. 2 (PDM/PSK), and the adaptive delta voice (ADVM) modems. The adaptive NBFM technique failed to achieve this level of performance, though not by far. One modem, the Hybrid No. 1, achieved PB word intelligibility in excess of 70% at 40 dB-Hz. Over the range of 40 to 48 dB-Hz, a relative ranking of modems would place Hybrid No. 1 first, followed by ADVM, Hybrid No. 2, and ANBFM. It should be emphasized that the evaluations pertain only to word intelligibility and do not explicitly include pleasantness of sound, synchronization time, dynamic range, etc. Also, the two male speakers were found to be consistently more intelligible than the two female speakers, probably due to audio band-limiting effects.

b. No apparent degradation in word intelligibility was observed in spite of relatively high multipath levels. Results for S/I = 3 dB showed little difference from the no-multipath performances for all modems tested. This is believed due to the natural waveform redundancy of speech and the fact that the distortion due to multipath is largely subaudio.

c. When operated in the hybrid voice/data mode, both Hybrid No. 1 and 2 modems required approximately 3 dB additional C/N_o to achieve the same intelligibility registered in the voice-only mode, as expected.

d. Though less costly to conduct, SCIM evaluations do not appear to provide a universal performance evaluation since the relation between SCIM score and word intelligibility is modem dependent. Further discussion and supporting data may be found in appendix A.

5. DIGITAL DATA MODEM TEST RESULTS

This section reports performance results of five PSK data modems, operating at 1200 bps in various aeronautical satellite channel conditions. The modems represented different implementations of differentially encoded, coherently detected phase-shift keying (DECPSK) and differentially coherent phase-shift keying (DPSK). Tests were conducted in the Rosman/ATS-6/KC-135 link configuration. Reception was with representative operational aircraft antennas (Type I tests) at angles ranging from 10^{o} to 30^{o} and with a simulated multipath-contaminated channel (Type II tests) at an elevation angle of 15^{o}.

5.1 DIGITAL DATA MODEMS TESTED

The five modems tested are briefly characterized below.

Hybrid No. 1: This modem implements DECPSK. In the data-only mode, detection is performed using a Costas-type demodulator (B_L = 130 Hz), and baseband matched filtering. Coherent AGC is employed and the narrowest IF filter bandwidth is 30 kHz. The unit can operate in the combined voice/data mode, for which demodulation is accomplished with a narrowband second-order phase-lock loop tracking a residual carrier. Bell Aerospace Company manufactured the modem under contract to DOT/TSC.

Hybrid No. 2: This unit was developed by Magnavox Research Laboratories under DOT/TSC contract. DECPSK is the data modulation and detection strategy. In the data-only mode, the modem uses Costas-loop demodulation ($B_L \simeq 150$ Hz) and baseband matched filtering. Coherent AGC is also utilized and no modem RF bandwidths are less than 50 kHz. This unit may also operate in an hybrid voice/data mode by placing one-half the signal power in a pulse-duration modulation (PDM) speech signal in phase quadrature to the data carrier.

NASA DECPSK: This modem also performs DECPSK transmission with a Costas-type demodulator, whose noise bandwidth is approximately 450 Hz. The predetection filter bandwidth is 15 kHz, and coherent AGC is employed. Operation is data-only at 1200 bps. The unit was developed for NASA by Bell Aerospace Company as part of the PLACE program.

FAA CPSK: The fourth modem performing DECPSK was developed for the DOT/FAA by Philco-Ford Corporation. The modem operates at either 1200 or 2400 bps with a Costas demodulator (B_L = 210 Hz). The signal processing is largely digital, including

the carrier and bit-timing loops and the integrate-and-dump detector. Coherent AGC is used for IF leveling, and band-limiting distortion is negligible. Previous testing has been accomplished under the DOT/FAA ATS-5 experiments, reported in reference 5-1.

FAA DPSK: This unit represents the only tested version of DPSK. Detection requires carrier phase stability only over two-bit intervals. The center frequency is continually estimated with a quadricorrelator automatic frequency-control (AFC) loop, and a signal-controlled AGC circuit is employed. Philco-Ford developed the modem for the FAA ATS-5 experiments. The unit uses largely digital signal processing.

All of the modems are devoid of nonlinear processing effects such as hard-limiting at IF. Intersymbol interference due to band-limiting may be ignored in all cases for the 1200-bps data rates tested here.

5.2 *DIGITAL DATA TEST SIGNAL DESCRIPTION*

5.2.1 PN Test Sequence

For all modems and test conditions, a maximum-length 2047-bit sequence was used as the test pattern. This provided a signal having adequate randomness properties, and was easy to replicate and synchronize in a general-purpose computer for error analyses. Also, the Hybrid No. 1 and 2 modems had internal error checkers using this sequence for quick-look evaluation. The code generator polynomial used was $X^{11} + X^2 + 1$ with arithmetic defined as usual on the binary field.

During hybrid mode tests (voice and data simultaneous), the same test sequence was used, and PB word list tapes were input to the respective modulator audio inputs.

5.2.2 RF Link Transmission Formats

Since all modems operate on versions of PSK signaling, a single data signal was sufficient for transmission from Rosman. The uncertainty arising from power balance of several PSK carriers was thus eliminated and intermodulation effects were minimized. During data-only tests, two additional cw carriers were FDM multiplexed into the transmitted signal. One, the PLACE S&R carrier, was necessary to lock up the NASA modem. The second carrier was placed 12.5 kHz removed from the data carrier and was used for analysis of the channel C/N_0 and S/I at a frequency very close to that of interest. This probing signal was also down-translated and recorded for possible future analyses. Also,

an NBFM carrier was included for coordination purposes, though normally the signal was unmodulated. The frequency assignments referenced to the satellite L-band output were:

1550.0750 MHz	PLACE S&R carrier
1550.2500 MHz	NBFM coordination channel
1550.6750 MHz	PSK data signal, 1200 bps
1550.6875 MHz	CW probing signal.

During the hybrid voice/data tests, signal commonality was no longer present since the Hybrid No. 1 and 2 modems have distinct modulations. The NASA and FAA modems were not tested during these periods, and the composite transmitted signal was

1550.0750 MHz	CW carrier
1550.2500 MHz	Hybrid No. 1 modem signal
1550.6000 MHz	Hybrid No. 2 modem signal
1550.6750 MHz	PSK data signal (not used by DOT/TSC aeronautical tests).

Both frequency plans were chosen to ensure that low-order intermodulation products are out-of-band. Any in-band products occur at a negligibly small level.

5.2.3 Channel Power Equalization

Channel signal-to-noise ratio measurements for the data test were made by analyzing the cw probe signal under the assumption that this value also applies for the other carriers in the composite spectrum. Such an assumption obviously implies careful power equalization among channels. This equalization was accomplished by continuous monitoring at Rosman of the forward-link L-band test signal radiated by the satellite.

Spectrum analyses permitted detection of power imbalance as small as 0.2 dB. Appropriate uplink level adjustments were then made on a closed-loop basis.

5.3 REDUCTION AND ANALYSIS OF DIGITAL DATA

This section highlights the reduction and analysis features associated with the digital data tests. More detail may be found in volume IV of this report.

5.3.1 Conversion to Digital Tape

Detected bit patterns as received on the KC-135 are recorded on an instrumentation recorder using direct analog recording at 3-3/4- or 7-1/2-ips drive speed. Five separate analog tracks convey the five modem outputs. Each track is recorded in Manchester format. Also, time code and the output of the envelope detector are FM recorded on separate tracks.

Source tapes are translated into computer-compatible seven-track tape at Boeing's Test Data Processing Center. Five independent bit synchronizers acquire and track the five analog Manchester data tracks. Data is packed in records containing 2460 bits from each of five channels, with each record containing a time code and identification header.

In addition to data stream records, a record of 1025 samples of the envelope detector output is written every 15 sec (real time). This signal is sampled at a 2000-Hz rate and the quantizing is to 10-bit accuracy. This batch of envelope samples is subjected to computer analysis to determine C/N_O and S/I.

5.3.2 Bit-Error-Rate Determination

Bit-error events are located with bit-by-bit comparison of the received data stream with a computer-generated replica. Generation of the local replica requires synchronization of the replica with the received data. This is done in a trial-and-check fashion until the detected error rate is below a 10% threshold. Once synchronization is initially established, subsequent records are processed synchronously unless the error-rate threshold is exceeded, in which case resynchronization is performed.

For each modem track, the error locations are accumulated within a record since there is sufficient information for error analyses. As records are processed, the total number of bits and total number of errors are totaled. This yields average error probability at the end of a time segment, typically several minutes in duration.

5.3.3 Error Spacing Analysis

Aside from average error rate over the time segment, information is tabulated on error spacings and the tendency for error bunching. Histograms of the spacing between errors (intererror spacings) and of the number of occurrences of zero, one, two, etc. errors per 24-bit block are constructed and updated at the end of each record. Separate histograms are maintained for each of the five modems.

5.3.4 C/N_0 and S/I Calculation

Using the samples of the envelope detector output, C/N_0 and S/I estimates are obtained at 15-sec intervals throughout the time segment of interest. Presuming these parameters to be constant unless contrary evidence exists, final estimates are taken as the segment average of the individual parameter estimates.

The method for obtaining these estimates is described in detail in volume IV, section 7. Briefly stated, a smoothed spectral estimate of the detector output is generated with the discrete Fourier transform. Certain characteristics of this spectrum (noise floor and power in the 0- to 250-Hz region) are used to estimate C/N_0 and S/I based on theoretical relationships generated from the detector model and from modeling of the received composite signal. The validity of this approach has been checked in the additive-noise environment by laboratory evaluations. The accuracy of reported quantities obtained in this manner is estimated to be ± 0.5 dB for C/N_0 and ± 1 dB for S/I.

5.4 BASELINE LABORATORY BER MEASUREMENTS

Prior to commencement of the flight test program, the bit-error probability of each modem was measured in the laboratory as a function of C/N_0 at 1200 bps. These measurements were conducted to gain operating insight and to establish a baseline performance for each.

The input to each demodulator was a PSK signal, set to the modem's required input level plus variable-level additive white noise. C/N_0 was measured repeatedly with a calibrated narrowband wave analyzer.

Figures 5-1 through 5-4 compile the test data for the various DECPSK modems. DPSK performance was measured at only two points and is not graphed. Relative to the appropriate theoretical performance, the modems exhibited the following inefficiencies at $P_e = 10^{-4}$.

Hybrid No. 1	1.2 dB
Hybrid No. 2	1.5 dB
NASA DECPSK	2.6 dB
FAA CPSK (DECPSK mode)	1.5 dB
FAA DPSK	0.8 dB

A similar series of tests conducted on DOT/TSC's laboratory simulator is reported in reference 5-2 and reveals generally similar conclusions.

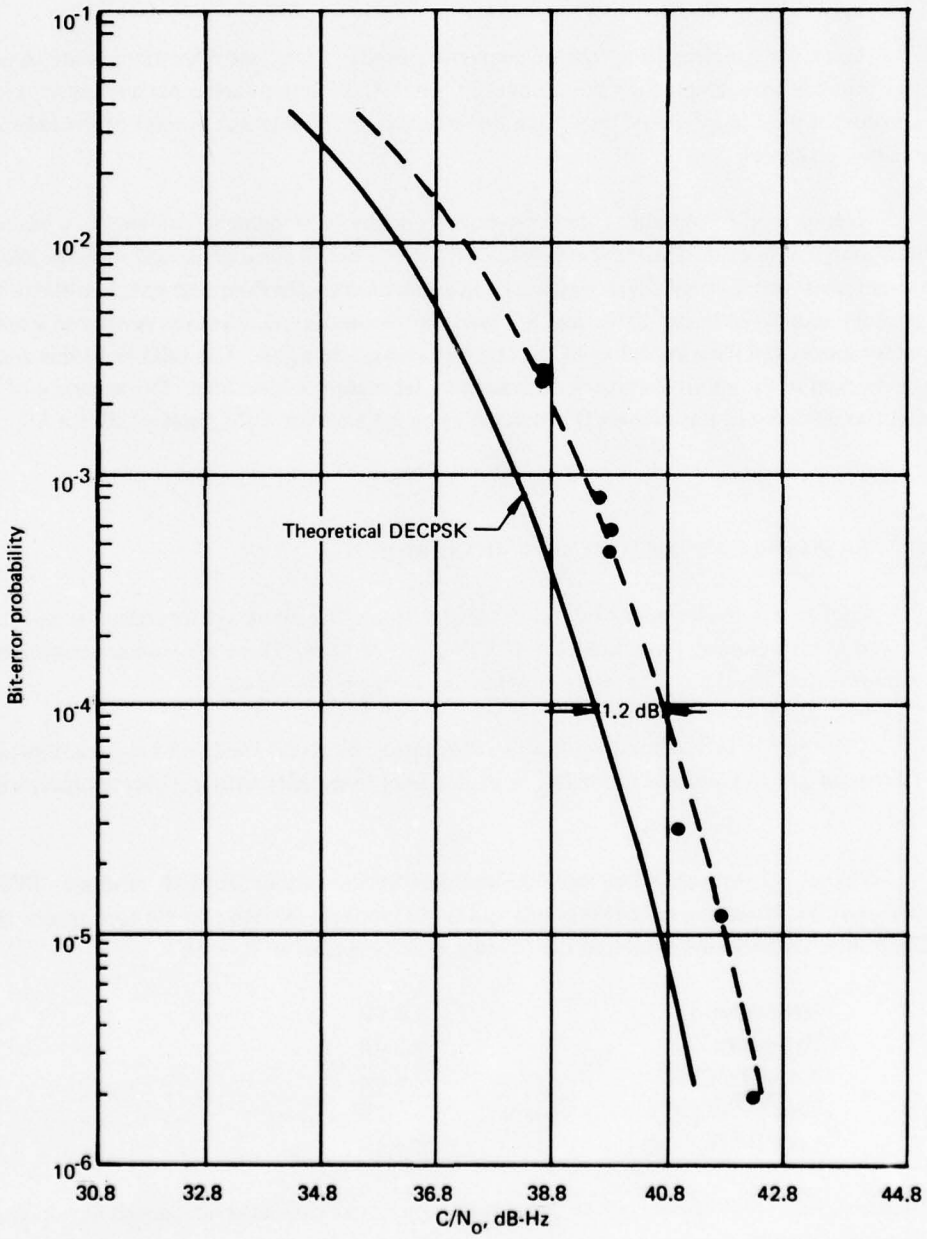

Figure 5-1. Laboratory Baseline Bit-Error-Rate Performance of Hybrid No. 1 DECPSK Demodulator, 1200 bps, August 1974

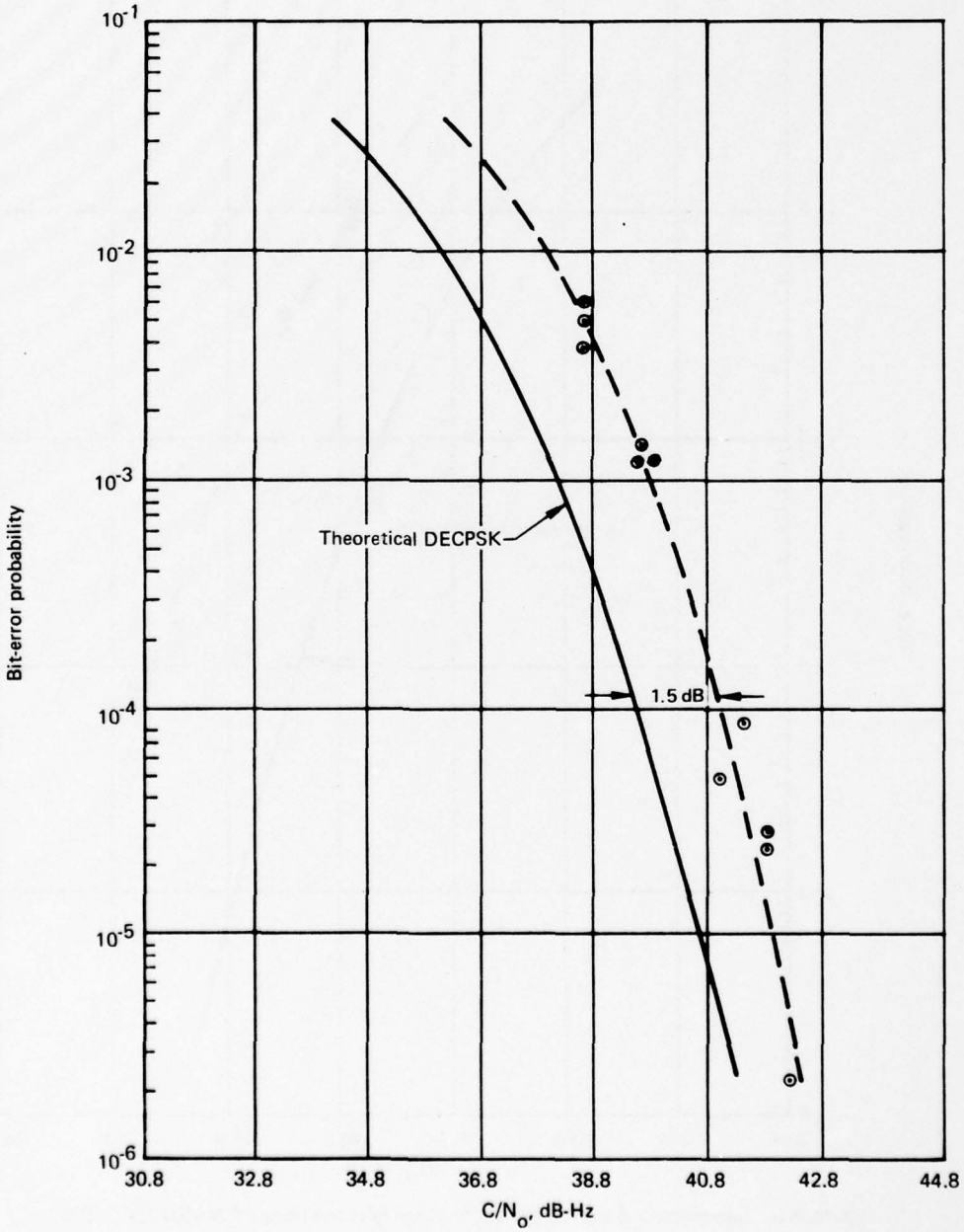

Figure 5-2. Laboratory Baseline Bit-Error-Rate Performance of Hybrid No. 2 DECPSK Demodulator, 1200 bps, August 1974

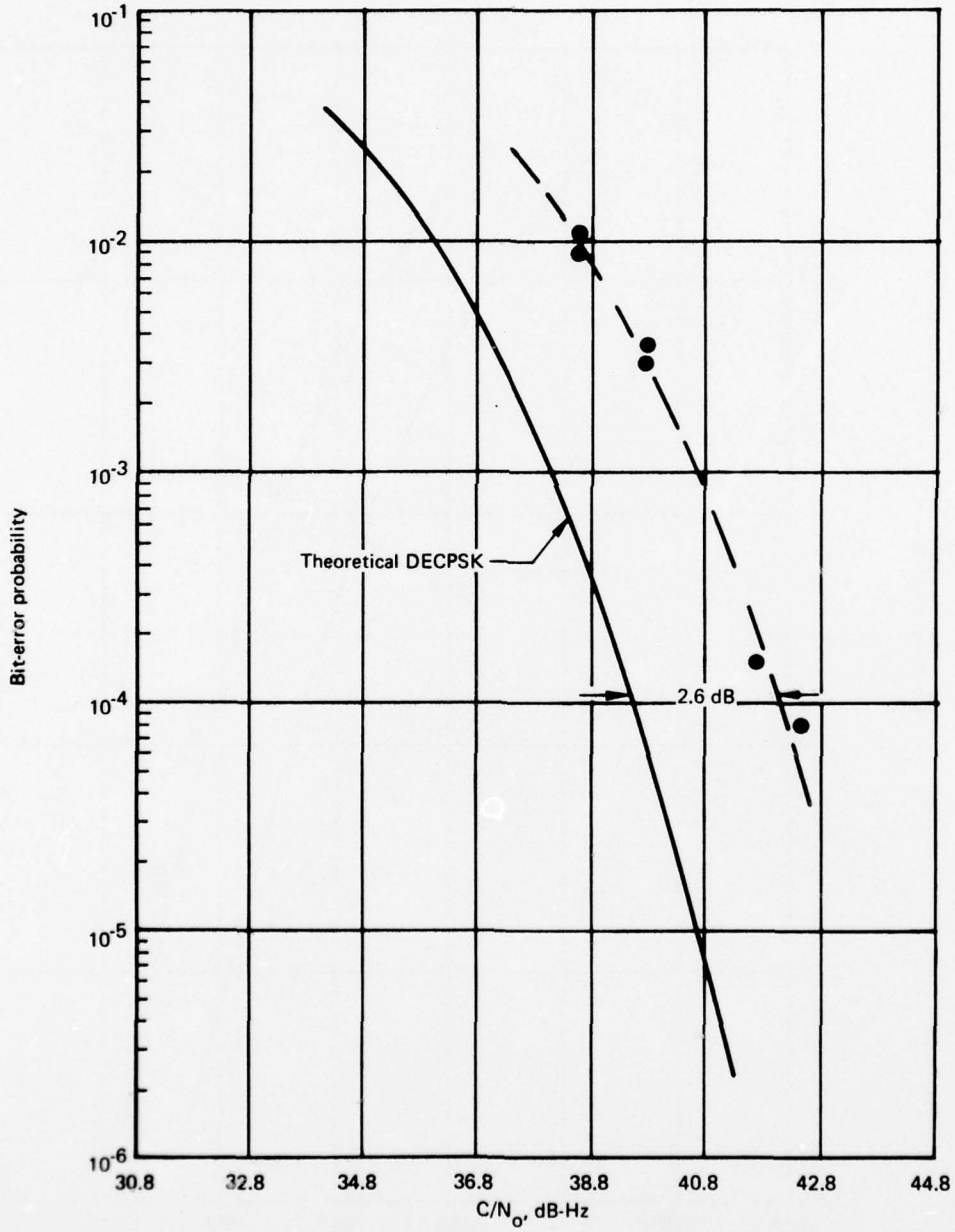

Figure 5-3. Laboratory Baseline Bit-Error-Rate Performance of NASA DECPSK Demodulator, 1200 bps, August 1974

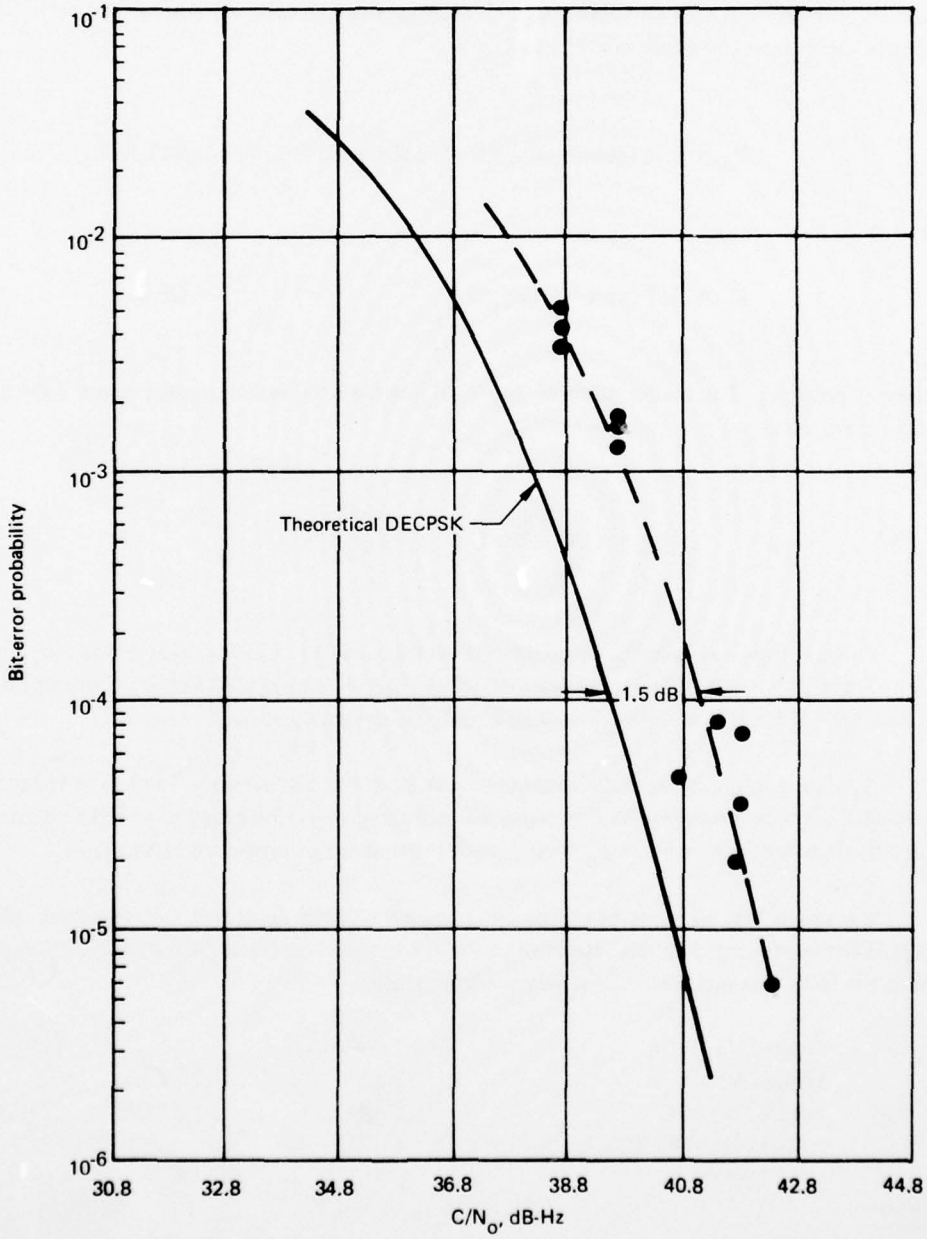

Figure 5-4. Laboratory Baseline Bit-Error-Rate Performance of FAA CPSK Demodulator, (DECPSK Mode), 1200 bps, August 1974

5.5 TYPE I TEST BER PERFORMANCE, DATA-ONLY MODE

Test results for all Type I test series are presented in figures 5-5 through 5-9 for the Hybrid No. 1, Hybrid No. 2, NASA DECPSK, FAA CPSK, and FAA DPSK modems, respectively. The reference theoretical curves are given by

$$P_e = \text{erfc}\,[(CT/N_o)^{1/2}]\,(1 - 1/2\ \text{erfc}\,[(CT/N_o)^{1/2}]) \qquad \text{DECPSK},$$

and

$$P_e = 1/2 \exp\,[-(CT/N_o)] \qquad \text{DPSK}.$$

In these expressions, T is the bit duration and C/N_o is the total signal-to-single-sided noise power density ratio. Also,

$$\text{erfc}\,(x) = [2/(\pi)^{1/2}] \int_x^\infty e^{-Z^2}\,dZ.$$

These theoretical curves are well-known expressions (ref. 5-3) for error probability in the presence of additive white Gaussian noise. Matched filter detection with no synchronization error is also assumed. It is believed the Type I tests closely simulated these conditions.

All data points represent the recording of at least 10 error events, except as noted for some points with very low error probability. Also, some intervals were recorded in which no errors were observed. This data is plotted at $P_e = 10^{-6}$ with the number of processed bits noted.

It is noted that all modems exhibit the exponential dependence on signal-to-noise ratio expected for nonfading channels. Relative to the respective theoretical performance, the modems exhibit the following inefficiencies at an error probability of 10^{-4}:

Hybrid No. 1	0.9 dB
Hybrid No. 2	1.2 dB
NASA DECPSK	1.9 dB
FAA CPSK (DECPSK mode)	1.4 dB
FAA DPSK	1.2 dB[1].

[1] Relative to DPSK theoretical, which is about 0.6 dB less efficient than DECPSK at 10^{-4} error probability.

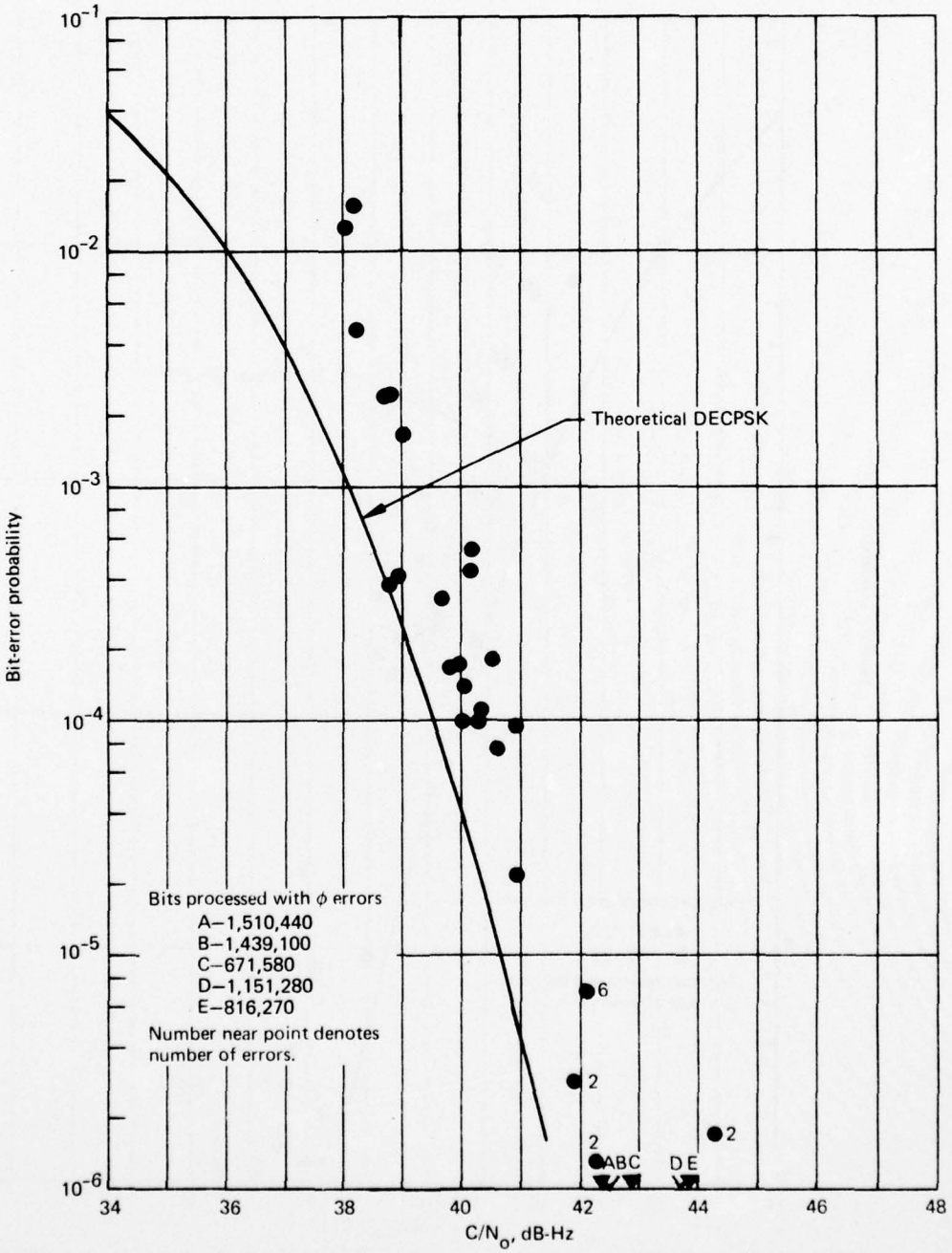

Figure 5-5. Bit-Error-Rate Performance of Hybrid No. 1 DECPSK Demodulator, 1200 bps, Type I Tests

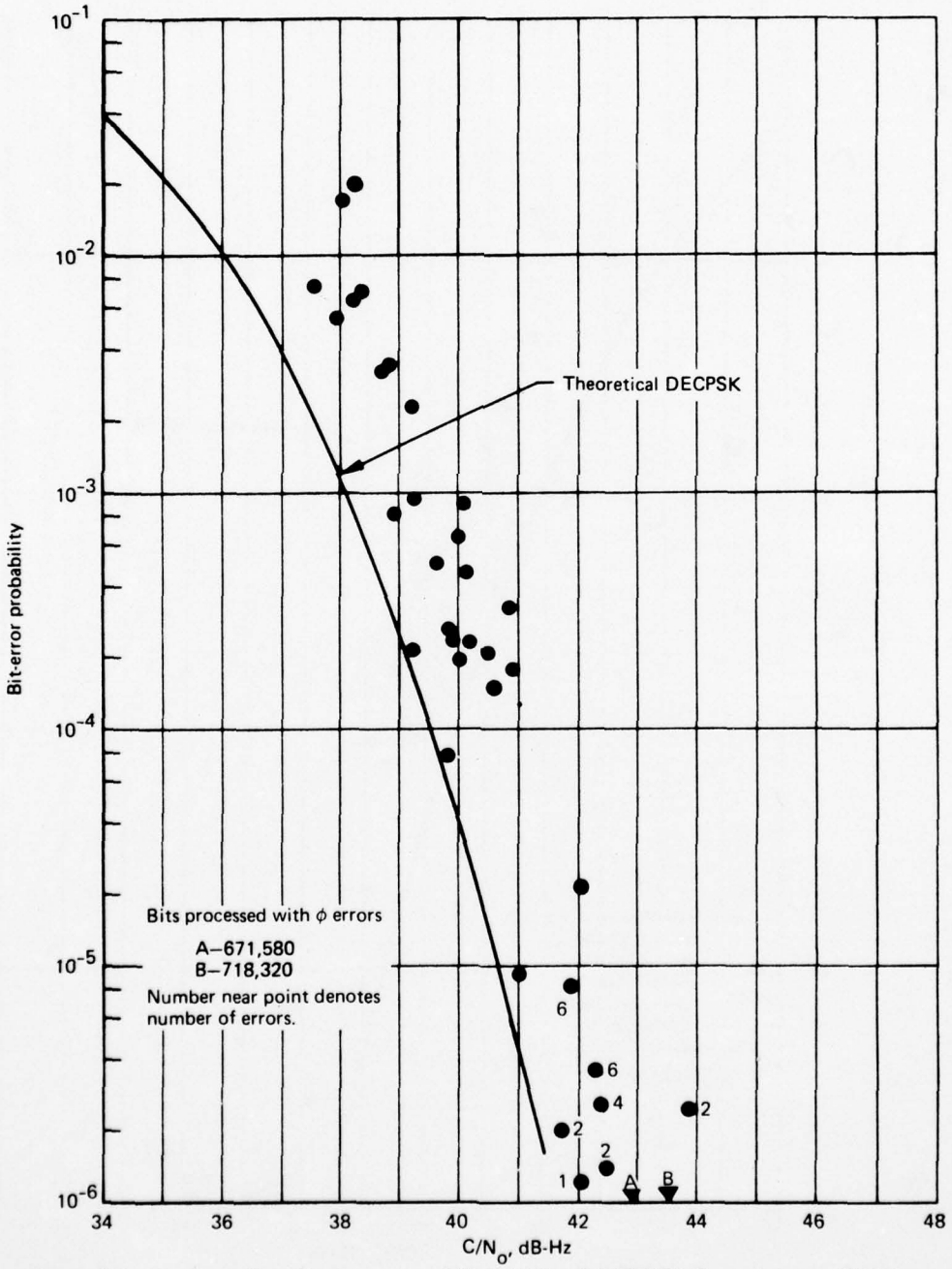

Figure 5-6. Bit-Error-Rate Performance of Hybrid No. 2 DECPSK Demodulator, 1200 bps, Type I Tests

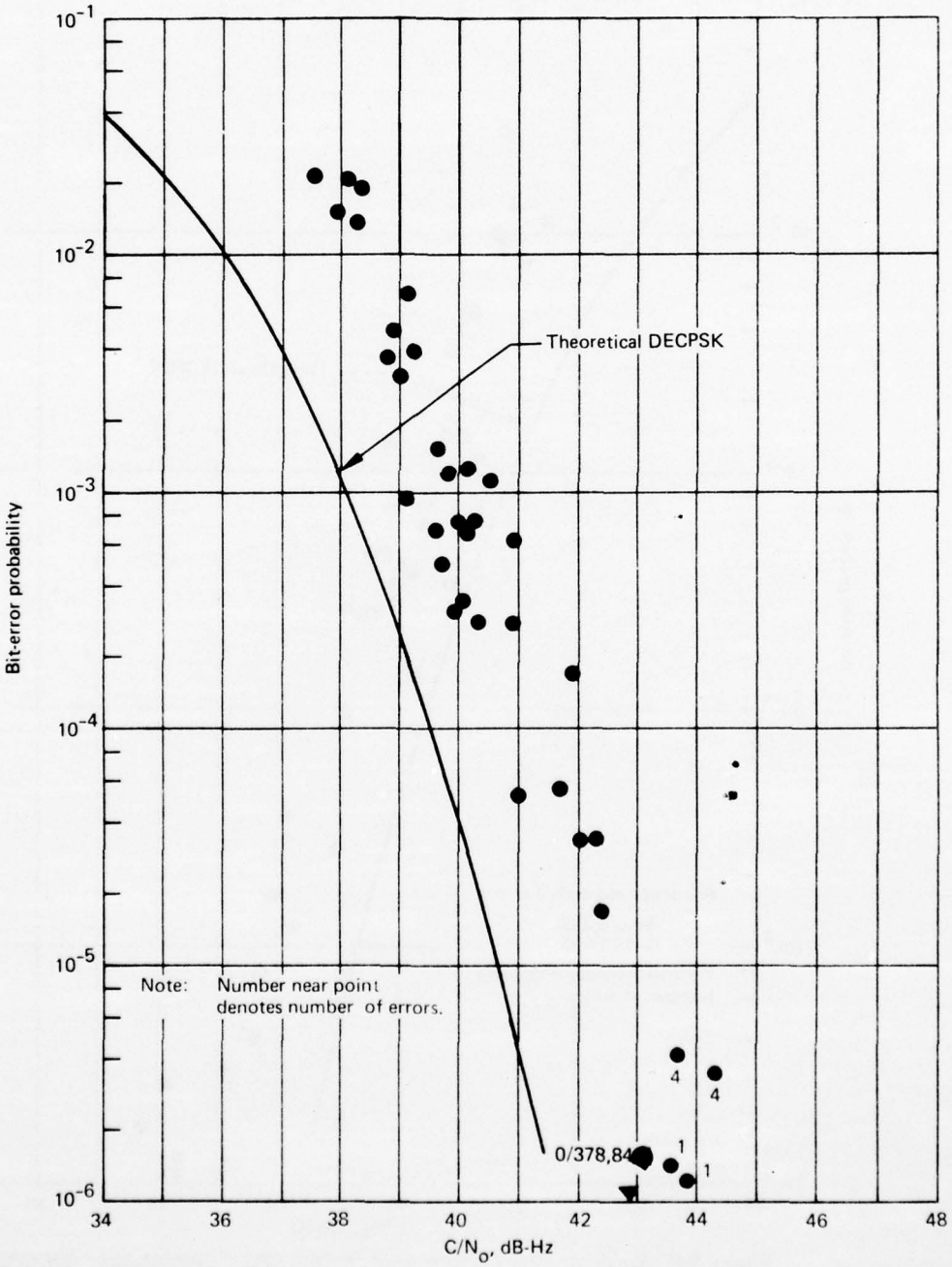

Figure 5-7. Bit-Error-Rate Performance of NASA DECPSK Demodulator, 1200 bps, Type I Tests

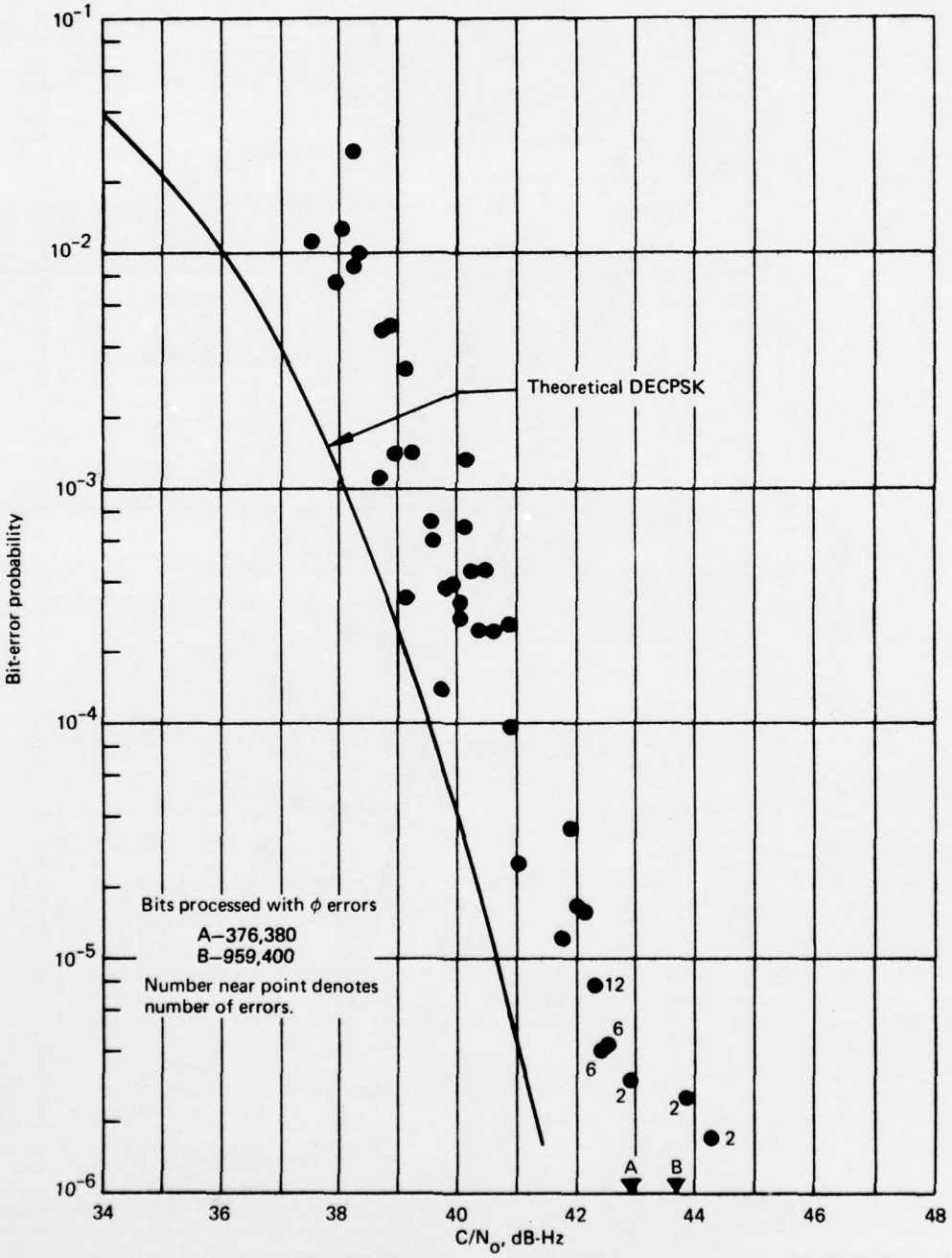

Figure 5-8. Bit-Error-Rate Performance of FAA CPSK Demodulator (DECPSK Mode), 1200 bps, Type I Tests

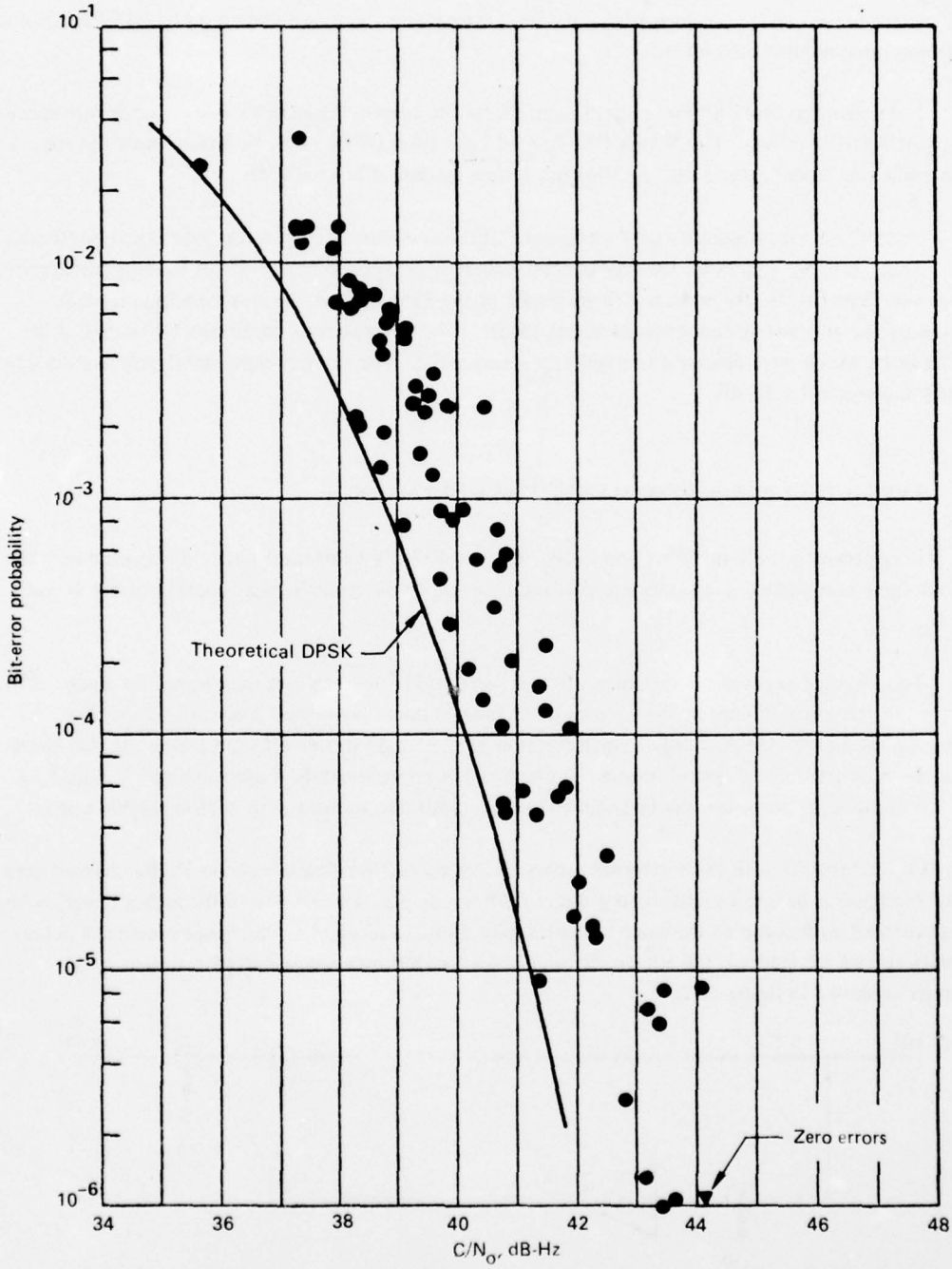

Figure 5-9. Bit-Error-Rate Performance of FAA DPSK Demodulator, 1200 bps, Type I Tests

These inefficiencies can be attributed to implementation losses, such as nonideal matched filtering, and carrier and bit synchronization jitter.

Note also that at 43 dB-Hz, each modem meets the current AEROSAT system error-rate specification of 1×10^{-5} or less. The NASA DECPSK and the FAA DPSK modems barely meet the specification while the others exceed the specification with a margin of at least 1 dB.

Since the error probability performance exhibits no divergence from the theoretical nonfading performance as C/N_o increases, we may conclude there is no appreciable multipath fading phenomenon for the Type I tests. By inference from results of the next section, we may conclude the S/I achieved by the antenna system exceeds about 15 dB. This conclusion is confirmed by results of the antenna tests, which were designed to explicitly measure S/I. The top-left-right slot-dipole system consistently showed $S/I > 15$ dB.

5.6 TYPE II TEST BER PERFORMANCE, DATA-ONLY MODE

In contrast to the setup for Type I tests, a controllable level of multipath was injected into the received signal composite. Thus, modem performance can be determined as a function of S/I as well as C/N_o.

To minimize experiment variables, all tests were conducted at a common elevation angle: 15^o. With the aircraft altitude kept in the vicinity of 31,000 ft, the delay between direct and specular returns was 16.3 μsec, which is only a small fraction of the total bit interval (833 μsec). At this elevation angle, multipath delay spread (minus 10-dB value) is approximately 4 μsec (see vol. V, sec. 5.3). Thus for all practical purposes, the intersymbol interference due to multipath is of negligible impact.

Commensurate with the scattering theory described and verified in volume V, the channel may then be modeled as having an undistorted direct-path signal, plus a signal passed through a linear, time-varying channel with complex Gaussian statistics, plus additive receiver noise. Since multipath delay and delay spread are ignored, the Rician channel is synthesized by a single complex time-varying multiplier as shown in figure 5-10.

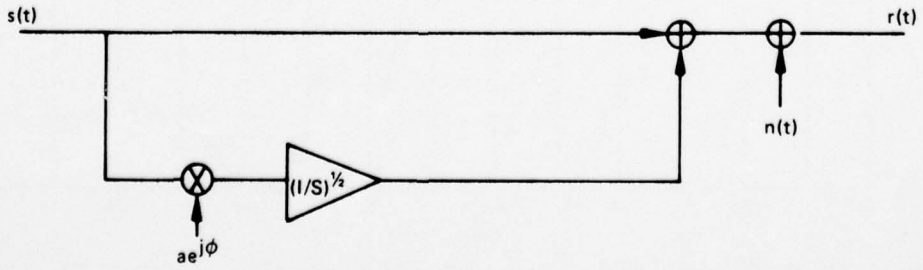

Figure 5-10. Multipath Channel Model

The random amplitude, a, is Rayleigh distributed with unity mean square value, and ϕ is uniform on $[0, 2\pi)$. The remaining variable is the spectral bandwidth of the time-varying complex gain; this bandwidth is typically 50 Hz, one-sided, for L-band carrier frequencies and nominal cruise velocities. Thus, a first approximation to performance is to assume fading is constant over the detection interval and average over the distributions for amplitude and phase to obtain the unconditional (long-term) error probability.

Presentation of the DPSK results utilizes a refinement of the above long-term fading model that accounts for phase decorrelation over two bits (ref. 5-4). This model was well verified in ATS-5 test results for DPSK (ref. 5-1) and is used again here.

The bit-error probability formulation for DECPSK is less concise, since performance now critically depends on the behavior of the coherent reference loop. The simplest treatment, pursued by Lindsey (ref. 5-5), is to assume that the carrier phase tracking loop estimates the composite signal phase perfectly. Thus, the bit-error probability is conditioned only on the phasor amplitude. By again assuming fading is slow over a bit interval, numerical integration can easily provide error probability versus C/N_o and S/I. These results may be found in reference 5-5.

Perfect tracking of the composite channel phase implies a loop bandwidth much greater than the multipath Doppler bandwidth. Increasing B_L subjects the loop to additional noise jitter and eventual threshold phenomena. Thus the existence of a loop bandwidth minimizing P_e is plausible. However, some simulation results (ref. 5-6) indicate that performance is insensitive to B_L until the threshold region is reached, implying frequent errors due to cycle slips. Apparently the additional detection efficiency gained by tracking the composite channel phase is balanced by the likelihood of the composite signal causing fades below the loop threshold.

We note that all DECPSK modem loop bandwidths exceed 130 Hz, so the perfect estimate results should be reasonably valid, ignoring cycle slip events. An intuitive approach presented in reference 5-7 models the detection performance for B_L on the order of the fading process bandwidth. A parameter γ is defined as

$$\gamma = \frac{B_L}{B_F + B_L} ,$$

so $\gamma \simeq 0$ indicates that only the direct-signal phase is estimated, whereas $\gamma \simeq 1$ indicates perfect composite phase is in effect, again ignoring noise effects. If we assume $B_F = 50$ Hz, typical of the 15^o elevation conditions, then

$$\gamma \geq \frac{130}{180} = 0.72 ,$$

for all modems. To present Type II test results, we use curves for $\gamma = 0.75$ in reference 5-7 as a common standard. The performance is not dramatically different from the perfect-estimate case except at very large C/N_0. To account for the error-rate magnification due to differential decoding, the error probability has been scaled by 2 as an approximation.

Figures 5-11 through 5-15 present the measured bit-error rate for each modem for all Type II tests. As for Type I tests, those intervals having less than 10 errors are noted, and intervals having no observed errors are also tagged.

Since S/I was a variable that could be only approximately set during flight conditions and estimated off-line later, the observed S/I values span a continuum from about 2 dB to in excess of 15 dB. To concisely present the data, the results have been grouped into cells of a particular S/I $\pm$1.5 dB. Thus the cell boundaries are 3 dB apart in the S/I variable. The $\pm$1.5 dB is not intended to be the measurement uncertainty associated with each point but merely the grouping uncertainty. As stated earlier, the estimated measurement uncertainty for S/I is 1 dB.

The performance of the Hybrid No. 1, Hybrid No. 2 and FAA CPSK demodulators is not appreciably different for larger C/N_0 values and for all S/I. For those cases where S/I is large and C/N_0 relatively small, the Hybrid No. 1 modem is slightly superior, followed by the Hybrid No. 2 modem and the FAA CPSK. This relative ranking is consistent with the findings of Type I tests, as one would expect, since S/I values usually exceeded 15 dB. The NASA DECPSK modem performed poorer relative to the other three DECPSK modems. This poor performance was especially noticeable at low S/I's, and appeared in the simulator data as well as flight test data. A plausible explanation is that the NASA modem's $B_L = 430$ Hz, (ref. 5-8) implying poorer threshold performance in noise, and this is accentuated by heavy fading.

It is also observed that BER performance is slightly poorer than predicted by the $\gamma = 0.75$ theory. Though the disagreement in terms of effective S/I is roughly 2 to 3 dB at lower S/I for the three best DECPSK modems (figs. 5-11, 5-12, and 5-14), this corresponds to a factor of only 2 to 3 in error probability for these cases. Agreement with theory at higher S/I is within the experimental uncertainty. We note that factors acting to make performance poorer than the theoretical curves are the implementation losses for each modem in the nonfading environment and the cycle-slipping phenomenon that is unmodeled by the reference curves. Empirical observations showed this was indeed significant for heavy-fading cases.

DPSK results (fig. 5-15) are in excellent agreement with the slow-fading model predictions (refs. 5-1, 5-4, and 5-9).[2] Note that the parameter values for S/I have been changed for the DPSK reference curves.

---

[2]The parameter ρ in figure 5-15 is a measure of channel gain correlation over a bit period and is given by the expression $(1-\rho) \approx \pi^2 B_F^2 T^2$. Additional details are available in the references.

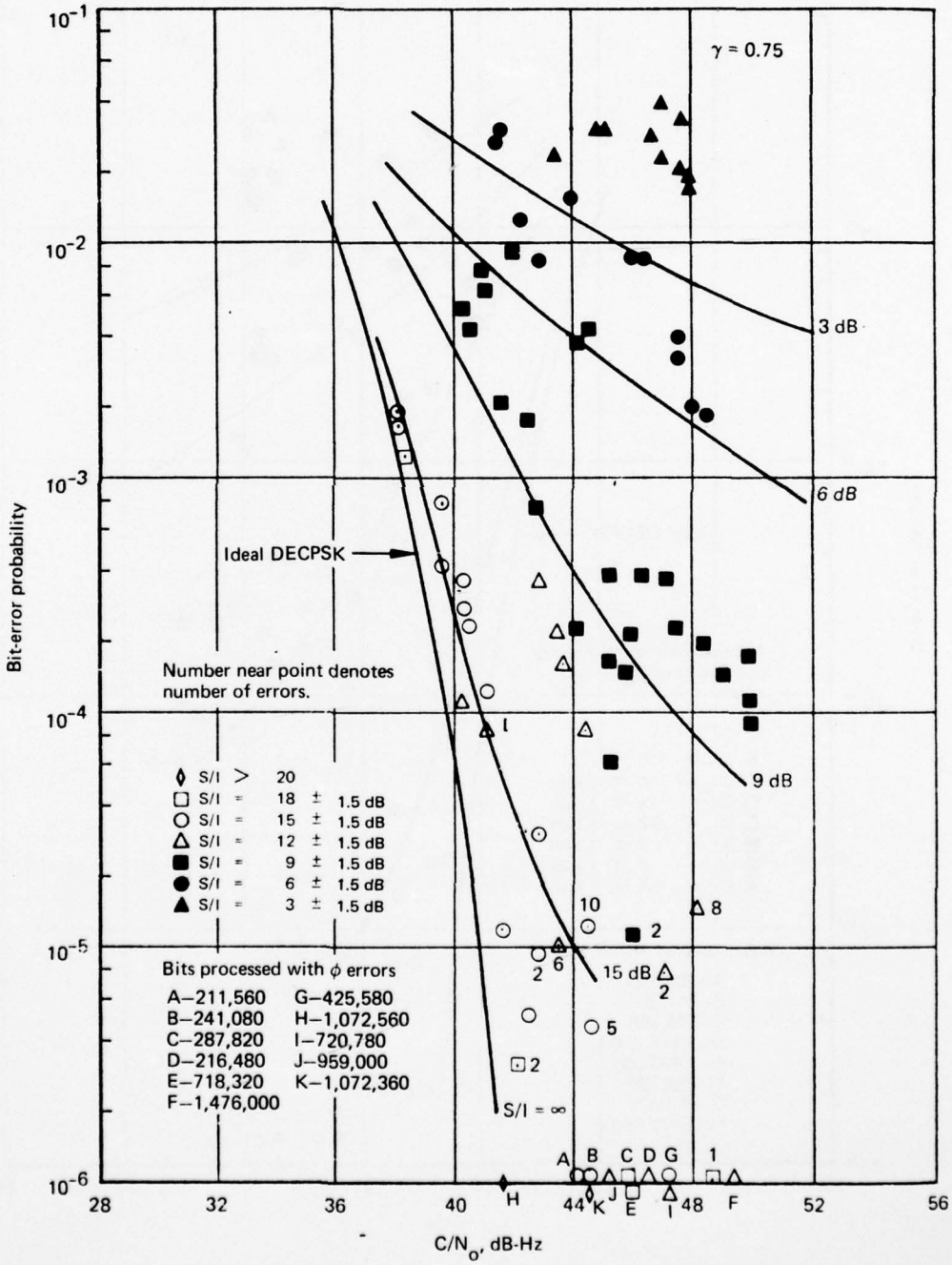

Figure 5-11. Bit-Error-Rate Performance of Hybrid No. 1 DECPSK Demodulator, 1200 bps, Type II Tests

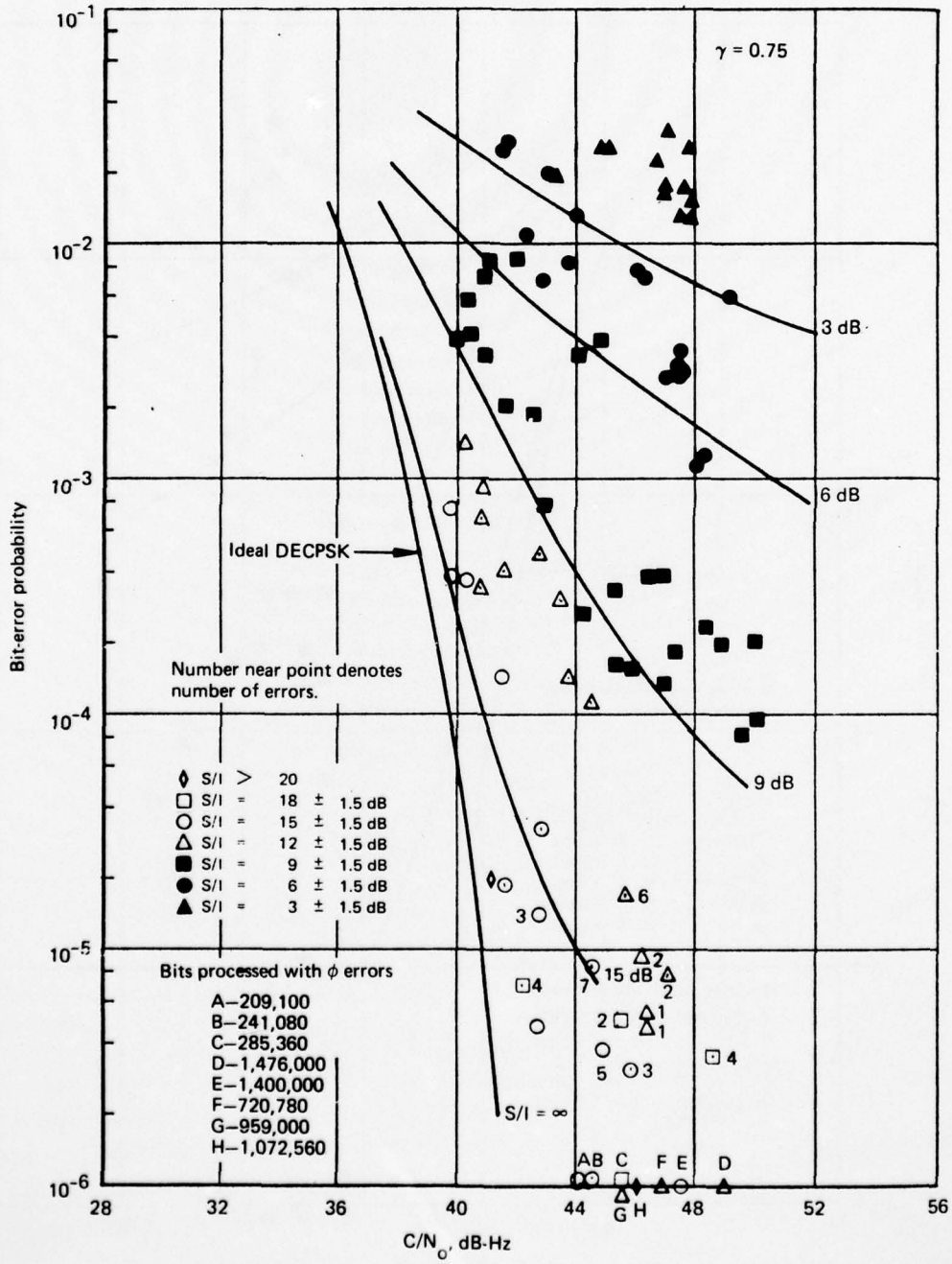

Figure 5-12. Bit-Error-Rate Performance of Hybrid No. 2 DECPSK Demodulator, 1200 bps, Type II Tests

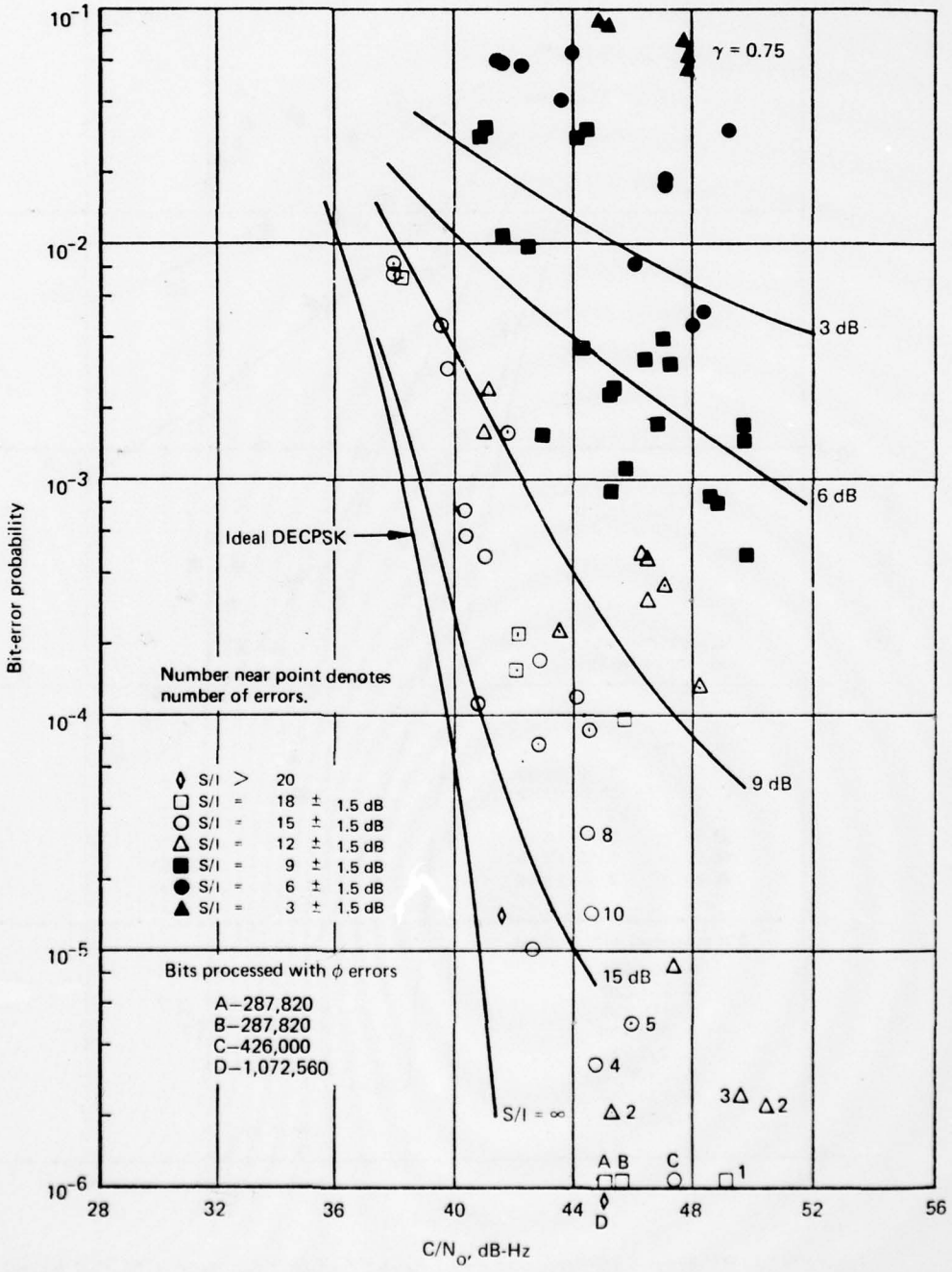

Figure 5-13. Bit-Error-Rate Performance of NASA DECPSK Demodulator, 1200 bps, Type II Tests

AD-A041 971 BOEING COMMERCIAL AIRPLANE CO SEATTLE WASH F/G 17/7
AIR TRAFFIC CONTROL EXPERIMENTATION AND EVALUATION WITH THE NAS--ETC(U)
SEP 76 S G WILSON, C V PAULSON, I R REESE DOT-TSC-707-6
UNCLASSIFIED D6-44051 FAA-RD-75-173-6 NL

2 OF 2
ADA041-971

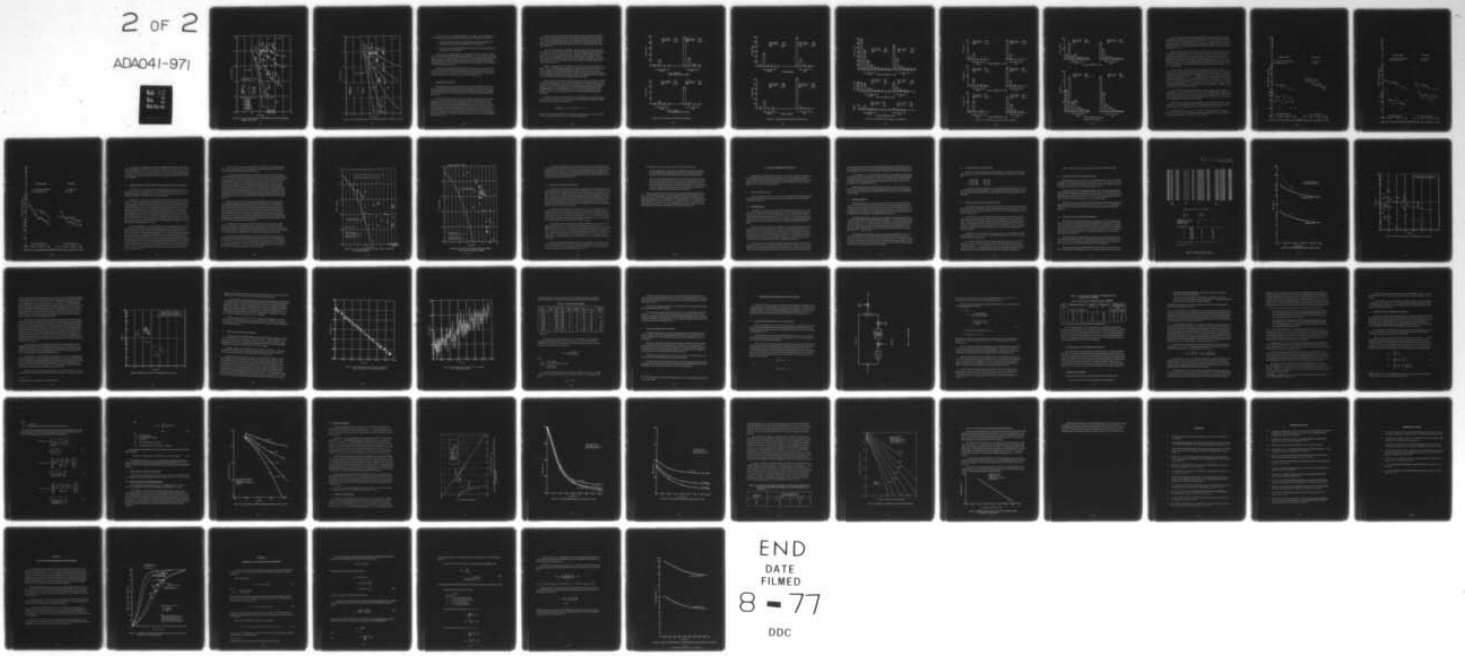

END
DATE FILMED
8-77
DDC

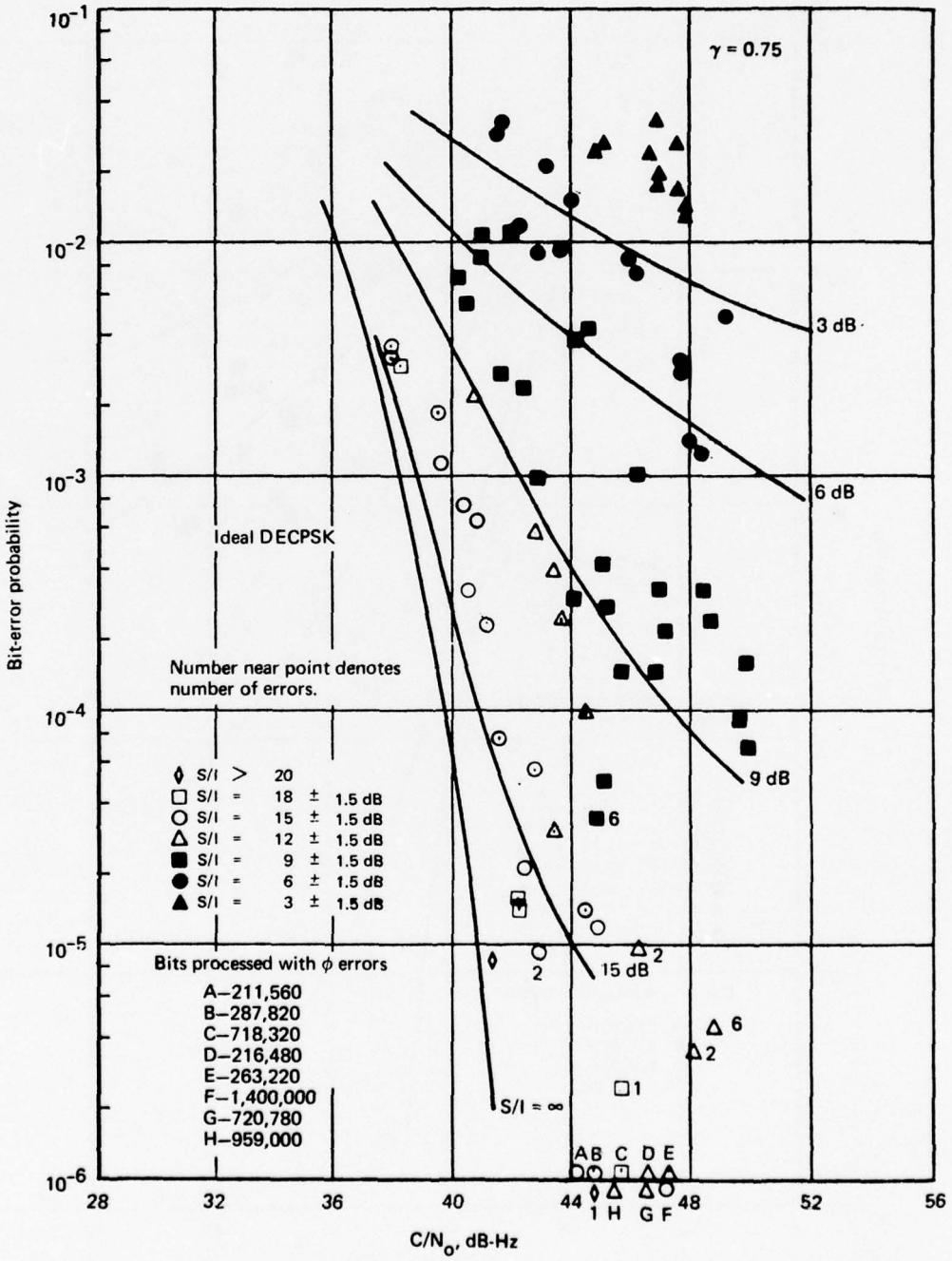

Figure 5-14. Bit-Error-Rate Performance of FAA CPSK Demodulator (DECPSK Mode), 1200 bps, Type II Tests

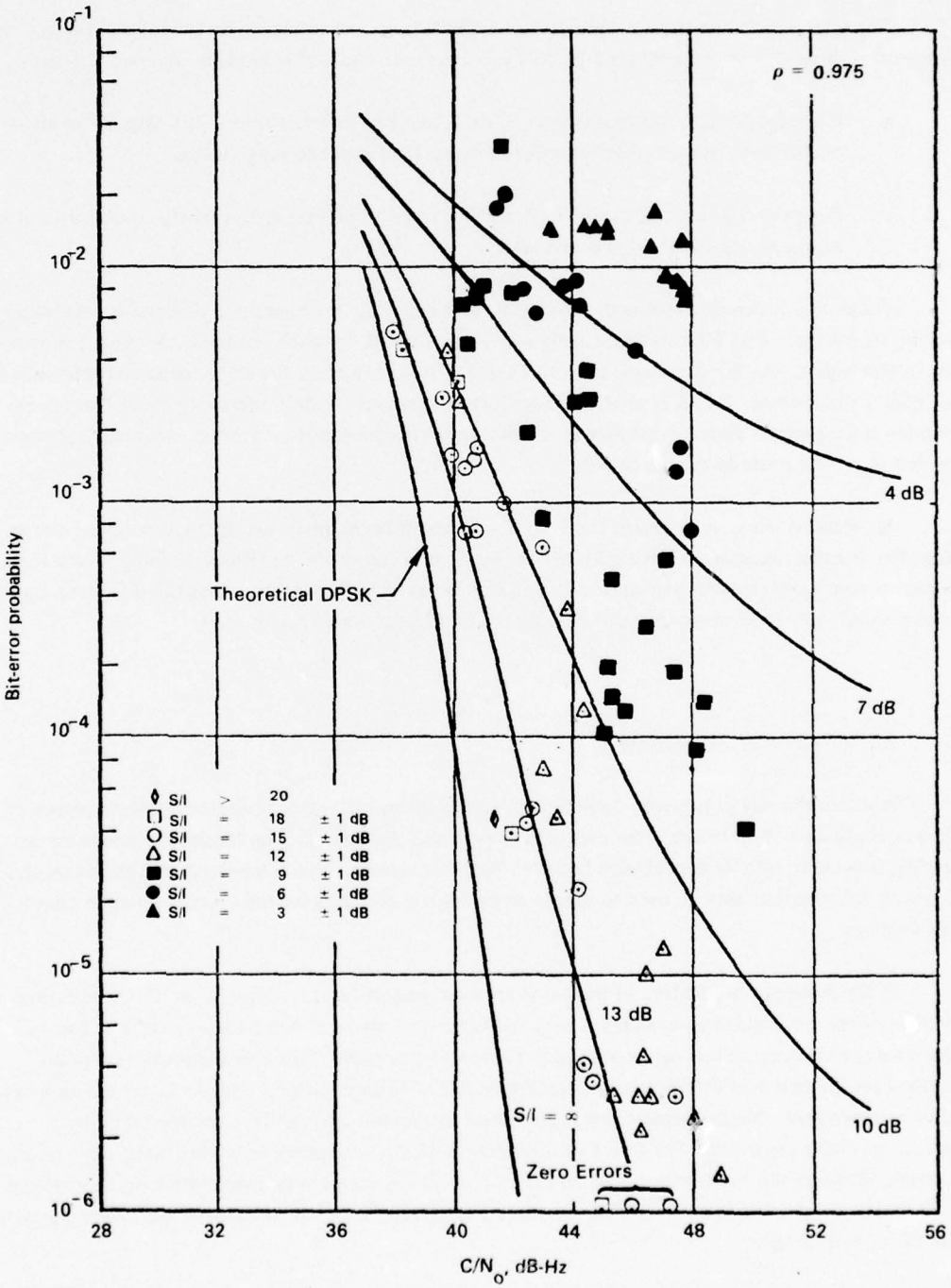

Figure 5-15. Bit-Error-Rate Performance of FAA DPSK Demodulator, 1200 bps, Type II Tests

The relative performance of DPSK and DECPSK is also of interest. By comparing the actual error probabilities of the three better DECPSK modems with the DPSK modem, it is found that:

a. For large S/I (greater than about 10 dB), DECPSK outperforms DPSK slightly in error probability, but less than an order of magnitude over the range tested.

b. For poor S/I, say less than 10 dB, DPSK begins to exhibit a superiority, but again not by a large factor in bit-error probability.

These results can be explained intuitively. For large S/I, the channel is essentially nonfading and it is well known that DECPSK is slightly superior to DPSK for such channels. Section 5.5 provides data in this regard. As S/I decreases, however, the ability to maintain the stable coherent reference for DECPSK is diminished. DPSK is relatively unaffected, however, as only relatively crude frequency accuracy is necessary. Thus a crossover in relative performance is not surprising. An identical observation has also been made in reference 5-2.

In terms of the system design for 1200/2400-bps data channels, no clear-cut winner emerges unless the channel character is decidedly nonfading or very heavy fading (Rayleigh-like). Even then, the performance difference is not dramatic, and it is believed by the authors that the differences are perhaps small relative to those that can be effected by careful design techniques.

5.7 ERROR BURST STATISTICS

Whereas the previous results have displayed the average bit-error probability over a period of minutes, the distribution of the error events in time is also important. The tendency toward error bursting, if present, affects the relation between bit-error rate and character-error rate, for example. Also, such information may be used to design error-control schemes for the specific channel conditions involved.

In the presence of additive white Gaussian noise and without fading effects, the correlation structure of the error patterns associated with the various modems is well understood. For the DECPSK-type strategy, errors occur with high probability in pairs. This arises from the fact that decisions are the result of differentially decoding matched-filter decisions, and the latter are approximately independent. Single isolated errors are rather infrequent and can be explained only by a carrier-loop phase-slip event. For true DPSK detectors, this strong propensity for paired errors is not observed, although the decision is based on the phasor difference over two successive signal intervals. Single errors still predominate for DPSK on nonfading channels, except perhaps at very poor signal-to-noise ratios (ref. 5-10).

Figures 5-16 and 5-17 provide block-error histograms for additive Gaussian noise conditions (Type I tests) for four different test intervals. The histogram independent variable is the number of bit errors per 24-bit contiguous block of data. The vertical axis is the number of occurrences registered. Two DECPSK modems (Hybrid No. 1 and FAA CPSK) were chosen for presentation, with similar results for the DPSK modem. DECPSK modem results for the remaining two units showed very similar character.

First, the expected superiority of DECPSK is observed for the total number of error events. This corresponds to results of the previous sections. The relative frequency of single and double errors is markedly different, however, for the two detection algorithms. DECPSK exhibits the expected paired-error tendency, while DPSK results show that isolated single errors predominate. These conclusions hold for all signal-to-noise ratios presented. The same behavior was observed on a qualitative basis at higher C/N_0; however, the number of error events observed was not large enough to yield statistically significant results.

Figure 5-18 provides block-error histogram data for a Type II test interval for various S/I conditions. C/N_0 was held approximately constant at 46.5 dB-Hz over the test. We observe that for S/I = 9 dB, the histograms for both DECPSK and DPSK are roughly the same in character. For both detection strategies, as S/I decreases (fading becomes stronger), the average error probability increases. Also, for DECPSK, the predominant error mechanism changes from isolated paired errors to single errors per block, indicating that carrier-loop cycle slipping is becoming significant.

Figure 5-19 presents similar data for a Type II test with C/N_0 held in the vicinity of 43 dB-Hz and with S/I varying between 13.5 and 4.5 dB. For the higher S/I cases, we observe the character associated with the nonfading additive-noise channel. As S/I decreases, the average error rate progressively increases as expected. The relative frequency of multiple-error events per block increases for both DECPSK and DPSK. Also, for DECPSK detection, we note (fig. 5-18) the transition from purely paired-error events to a situation where single errors are very prevalent, indicating the presence of cycle slipping.

An alternate viewpoint for studying the memory, or interdependence, of channel error patterns is that of the spacings between errors. If the error process is truly memoryless, the spacing, or waiting time between errors, is geometrically distributed; i.e.:

$$\text{Prob [spacing = k]} = P_e(1 - P_e)^{k-1}, \quad k = 1,2, \ldots,$$

where P_e is the average error probability. As the channel or modem induces memory, the frequency of lesser waiting times increases relative to that of a geometric distribution.

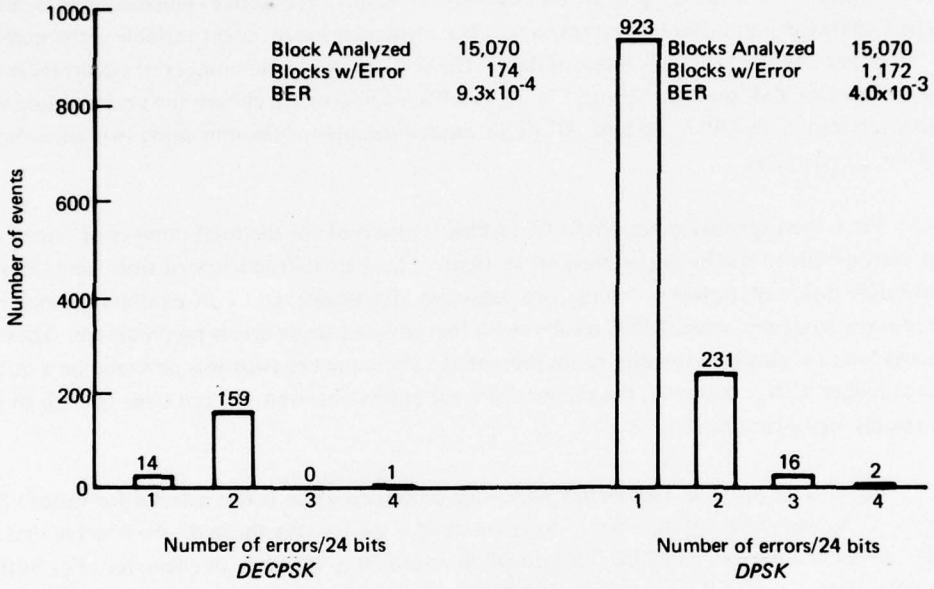

(a) C/N_o = 38.8 dB-Hz
Date = April 2, 1975 (10:51-10:56)

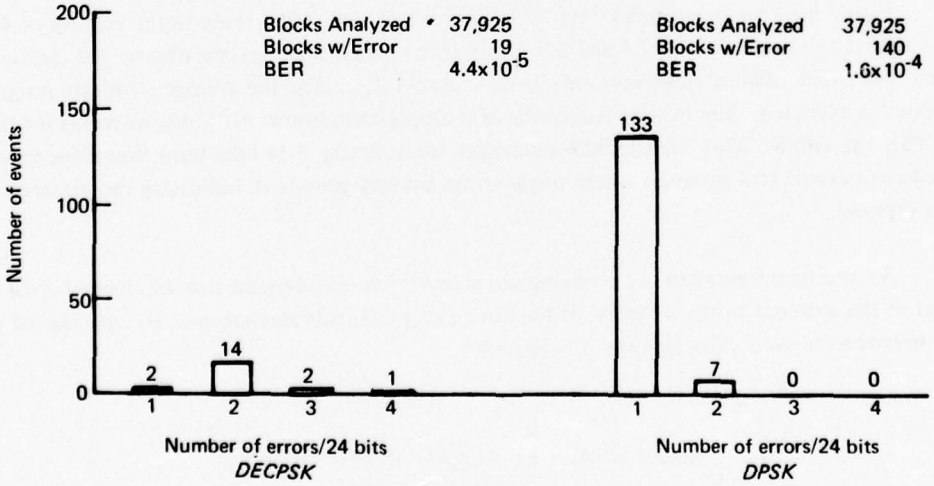

(b) C/N_o = 40.8 dB-Hz
Date = March 25, 1975 (12:06-12:19)

Figure 5-16. Type I Block-Error Histograms (First Example)

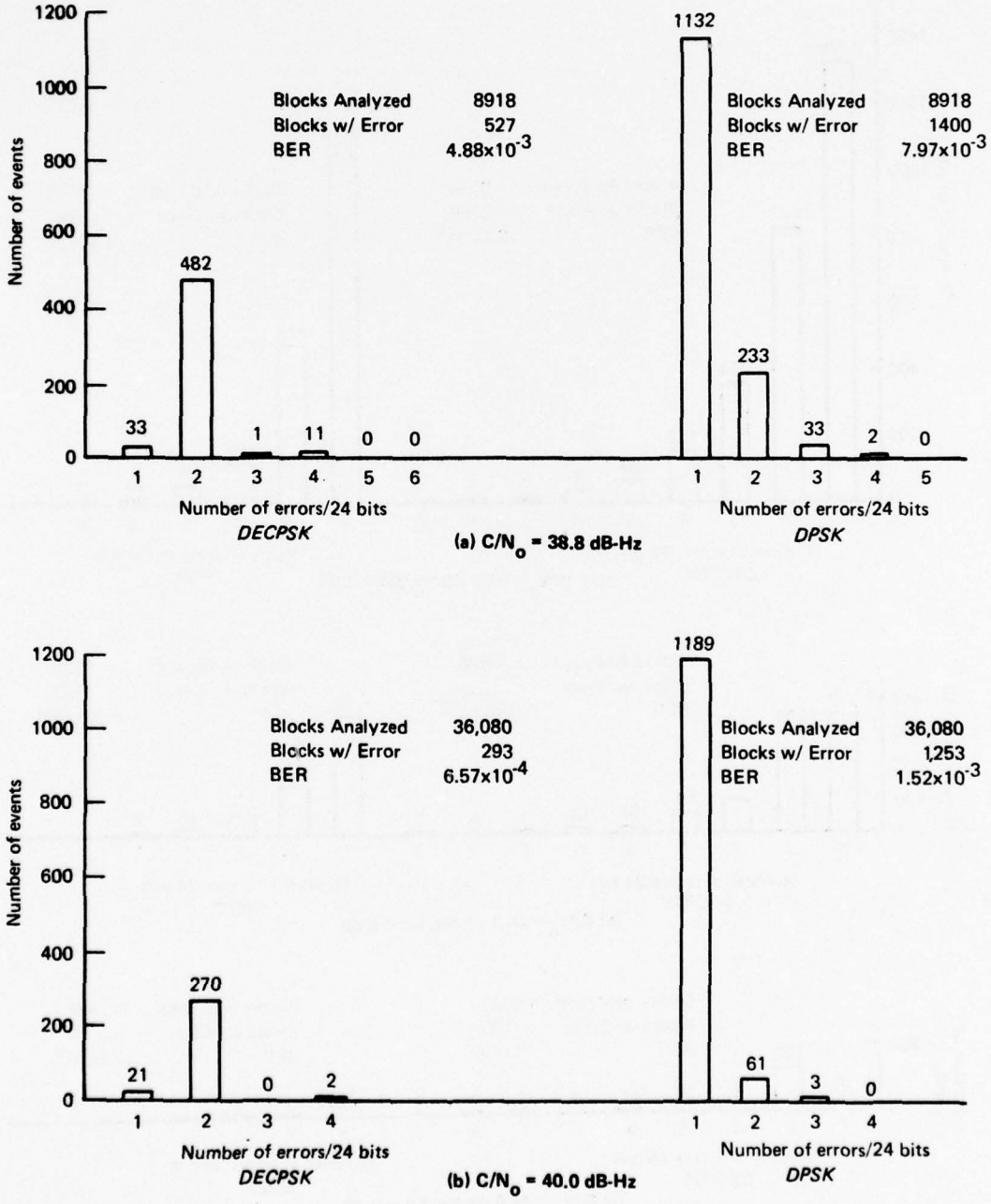

Figure 5-17. Type I Block-Error Histograms (Second Example)

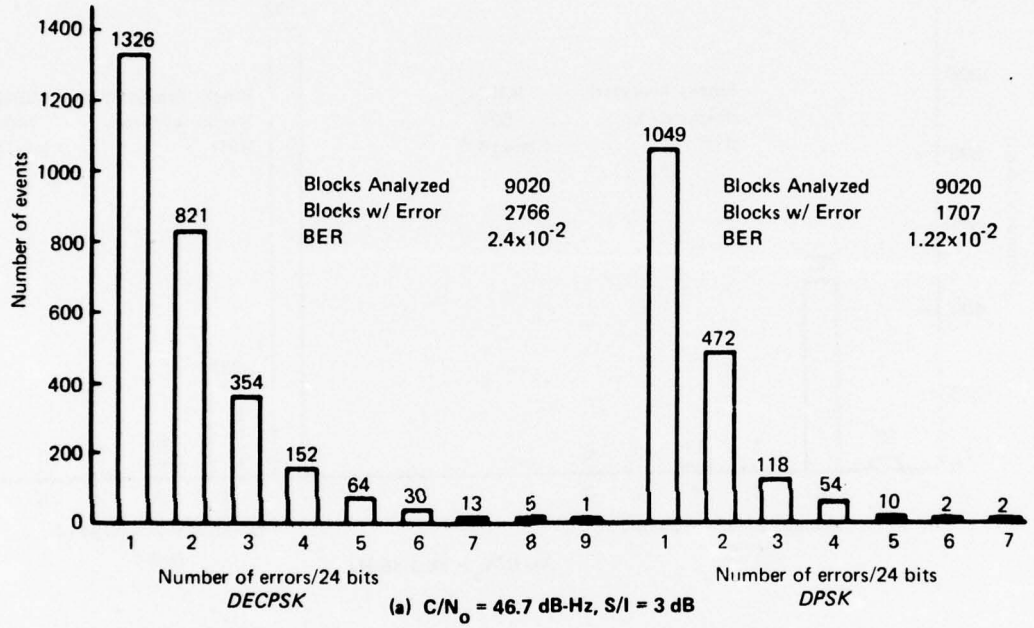

(a) C/N_o = 46.7 dB-Hz, S/I = 3 dB

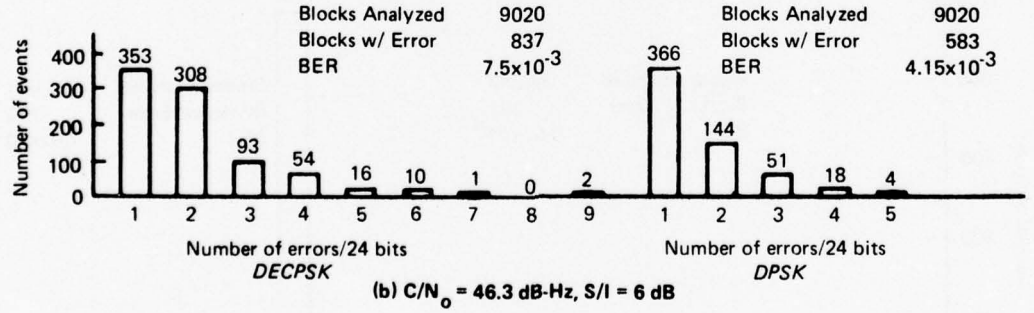

(b) C/N_o = 46.3 dB-Hz, S/I = 6 dB

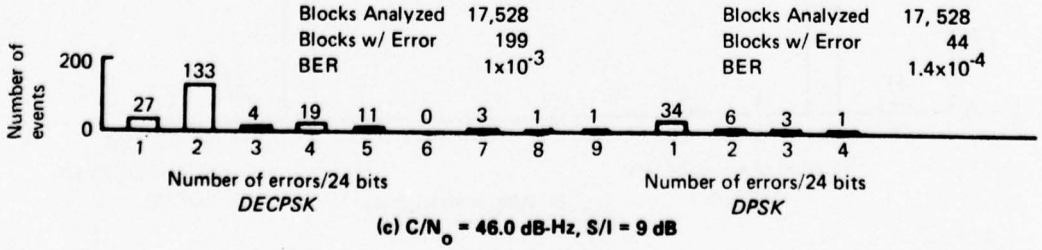

(c) C/N_o = 46.0 dB-Hz, S/I = 9 dB

Figure 5-18. Type II Block-Error Histograms, $C/N_o \cong 46$ dB-Hz

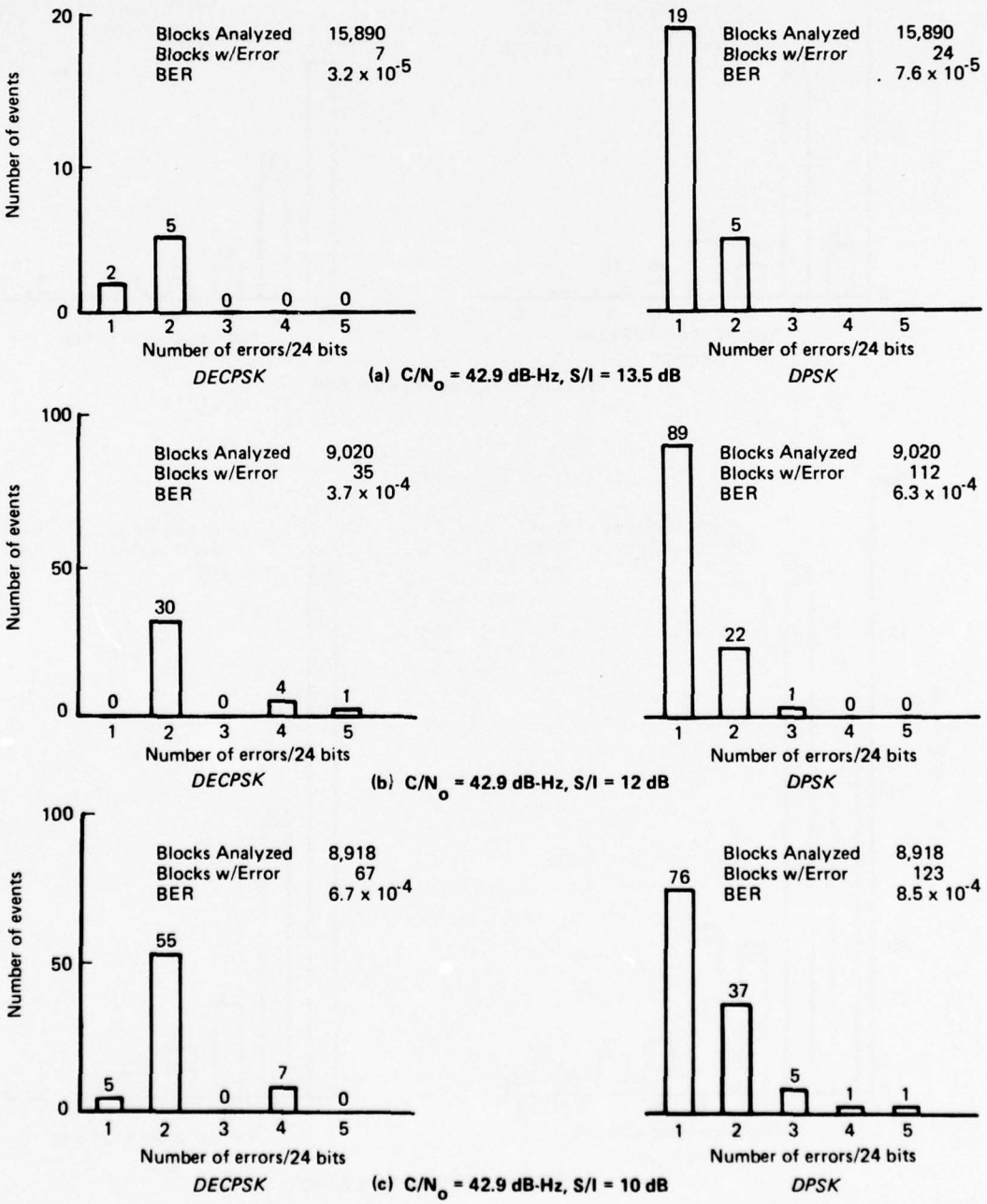

Figure 5-19. Type II Block-Error Histograms, C/N_0 = 43 dB-Hz

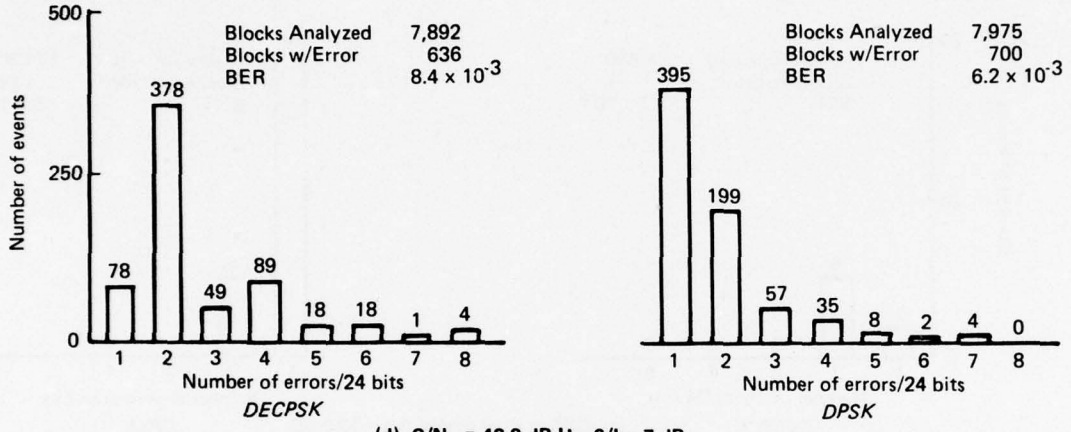

(d) C/N_o = 42.8 dB-Hz, S/I = 7 dB

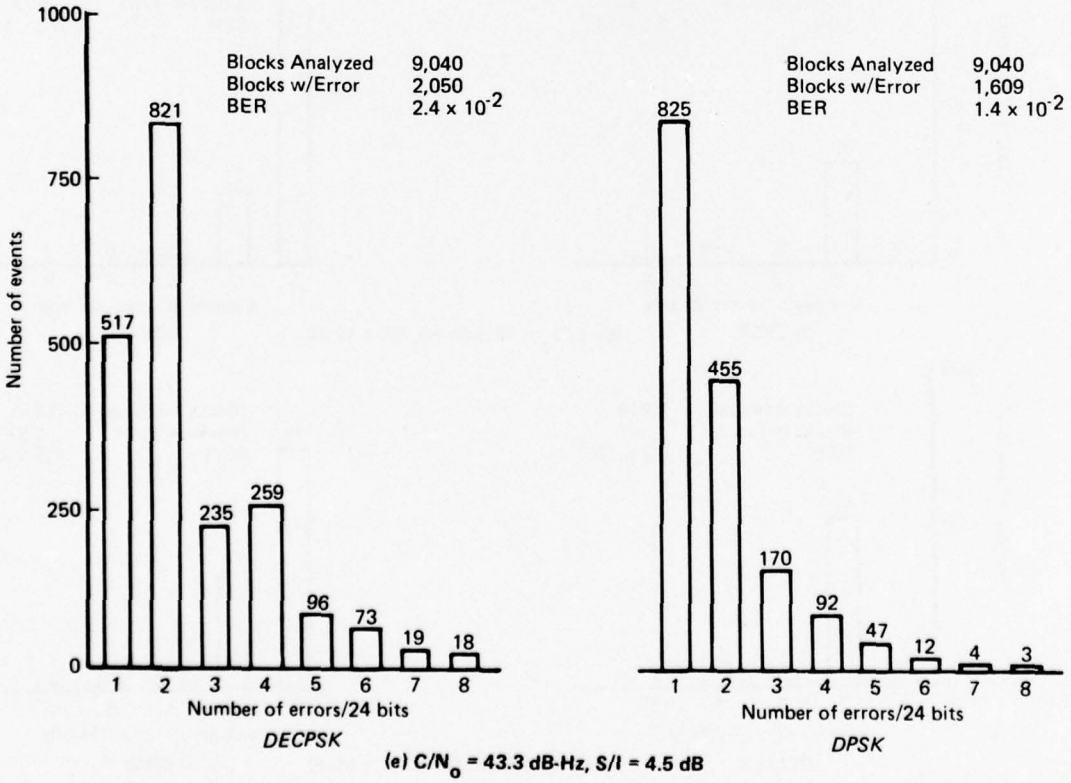

(e) C/N_o = 43.3 dB-Hz, S/I = 4.5 dB

Figure 5-19. (Concluded)

Figures 5-20 through 5-22 show error-spacing distributions for the Hybrid No. 1 and DPSK modems for three distinct channel conditions. These distributions have been calculated by counting the number of times the spacing between errors was k, k = 1,2, . . . , 40, and dividing each total by the total number of errors. This provides an estimate of the waiting-time density function. On the same figures, the distribution of spacings assuming a memoryless process with the *same* error probability has been plotted for contrast.

Figure 5-20 is for a Type I test with C/N_0 = 38.2 dB-Hz and S/I > 20 dB. We observe that the error process has significant memory over two bits in each case; then the probability of spacing k > 2 falls off, with slope characteristic of a memoryless process. Of course, this is the expected result for additive-noise environments due to the detection involving two adjacent bits. Also note that for DECPSK, given an error event, the probability is one-half that another error follows. This is in agreement with theory (ref. 5-1). The corresponding probability for DPSK is 0.186, meaning back-to-back errors are less likely. This value is in very good agreement with the calculations of reference 5-9 (0.19 at C/N_0 = 38.2 dB-Hz).

Figure 5-21 depicts a case with greater C/N_0 and moderately heavy fading. This case was chosen since the average error probabilities were roughly the same as those of figure 5-20. Here both modems exhibit a two-mode characteristic in the density function. Namely, the density exhibits relatively large weighting for spacings 1,2, . . . , 7, then decays slowly in accord with a memoryless process with small error probability. Thus, we may conclude that for C/N_0 = 41.6 dB-Hz and S/I = 6 dB, the effective memory length of the error process is on the order of seven bits at 1200 bps. An error-correcting code should have capability for correcting bursts of time duration equivalent to seven bits, as well as having modest random-error-correcting power. If the code rate is one-half, for example, the burst-correcting power should be 14 channel symbols.

Figure 5-22 illustrates an extreme multipath case, with the average error probability approximately the same as for the example of figure 5-20. Here C/N_0 = 47 dB-Hz and S/I = 2.5 dB. Again, we observe a dual-mode character in the density function for error spacings, but the transition region is now displaced to about 14 bits. For this heavy-fading situation, a longer burst-error-correcting span would be appropriate to fully combat channel memory.

We note that the memory time of the fading process has not changed for figures 5-21 and 5-22, only the relative levels of multipath and noise. An increasing noise level tends to mask the multipath fading effects somewhat, thereby shortening the effective memory of the error process.

Memory times of as great as 14 bits at 1200 bps are certainly plausible for the AEROSAT channels. If one assumes a two-sided Doppler bandwidth of the multipath process to be 100 Hz, then the process decorrelation time is 10 msec, or 12 bits at 1200 bps.

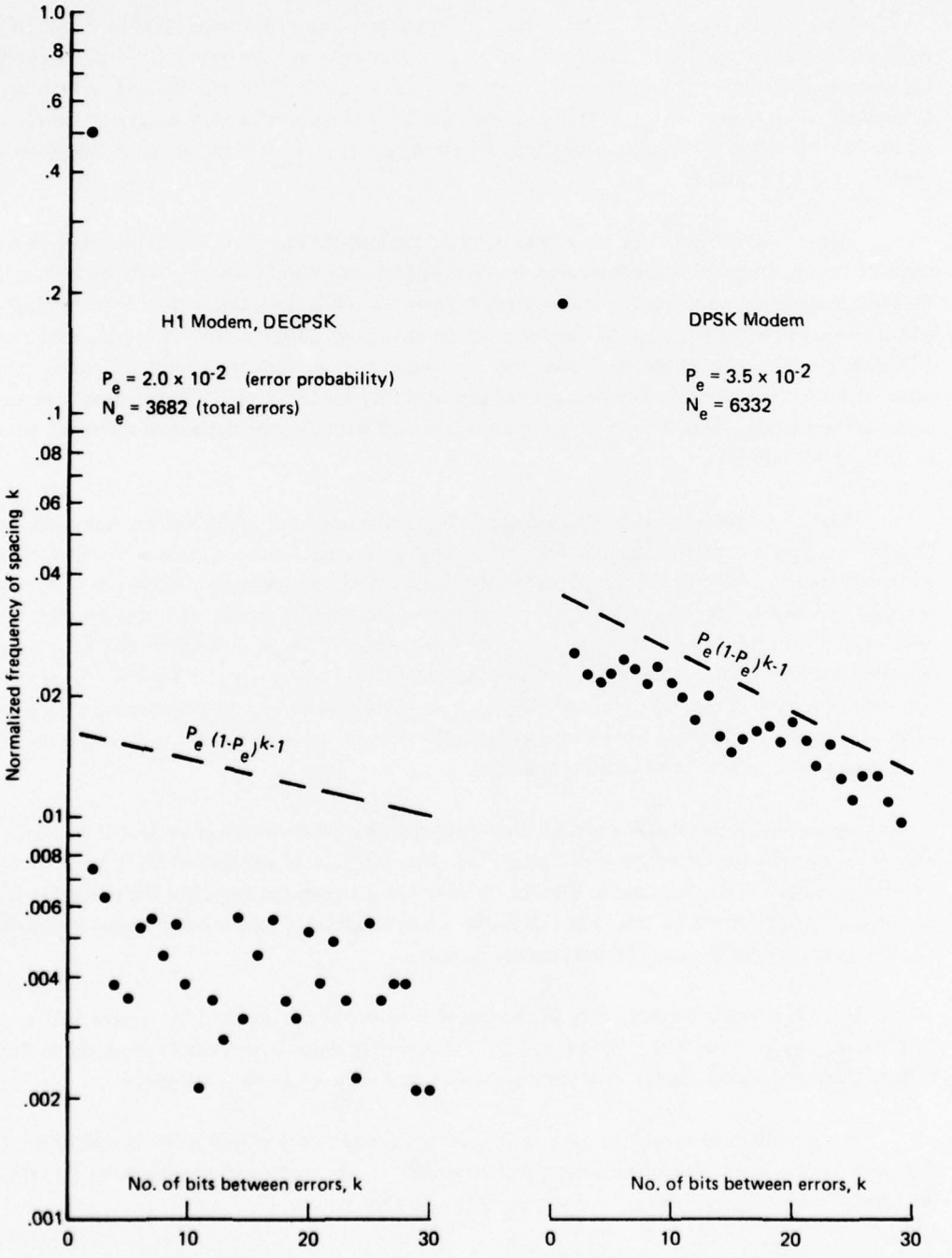

Figure 5-20. Error Spacing Distributions, DECPSK and DPSK, C/N_0 = 38.2 dB·Hz, S/I = 20 dB

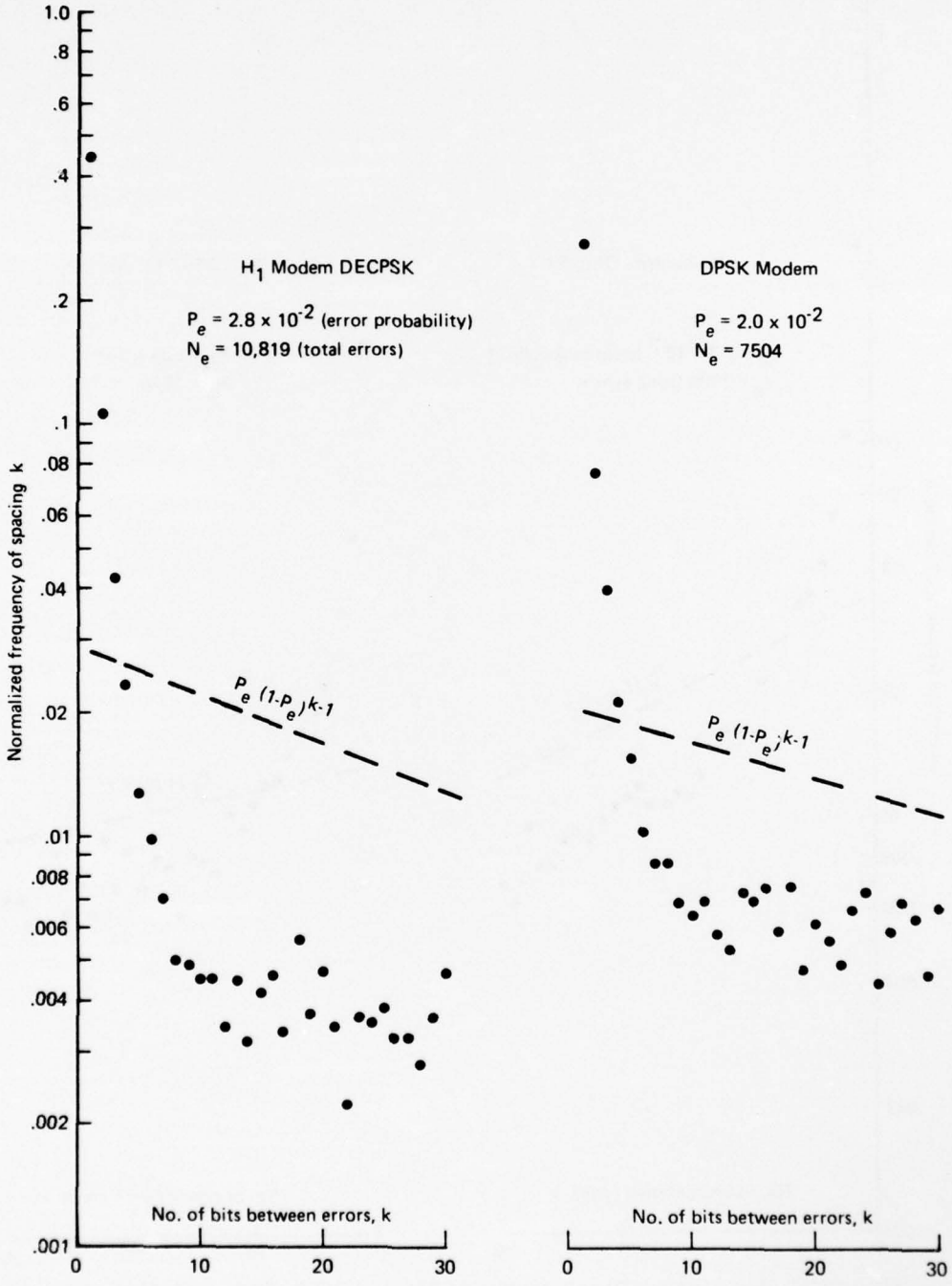

Figure 5-21. Error Spacing Distributions, DECPSK and DPSK, C/N_o = 41.6 dB-Hz, S/I = 6 dB

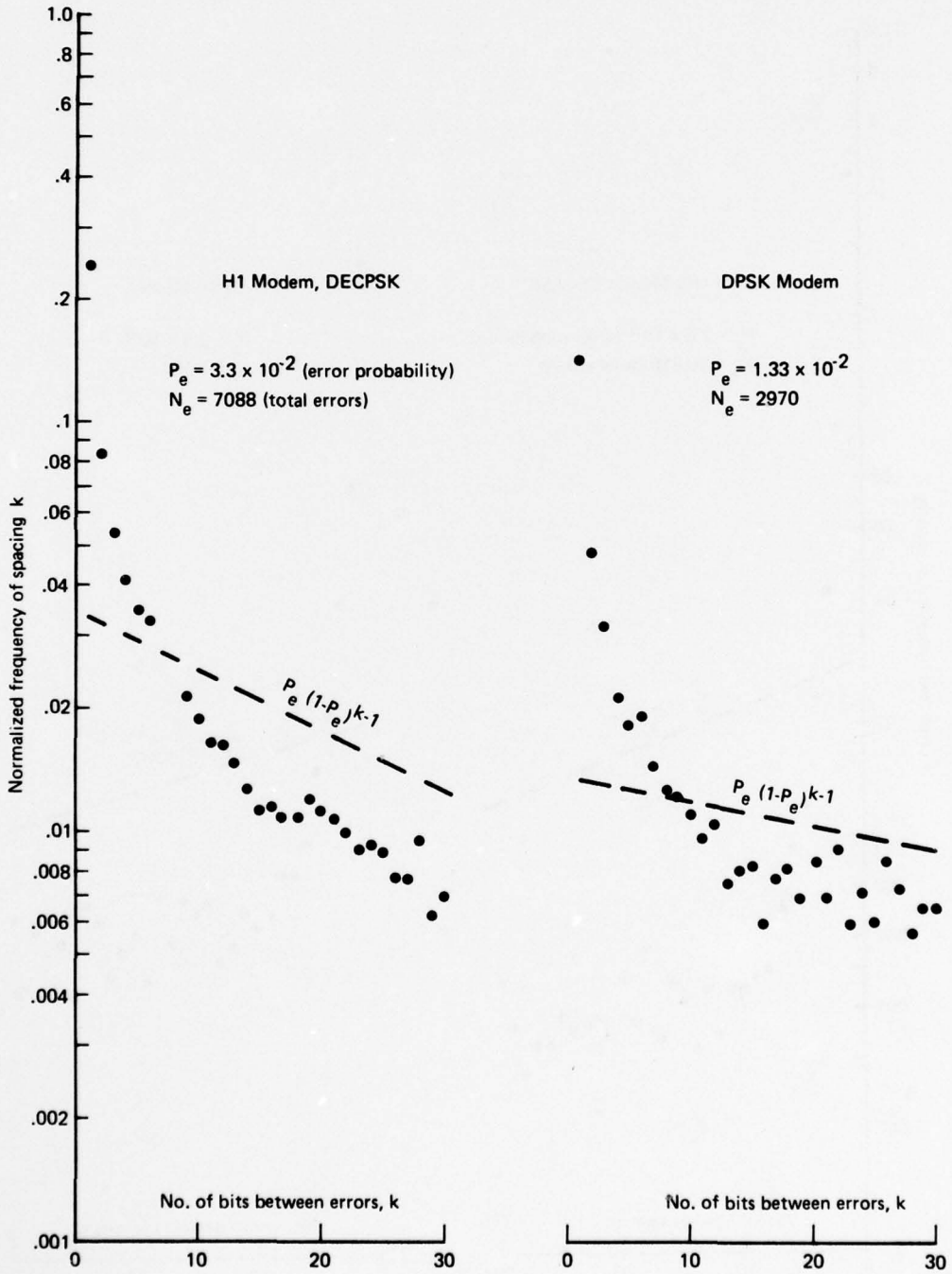

Figure 5-22. Error Spacing Distributions, DECPSK and DPSK, C/N_o = 47 dB-Hz, S/I = 2.5 dB

A note relative to the amplitudes of the density function in the tail region is in order. Typically, the tail probability for DPSK is greater than that for DECPSK. This is simply a manifestation of the fact that DPSK tends to possess errors that are more scattered in time, once the average error rate is normalized. In particular, the frequency of paired errors is less. Since a density function must have a sum of unity, it is expected that the probability measure of large spacings will be higher for DPSK than for DECPSK.

5.8 BER PERFORMANCE OF HYBRID MODEM IN COMBINED VOICE AND DATA MODE

The Hybrid No. 1 and 2 modems have the capability of transmitting speech and data simultaneously on a single constant-envelope carrier. Tests were performed to measure bit-error rate (and speech intelligibility) when operating in the hybrid mode. Before presenting the results, the two methods of modulation are reviewed to assess the expected behavior.

The Hybrid No. 2 modem is more easily analyzed because in the hybrid mode the transmitted signal is the sum of constant-amplitude speech and data carriers placed in phase quadrature. The data carrier is modulated in NRZ/PSK fashion while the speech carrier is suppressed-clock pulse-duration modulated (SCPDM). Each carrier level is adjusted so that one-half the total signal power is allocated to each. Thus, in the absence of any crosstalk induced by nonquadrature phase error or by carrier tracking jitter, the BER performance can be expected to be degraded 3 dB relative to the situation where all signal power is in the data channel. Since speech/data crosstalk can on the average only degrade the BER, 3 dB represents a lower bound on the degradation in the hybrid mode. To summarize, if the modem achieves a certain error probability at 41 dB-Hz in the data-only mode, at least 44 dB-Hz is likely to be needed to achieve the same error probability in the hybrid mode. Also, since the data signal power is time invariant (in contrast to the case for the Hybrid No. 1 modem), no clustering of bit errors is anticipated during speech intervals.

Conversely, the Hybrid No. 1 modem is implemented such that during speech pauses, all signal power reverts to the data channel, and during periods of speech activity, the instantaneous power division is dependent on the speech level. The transmitted signal is the limited vector sum of a PSK data carrier in quadrature with a DSB-AM modulated speech carrier. The net modulation can be viewed as a phase modulation and, as aligned for the test program, the maximum phase deviation was held to 58°. During speech pauses, all power reverts to the data channel, while during high dynamic speech peaks, the maximum short-term reduction of data channel power is determined by the maximum angle of voice modulation (58°). Given the statistical description of the speech modulation, one may do the necessary averaging to predict the long-term average error probability. Due to the speech/data interaction, the bit-error sequence will not be a stationary process but will have error events concentrated in periods of speech activity. This discussion has considered only the time-varying power division and ignores crosstalk phenomenon.

Figures 5-23 and 5-24 present the measured BER for the Hybrid No. 1 and 2 modems, respectively. Tests were conducted in the Type I condition, i.e. no appreciable multipath interference is present, except for the points tagged with circled S/I values.

It is noted that the experimental data for the Hybrid No. 1 modem shows a rather dramatic divergence from the theoretical data-only performance at low bit-error rates. Data channel performance is, in fact, expected to be somewhat dependent upon the voice channel due to the speech/data adaptive power-sharing techniques inherent in the design of the modem. It is also reasonable to expect the effects of speech/data adaptive power sharing to be most readily observable at low bit-error rates because the error probability is more dominated by the infrequent peaks in the speech signal that reduce the effective power available to the data channel. Although the general behavior apparent in the experimental result is partially supportable by the above considerations, the acceptance test data furnished by the modem manufacturer and laboratory measurements made by DOT/TSC after completion of the field tests do not show the large divergence observed in the experimental data. Laboratory performance measurements for both the data-only and hybrid voice/data modes are included in figure 5-23.

In an effort to isolate the reason for the performance differences cited, several factors have been investigated including (1) sensitivity of data channel performance to the voice channel audio input level and (2) possible presence of multipath degradation during Type I tests. Measurements made by DOT/TSC indicate that audio-level-setting errors of +6 dB do not degrade error-rate performance by more than 1 dB relative to the error-rate performance achieved with the correct audio level. Multipath degradation was also ruled out as a potential cause since S/I values were found to exceed 18 dB in all cases. Hence the disparity between laboratory performance measurements and field test data for the BER hybrid voice/data mode performance of the Hybrid No. 1 modem remains largely unresolved. It appears likely that the laboratory performance data more closely approximates the achievable performance than does the field test data.

It should be stated that the results exhibited herein pertain to the regular utterance of PB words at 2.5-sec intervals. In operational use, where verbal messages are conveyed, the data BER during voice channel activity may differ somewhat from the results obtained using PB word lists because of the different dynamics associated with the voice channel modulation for the two cases. During periods of voice channel inactivity, the BER would be essentially that achieved in the data-only mode.

The Hybrid No. 2 modem performance (fig. 5-24) seems consistent with the expected 3-dB shift discussed above. Relative to the data-only mode performance at $P_e = 10^{-5}$, the actual difference is approximately 3.5 dB. According to the field test data, it is noted that very low error probability, say 1×10^{-5}, was achieved with less C/N_o for the Hybrid No. 2 than for the Hybrid No. 1 modem. On the other hand, the Hybrid No. 1 modem was more efficient at higher error rates. Again, these judgments pertain to the particular speech duty cycle used for these tests.

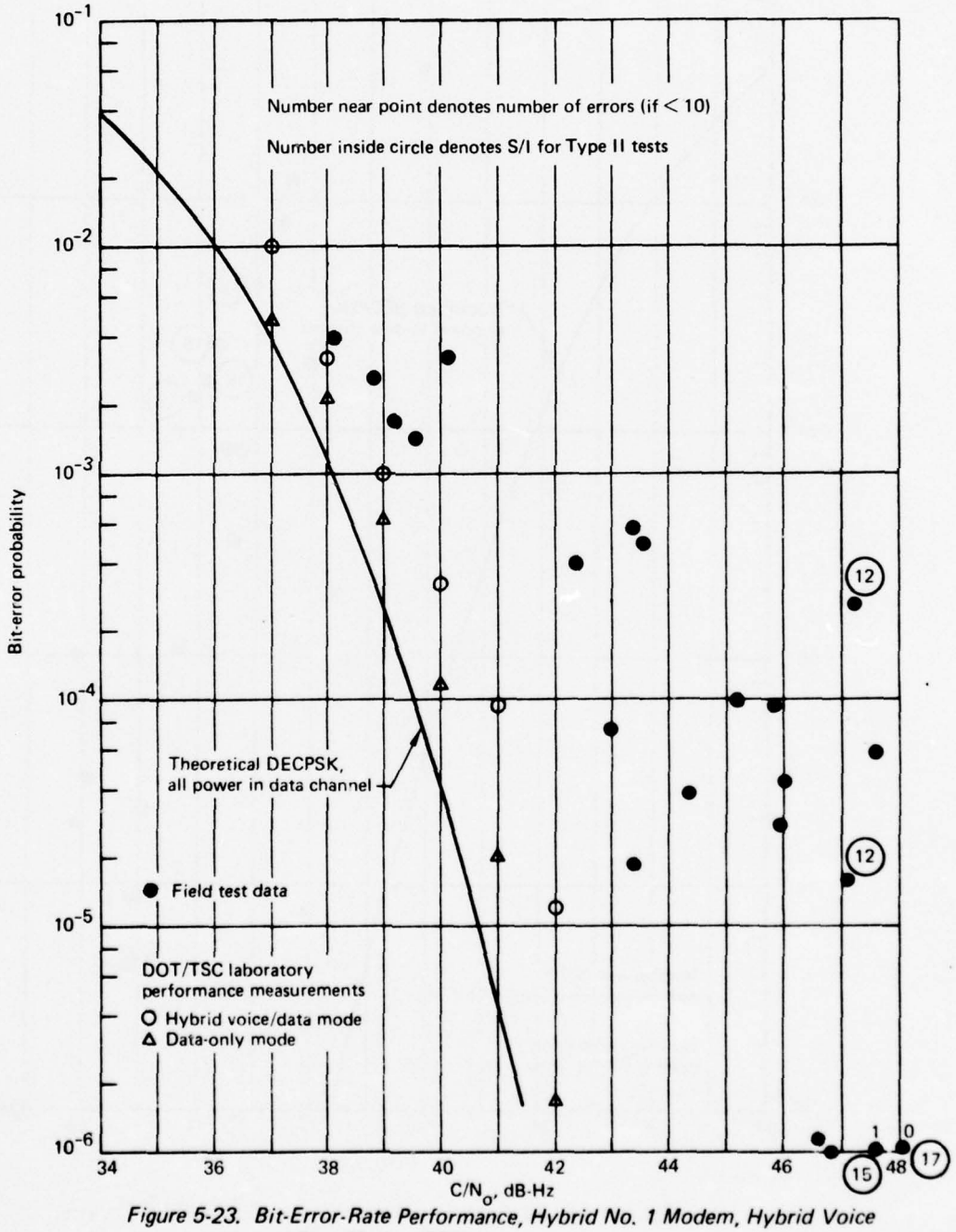

Figure 5-23. Bit-Error-Rate Performance, Hybrid No. 1 Modem, Hybrid Voice and Data Mode, 1200 bps

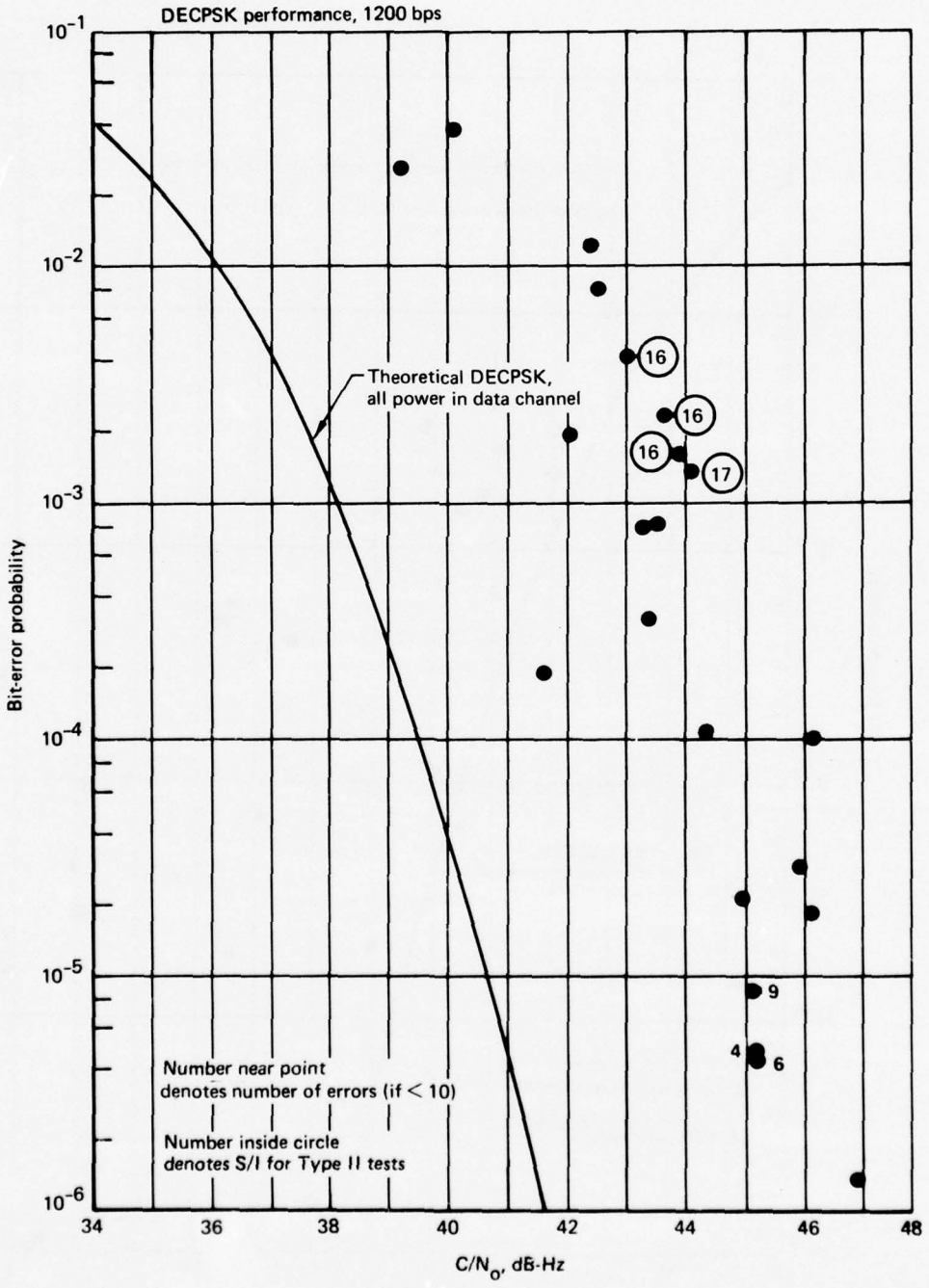

Figure 5-24. Bit-Error-Rate Performance, Hybrid No. 2 Modem, Hybrid Voice and Data Mode, 1200 bps

As discussed, the Hybrid No. 1 modem can be expected to have an error bunching tendency. An attempt was made to investigate this effect by examining whether error events tended to be located at regular intervals 2.5 sec apart. No conclusive evidence was produced from this investigation, primarily due to the fact that the error rate is extremely small where the bunching phenomenon would be most observable. Careful laboratory investigation with deterministic "speech" modulation would undoubtedly demonstrate the bunching effect.

5.9 DIGITAL DATA MODEM CONCLUSIONS

The digital data tests have revealed or verified several significant conclusions applicable to the configuration of aeronautical satellite data link channels. First, the bit-error rates achieved with reception via a representative switched antenna system (the top-left-right slot-dipole configuration) are less than 1×10^{-5} at $C/N_o = 43$ dB-Hz. The latter corresponds to the current AEROSAT system specification, and the conclusion holds for four distinct DECPSK modems and one DPSK modem. Relative to theoretical limits for additive Gaussian noise environments, the modems exhibited inefficiencies of 0.9 to 1.9 dB. By implication, the net S/I achieved by the antenna system for the various Type I geometries exceeded 15 dB since none of the characteristic divergence from theoretical nonfading performance was observed as C/N_o was increased.

When operated on a synthetic Rician fading channel (Type II tests), the DPSK modem performed in general accord with existing theoretical results and with previous experimental flight test results. For example, if the S/I achieved by the antenna system is only 10 dB, an additional 8 dB of channel power is necessary to reduce the error probability to 1×10^{-5}. As concluded in other investigations, error-control coding or multipath-tolerant waveform design appears to be a necessary adjunct to the existing modem designs if S/I values of only 10 dB are anticipated.

The performance of the coherent-detection technique (DECPSK) was rather different for the various modems, possibly due to the different loop bandwidths involved and the impact of cycle slipping. The bit-error rate versus C/N_o observed for these modems was slightly lower than for DPSK when S/I was large, say greater than 10 dB; as S/I decreased below 10 dB, however, the DPSK technique exhibited better performance. In ranking the DECPSK modems qualitatively, we conclude that the Hybrid No. 1 modem performed best, followed by the Hybrid No. 2, the FAA CPSK, and the NASA modems. The NASA modem seemed to exhibit particularly severe degradation in a multipath environment.

Relative to the DPSK versus DECPSK question, it is our judgment that the difference in performance is not significant in either's favor over a typical operating region of S/I and C/N_o. Other factors not evaluated here, such as acquisition performance, complexity of design, and reliability of operation, probably outweigh any observed bit-error-rate factors.

Investigation of the memory characteristics of the error patterns revealed that:

a. In nonfading additive-noise environments, the DECPSK errors generally occur in pairs whereas the DPSK errors are predominantly isolated single errors and, less frequently, paired-error events. Both of these results have been earlier theorized and verified.

b. As the level of multipath interference increases, the likelihood of error bursts increases; that is, the short-term error probability varies over orders of magnitude due to constructive and destructive interference. Also, for DECPSK, cycle slip events become more obvious as evidenced by the increase in frequency of isolated errors. For either technique, if burst-correction coding is used, the burst-correcting span should be on the order of seven bits at 1200 bps (14 code symbols in a rate one-half code).

Finally, the performance of the two hybrid voice/data modems was evaluated in the hybrid mode. For the Hybrid No. 2 modem, the C/N_o increase required to maintain equivalent error performance was about 3.5 dB due to the equal power sharing. The Hybrid No. 1 modem exhibited a more complex relationship: for high error rates ($\approx 10^{-2}$), speech and data could be conveyed with only 1 dB additional power, whereas at a 10^{-5} error rate, the necessary increase in C/N_o for the hybrid mode was on the order of 4 dB. This is somewhat dependent on the duty cycle and statistics of the speech modulation. The impact of adding data to the speech signal is roughly 3 dB.

6. RANGING EXPERIMENT TEST RESULTS

The flight test program evaluated the performance of two distinct satellite-aircraft ranging techniques. Measurements were performed using a single satellite, whereas an operational surveillance system would necessitate additional measurements for a 3-D position solution. Because the true range between aircraft and satellite could not be readily determined, the ranging accuracy was evaluated relative to a best-fit estimate, rather than absolutely.

6.1 RANGING MODEMS TESTED

The two ranging techniques tested are referred to as TSC ranging and NASA ranging, the names deriving from the agencies sponsoring the respective modem developments. This section will briefly describe the two approaches.

6.1.1 TSC Ranging Modem

This modem was an in-house development at DOT/Transportation Systems Center. The technique utilizes a ranging signal first studied by Stiffler (ref. 6-1), which is a binary ranging code having rapid acquisition potential. Starting with an upper tone frequency of 156.25 kHz (or 19.53 kHz), binary submultiples are generated logically down to 76.3 Hz. These 12 (or 9) square waves are input to a majority logic unit that synthesizes the code state. The highest frequency determines the ranging modem precision, while the lowest frequency in the code determines the maximum unambiguous range.

Whereas a brute-force code search would examine 2^{12} (or 2^{9}) possible code phases to synchronize in the worst case, a more rapid procedure is allowed for this waveform. Namely, correlation of each subharmonic with the incoming code can be performed to determine if the polarity of that component is correct or not. If not, a simple logic inversion is performed. Following clock acquisition, sequential operation from highest to lowest frequencies requires 11 (or 8) polarity checks. If an incorrect polarity decision is made on any of the component frequencies, a large range error obviously ensues; this corresponds to what is generally called an ambiguity resolution error.

Several variations of the basic signal processing are available for selection. First, the choice that most dramatically affects performance is that of highest frequency (156.25 kHz or 19.53 kHz). The weighting of the highest frequency component prior to generation of the composite code is also selectable. Increasing the weighting provides more clock energy but decreases the correlation with each of

the remaining component square waves, thus increasing the ambiguity error probability. Also selectable is the number of code cycles used in performing a polarity decision on each component; increasing the integration time reduces the error probability in random noise but lengthens acquisition time.

Carrier modulation is ± 1.2 radians peak phase modulation, and demodulation is coherent with the aid of a narrowband carrier-tracking loop. Range measurements are made by comparing the phase of the regenerated range code with that of a reference code. A 40-MHz clock is counted to provide this measure, and each time a range measurement is performed, a 20-bit range count is formed, the least significant bit corresponding to 25 nsec.

Formatted along with the range count are eight code-format bits, which indicate the clock frequency and its weighting, plus five status bits, relating modem lock conditions. For each measurement, these data bits are inserted into a 305-bps Manchester stream, which is recorded and processed off-line in Seattle.

6.1.2 NASA Ranging Modem

This modem implements a cw sidetone ranging technique (ref. 5-8) developed for NASA as part of the PLACE system. Modems were located on the aircraft and at Rosman, and the two-way round-trip range was computed at Rosman. Rosman continuously emitted the S&R (surveillance and ranging) signal, which was acquired and tracked by the aircraft modem, as well as by other users. Aircraft emissions were in response to an interrogation signal inserted into the forward-link waveform. In the high-rate mode used for these tests, an interrogation occurs each 6.4 sec.

The S&R surveillance signal is comprised of four ranging tones double-sideband modulated on a carrier and a 600-bps Manchester PSK channel in phase quadrature. The composite of these is limited to remove envelope variation. The signal is coherently demodulated with a carrier-tracking loop that tracks the residual carrier. Tone phase for each tone is computed by baseband correlation with reference tones. A digital computer resolves the phase ambiguities implied by the modulo-2π measurements and computes round-trip range. The 600-bps data channel is used for polling of various terminals, transmission of onboard altitude, etc.

The responses received at Rosman were processed and written on digital tape, which in turn was supplied to Boeing for analysis. With the data processing performed, the two-way range error relative to a best-fit trajectory is calculated. Absolute accuracy could have been evaluated if the satellite and aircraft positions were accurately known and if all equipment delays were calibrated. However, the relative excursions from best fit provide the information necessary to predict system performance on a 3-D basis, if it is assumed biases can be suitably removed.

6.2 RANGING TEST SIGNAL DESCRIPTION

The signal emanating from Rosman was an FDM composite of the S&R signal, the TSC digital ranging signal, and a cw carrier for envelope analyses. The frequencies, after translation at the satellite, were

1550.000 MHz	CW carrier
1550.075 MHz	S&R carrier
1550.600 MHz	TSC carrier.

As in other tests, carrier level equivalence was established by monitoring the downlink spectrum from the satellite and adjusting as appropriate. This was performed for unmodulated carriers; since the TSC modem output power is slightly less when code modulation is applied, a corresponding correction was applied.

6.3 REDUCTION AND ANALYSIS OF RANGING DATA

Analog instrumentation tapes recorded on the aircraft for the TSC modem tests were processed by Boeing in Seattle to yield a digital computer tape having formatted time, range, and signal envelope samples. This procedure is described in detail in volume IV, section 10. NASA ranging data is received directly in digital tape form.

For both types of tests, range versus time arrays are constructed for a test interval of several minutes' duration. Obvious outliers, or blunder errors, are purged from the data set as described in volume IV to yield a more meaningful calculation of error standard deviation. Using the remaining points, a second-order polynomial fit is performed, and an error array is defined by the deviations between each sample point and the best-fit estimate at the corresponding time. Thus, the experiment measures error deviations relative to a nominal trajectory. The rms value of this deviation is the primary test statistic.

Goodness-of-fit tests are performed for both experiments to test the assumption of normally distributed range error. The chi-square test is used with mean and variance of the hypothetical distribution computed from the error data.

For the TSC tests, the signal envelope samples are processed to provide C/N_0 and S/I estimates for the channel. The method is identical to that used for voice and data modems (detailed description in vol. IV, sec. 7). The forward-link C/N_0 for the NASA signal is assumed identical to that of the TSC signal. No corresponding C/N_0 and S/I data were available at the Rosman ground station relative to the return-link channel quality during tests of the NASA ranging modem.

Figure 6-1 illustrates a typical TSC ranging summary printout from CDC 6600 analysis.

6.4 LABORATORY BASELINE PERFORMANCE DATA

TSC has provided performance data taken in the laboratory that may be used for comparison with flight test data. The rms error, in meters, as a function of C/N_0 is shown in figure 6-2 for both wideband (156.25 kHz) and narrowband (19.53 kHz) modes. At each C/N_0 setting, a series of runs was made, and the range results for error standard deviation are shown.

Also shown in figure 6-2 are theoretical performance curves for the modem that account for additive Gaussian noise disturbances and modem quantization effects. The theoretical performance evaluation is found in appendix B. The precision in the limit of high C/N_0 is determined by the clock digital PLL phase correction interval, which is 1/128 of a cycle. This corresponds to an rms uncertainty of 34.6 m in the narrowband mode and 4.3 m in the wideband mode.

Sources of the discrepancy between measured and expected performance are probably various implementational losses, still under investigation by TSC. Also, at lower C/N_0 settings, the noisier tracking of the carrier-tracking loop acts to increase the rms range error beyond that modeled in appendix B.

6.5 TSC DIGITAL RANGING MODEM PERFORMANCE

Results presented for the TSC ranging modem are confined to the November 1974 through April 1975 test periods. Although data was collected during September and October 1974, this data could not be reduced due to a waveform anomaly in the modem output consisting of a phase discontinuity that appeared in the Manchester bit stream shortly prior to each range reading. This anomaly occurred only when the modem was forced to make entire code acquisition for each measurement; subsequently, the modem was operated in a four-readings-per-second mode where reacquisition is performed only if lock is broken.

Type I test results for standard deviation of range error in meters are found in figure 6-3 for both narrowband and wideband modes. Superimposed are best-fit curves from baseline laboratory data (sec. 6.4). For the narrowband data, the points straddle the laboratory curve but in general lie above. Also, data scatter is greater than that attributable to finite-sampling error.

One potential reason for the higher observed rms error in the flight test environment is the presence of small amounts of multipath interference. Although the slot-dipole antenna system used

POINT	273	ST.BIT	1 0 1 1 1	TIME	12/44/27.920	RANGE	109695	R.IN NSEC	365650
POINT	274	ST.BIT	1 0 1 1 1	TIME	12/44/28.130	RANGE	109695	R.IN NSEC	365650
POINT	275	ST.BIT	1 0 1 1 1	TIME	12/44/28.240	RANGE	109695	R.IN NSEC	365650
POINT	276	ST.BIT	1 0 1 1 1	TIME	12/44/28.450	RANGE	109695	R.IN NSEC	365650
POINT	277	ST.BIT	1 0 1 1 1	TIME	12/44/28.659	RANGE	109695	R.IN NSEC	365650
POINT	278	ST.BIT	1 0 1 1 1	TIME	12/44/28.869	RANGE	109575	R.IN NSEC	365250
POINT	279	ST.BIT	1 0 1 1 1	TIME	12/44/29.079	RANGE	109695	R.IN NSEC	365650
POINT	280	ST.BIT	1 0 1 1 1	TIME	12/44/29.288	RANGE	109695	R.IN NSEC	365650
POINT	281	ST.BIT	1 0 1 1 1	TIME	12/44/29.498	RANGE	109695	R.IN NSEC	365650
POINT	282	ST.BIT	1 0 1 1 1	TIME	12/44/29.708	RANGE	109575	R.IN NSEC	365250
POINT	283	ST.BIT	1 0 1 1 1	TIME	12/44/29.918	RANGE	109695	R.IN NSEC	365650
POINT	284	ST.BIT	1 0 1 1 1	TIME	12/44/31.127	RANGE	109575	R.IN NSEC	365250
POINT	285	ST.BIT	1 0 1 1 1	TIME	12/44/31.337	RANGE	109575	R.IN NSEC	365250
POINT	286	ST.BIT	1 0 1 1 1	TIME	12/44/31.547	RANGE	109575	R.IN NSEC	365250
POINT	287	ST.BIT	1 0 1 1 1	TIME	12/44/31.756	RANGE	109695	R.IN NSEC	365650
POINT	288	ST.BIT	1 0 1 1 1	TIME	12/44/31.966	RANGE	109575	R.IN NSEC	365250
POINT	289	ST.BIT	1 0 1 1 1	TIME	12/44/31.176	RANGE	109575	R.IN NSEC	365250
POINT	290	ST.BIT	1 0 1 1 1	TIME	12/44/31.386	RANGE	109695	R.IN NSEC	365650
POINT	291	ST.BIT	1 0 1 1 1	TIME	12/44/31.595	RANGE	109575	R.IN NSEC	365250
POINT	292	ST.BIT	1 0 1 1 1	TIME	12/44/31.805	RANGE	109575	R.IN NSEC	365250
POINT	293	ST.BIT	1 0 1 1 1	TIME	12/44/32.015	RANGE	109575	R.IN NSEC	365250
POINT	294	ST.BIT	1 0 1 1 1	TIME	12/44/32.224	RANGE	109455	R.IN NSEC	364850
POINT	295	ST.BIT	1 0 1 1 1	TIME	12/44/32.434	RANGE	109455	R.IN NSEC	364850
POINT	296	ST.BIT	1 0 1 1 1	TIME	12/44/32.644	RANGE	109575	R.IN NSEC	365250
POINT	297	ST.BIT	1 0 1 1 1	TIME	12/44/32.854	RANGE	109455	R.IN NSEC	364850
POINT	298	ST.BIT	1 0 1 1 1	TIME	12/44/33.063	RANGE	109575	R.IN NSEC	365250
POINT	299	ST.BIT	1 0 1 1 1	TIME	12/44/33.273	RANGE	109455	R.IN NSEC	364850
POINT	300	ST.BIT	1 0 1 1 1	TIME	12/44/33.483	RANGE	109455	R.IN NSEC	364850
POINT	301	ST.BIT	1 0 1 1 1	TIME	12/44/33.692	RANGE	109455	R.IN NSEC	364850
POINT	302	ST.BIT	1 0 1 1 1	TIME	12/44/33.902	RANGE	109575	R.IN NSEC	365250
POINT	303	ST.BIT	1 0 1 1 1	TIME	12/44/34.112	RANGE	109575	R.IN NSEC	365250
POINT	304	ST.BIT	1 0 1 1 1	TIME	12/44/34.322	RANGE	109455	R.IN NSEC	364850

Point index | Status bit | Time | Range, m

R A N G I N G S E G M E N T S U M M A R Y

DATE 3/28/75
START TIME 12/43/30.00
STOP TIME 12/44/35.00
MODE 1

2ND ORDER FIT COEFFICIENTS .0161 -40.7511 -97.7140
NUMBER OF POINTS 319
NUMBER OF POINTS CENSORED 0
MEAN ERROR, METERS -.0
RMS ERROR, METERS 62.3

ERROR DISTRIBUTION

INTERVAL	MID POINT	NUMBER OF OBSER.	EXPECTED NO. OF OBS.
1	-137.066	9	7.3
2	-112.145	11	16.2
3	-87.224	19	19.2
4	-62.303	32	36.9
5	-37.382	38	42.3
6	-12.461	45	49.6
7	12.461	50	49.6
8	37.382	41	42.3
9	62.303	38	36.9
10	87.224	21	19.2
11	112.145	11	16.2
12	137.066	4	7.3

PROBABILITY THAT CHI-SQUARED VARIATE IS GREATER THAN TEST STATISTIC .342

CODE/STATUS BITS 0 0 0 0 0 1 0 0

Figure 6-1. Sample TSC Ranging Printout

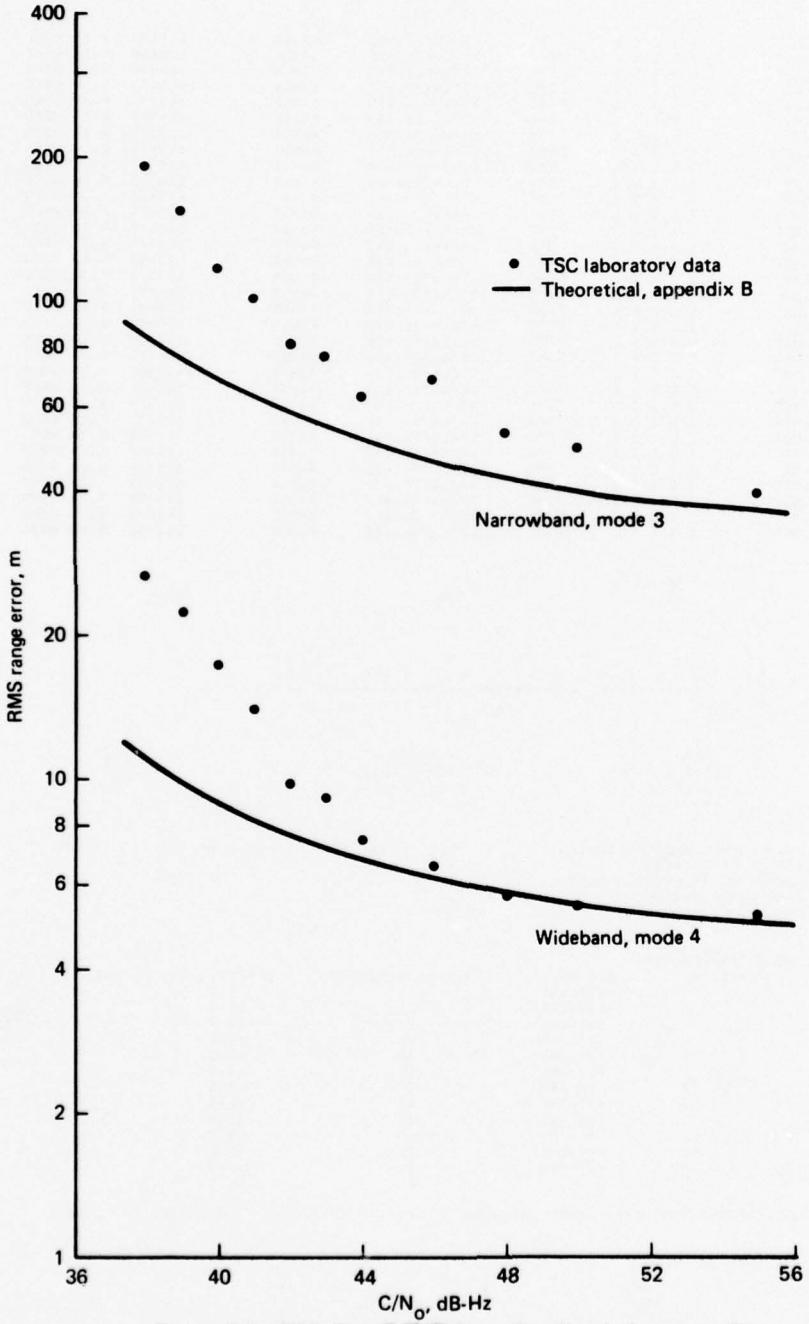

Figure 6-2. TSC Ranging Modem, Baseline Laboratory Data

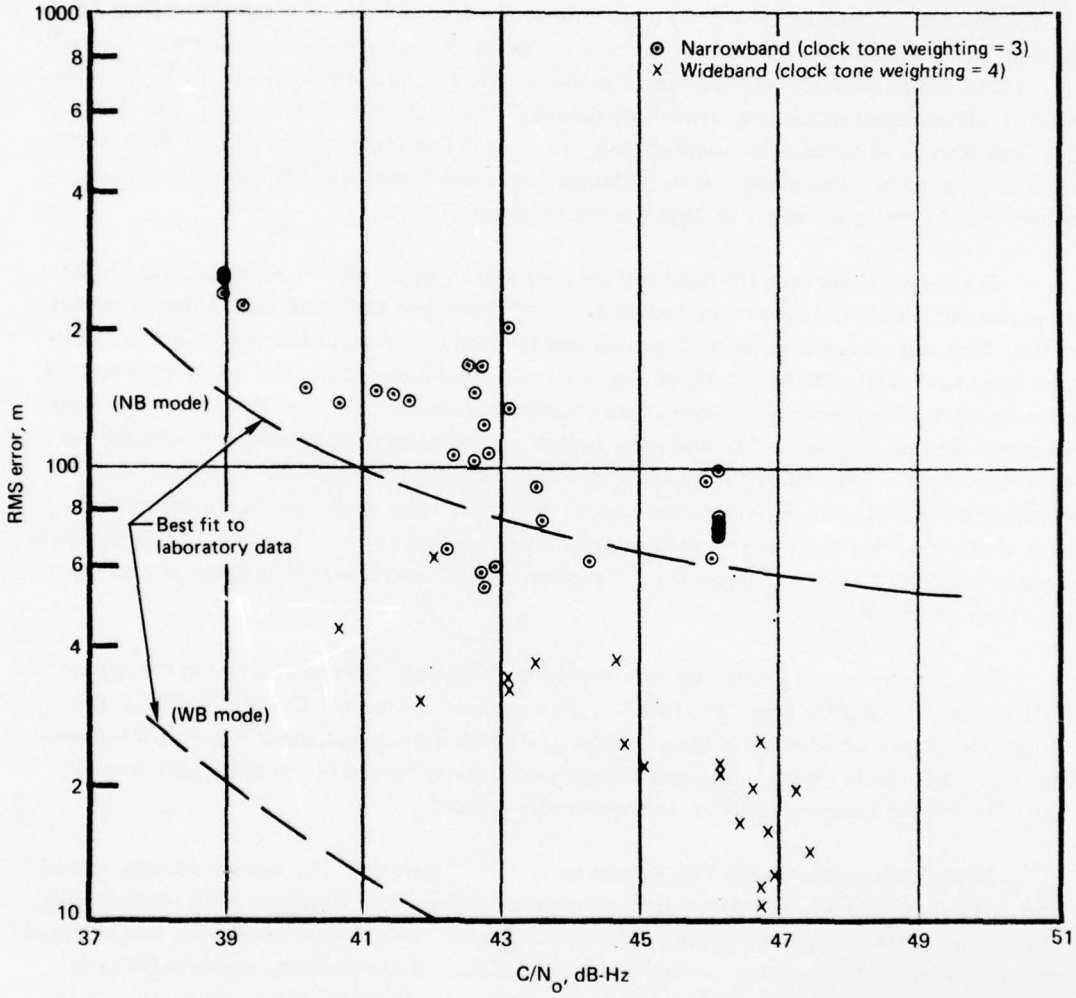

Figure 6-3. RMS Error Performance, TSC Ranging Modem, Type I Tests

in Type I tests provides rather large discrimination as determined from spectral analysis of the envelope detector output, even low multipath levels can increase the rms deviation significantly beyond that predicted for additive noise only. For example, with C/N_o = 43 dB-Hz, the clock loop signal-to-noise ratio is 38.9 dB (effective tone-power-to-noise ratio in B_L from app. B). The signal-to-multipath ratio may be calculated by assuming for the present that the S/I achieved by the antenna system is 20 dB. Also assuming the multipath one-sided bandwidth is 50 Hz and noting that $B_L \simeq 1$ Hz, an additional 17-dB rejection accrues via narrowband tracking. The loop output S/I then is 37 dB. This is approximately equal to the signal-to-noise ratio. Thus the net rms error will be larger than that calculated for noise alone. This points out the potential dominance of multipath effects in the ranging system error budget, particularly for high-precision systems.

For the *wideband* case, the flight test has considerably larger rms deviation than the laboratory measurements. Aside from multipath factors described above, two additional factors may contribute to this. First, experience with the modem indicated the carrier loop needed continual monitoring of loop stress to maintain optimum performance in the wideband mode. Since the operator's workload prevented this, the performance observed here could be expected to be poorer than laboratory measurements. Second, the assumed second-order aircraft trajectory may not be adequate to model the short-term motion of the aircraft due to gusting and flight control actions. These perturbations are insignificant when error deviations on the order of 100 m are under study. In the wideband mode, however, the ranging precision is on the order of a few tens of meters, and these unmodeled variations could be important. If so, the apparent rms deviation is inflated relative to that obtained with exact knowledge of aircraft motion.

It is also interesting to compare the observed performance with that required in the current AEROSAT system specification. The specified performance is 50 m rms at 43 dB-Hz C/N_o. The current TSC design achieves this in the wideband mode with the antennas used. However, for operation with 0.5-sec polling slots,[1] the signal averaging time would have to be less than that currently used. The ranging accuracy would be correspondingly reduced.

Type II test results for the TSC modem are found in figure 6-4. The number adjacent to each point is the computed S/I. The data is limited to those conditions for which the S/I is relatively high since the cases with stronger multipath yielded erratic modem performance, presumably due to loss of lock. It is noted that in both narrowband and wideband cases, data points lie roughly in the same location versus C/N_o as do the Type I data points. This is a reasonable result since the slot-dipole system effective S/I generally exceeds 20 dB for the test geometries flown.

In Type I and Type II tests, frequent range jumps were observed, either due to loss of lock or incorrect ambiguity resolution. The latter are identifiable as a range shift corresponding to a half wave-

[1] Polling slots of 0.5 sec are specified for the AEROSAT system.

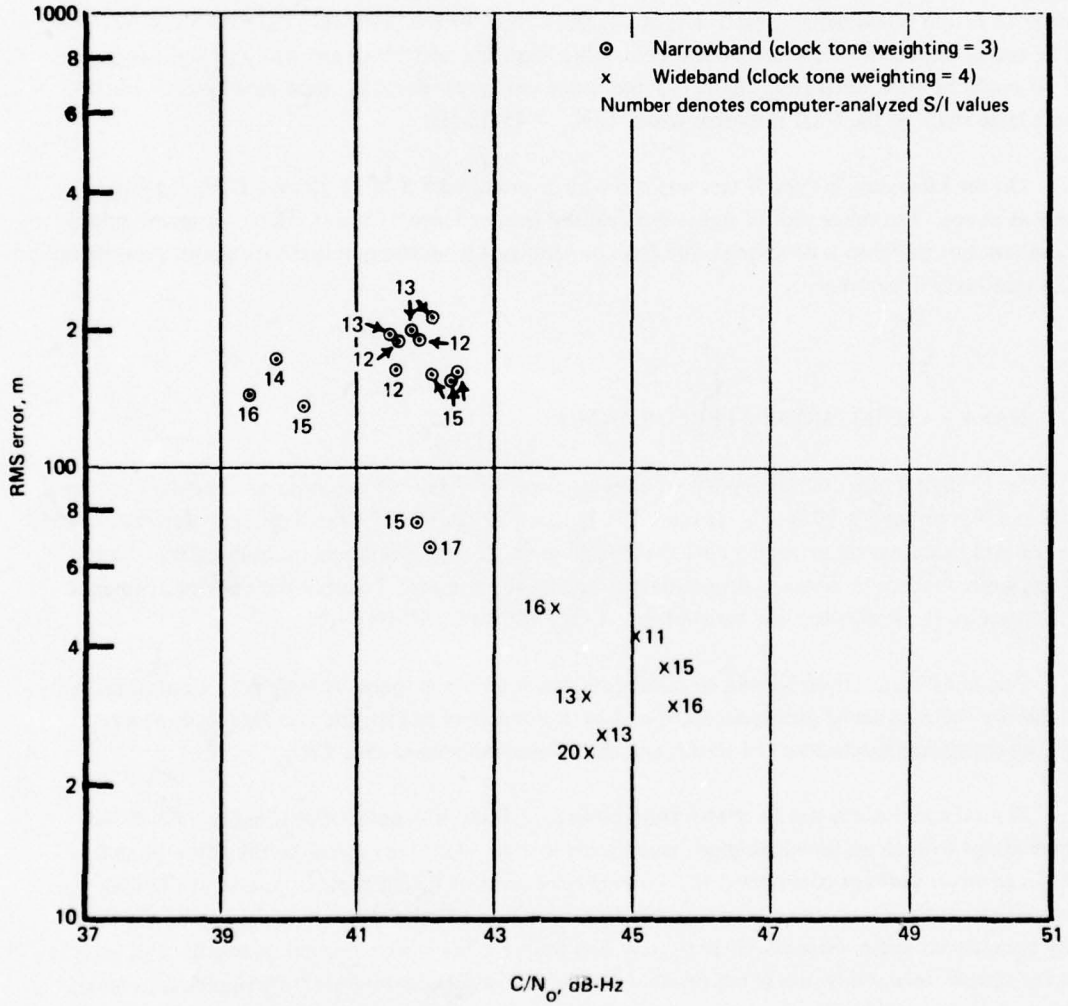

Figure 6-4. RMS Error Performance, TSC Ranging Modem, Type II Tests

length at one of the component frequencies. These points were censored from the data set unless the frequency of occurrence was too large to permit reasonable processing of the set.

As previously mentioned, the TSC modem has inherent range quantizing due to the digital nature of the clock tracking loop. Figure 6-5 illustrates the range trajectory for an interval in which nominal performance is observed. The range quantization associated with the clock tracking loop is clearly visible and corresponds to 120 m in the narrowband mode. (The quantum interval in the wideband mode is 15 m and is less perceptible.) The measured C/N_o for the interval of figure 6-5 was 42.7 dB-Hz, and no multipath interference was detectable from the analysis of the envelope detector samples. It might be concluded from figure 6-5 and other similar results that quantizing "error" contributes a large share of the total rms error when C/N_o = 43 dB-Hz.

On the same day, a Type II test was run with a measured S/I of 13 dB and C/N_o approximately as above. The range plot of figure 6-6 resulted (note change of scale). Here the quantizing is still evident, but the loop is deviating more than one interval from the nominal lock point, presumably due to multipath interference.

6.6 NASA RANGING MODEM PERFORMANCE

Seven digital tapes were supplied to Boeing, spanning 7 days of ranging experiments: November 13 and November 19, 1974, and January 23, January 29, March 27, March 28, and March 31, 1975. Upon careful examination it was decided that the January 23 tape contained no usable data. Range readings were very erratic and a malfunction was apparently present. Possibly the poor performance was induced by the somewhat low forward-link C/N_o (40 to 42 dB-Hz).

Pertinent information for the remaining six test intervals is found in table 6-1. Contained in the table are the number of points accepted and total number of points, the standard deviation of error, the chi-square goodness-of-fit result, and the measured forward-link C/N_o.

Several conclusions can be drawn from table 6-1. First, it is noted that roughly 25% of the range readings written on tape had large errors (greater than 10,000 m) and were therefore purged. These large errors perhaps correspond to incorrect resolution of the ambiguous phases of the four tones. Whatever the cause, the frequency of blunder errors would have to be reduced to be usable in any operational sense. Second, there is no strong basis for rejecting a normal distribution of error from chi-square tests. Only one batch produced a test statistic exceeding the 0.05 significance level; all other statistics could have been produced under the normal hypothesis with probability shown. However, due to the small sample sizes involved, the power of the test, i.e., the probability of rejecting the hypothesis when in fact the samples were not normally distributed, is probably not large. In other words, many near-Gaussian distributions, appropriately scaled, might be approved by the test. Since

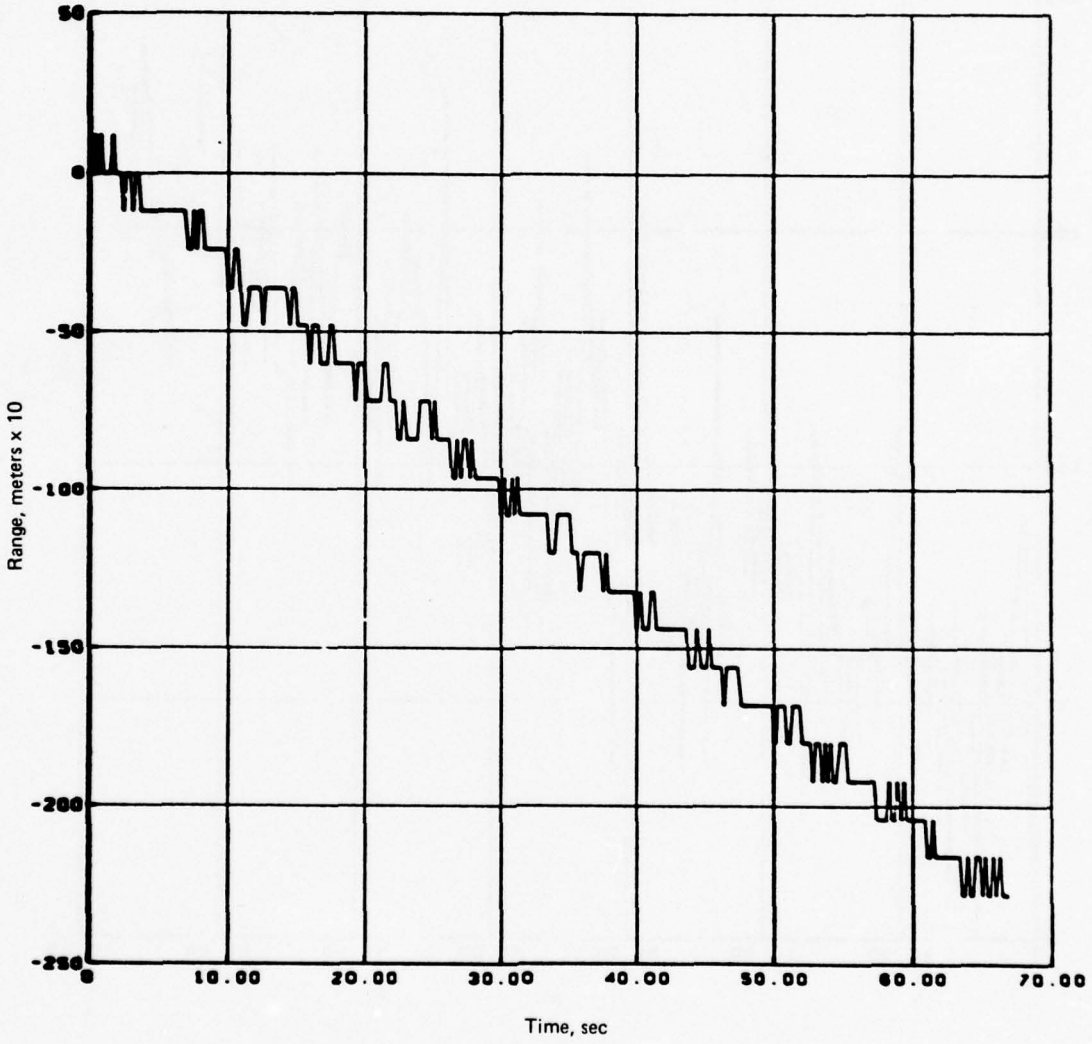

Figure 6-5. Sample Range-Time Trajectory Illustrating Quantizing, C/N_o = 42.7 dB-Hz, S/I = 20 dB, March 28, 1975

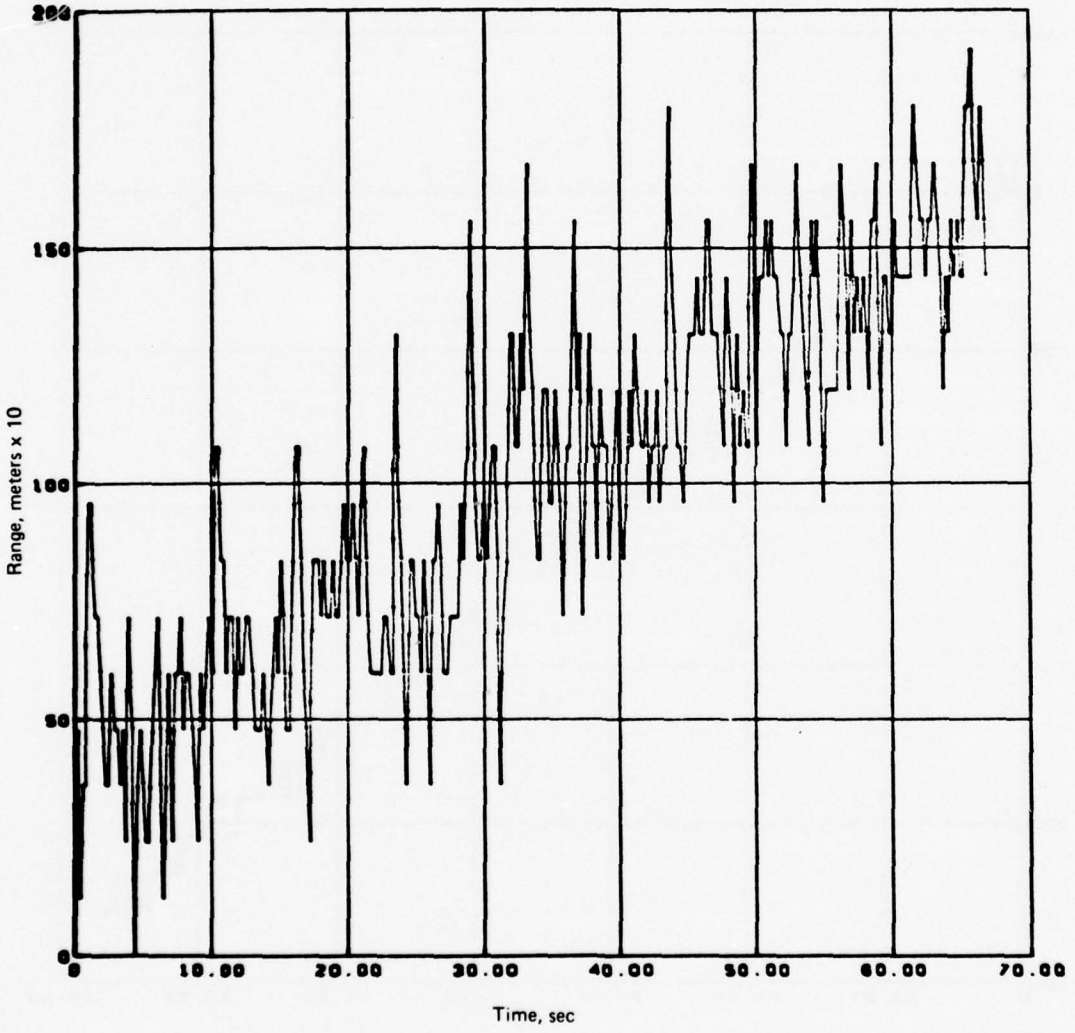

Figure 6-6. Sample Range-Time Trajectory, C/N_0 = 42.2 dB-Hz, S/I = 13 dB, March 28, 1975

there is physical basis for a Gaussian model and it is not rejectable from the data, it is plausible to invoke its assumption except perhaps for describing events lying in the far tail of the distribution.

TABLE 6-1. NASA RANGING SUMMARY

Date, mo-day-yr	Test type	Start time	Stop time	Total points	Points accepted	σ_R, meters	P ($\chi^2 > t$)	C/N_o, dB-Hz
11-13-74	II	0941	0946	42	32	298	0.70	42.0
11-13-74		0958	1007	79	69	248	0.27	–
11-13-74	II	1011	1016	32	23	332	0.62	44.5
11-19-74	II	1203	1208	43	23	225	0.79	–
1-29-75[a]	I	1020	1028	76	76	56	0.35	60
1-29-75[a]	I	1030	1038	67	67	125	0.92	46
3-27-75	II	1220	1233	127	120	334	0.03	44.6
3-28-75	I	1353	1359	48	45	236	0.75	42.7
3-31-75	II	1217	1221	33	27	263	0.27	42.0

[a]Ground test.

The average of observed rms deviations for C/N_o = 42 to 44 dB-Hz on the forward link is 276 m and is within the expected range. The highest frequency tone is 8575 Hz and the tone integration time is 120 msec. As is well known, the rms range deviation in the presence of Gaussian additive noise is for double-sideband modulation,

$$\sigma_R = \frac{c}{2\pi f_T}\left(\frac{N_o}{2 P_T T_I}\right)^{1/2} ,$$

where:

f_T = tone frequency
P_T/N_o = tone-power-to-noise density ratio
T_I = integration time
c = speed of light.

From reference 5-8, the available P_T/N_o is roughly 32 dB-Hz when total C/N_o is 42 dB-Hz, owing to the power sharing between the data subcarrier and the four tones. Substituting the above yields

$$\sigma_R = 285 \text{ m}.$$

Although only the forward-link C/N_o was measured directly, link calculations indicate the return link should contribute little additional noise. Thus, 42 to 44 dB-Hz round-trip C/N_o may be expected for most of the cases in table 6-1, and we see that the observed standard deviation is roughly what should be expected.

The ground test conducted on January 29, 1975, revealed that for strong signal conditions, the rms error can be reduced to the 50-m region.

It is noted that the rms range error achieved falls short of the current AEROSAT system specification of σ_R = 50 m at 43 dB-Hz. (The modem obviously was not designed to achieve this performance.)[2] Satisfaction of the specification with a tone-ranging format will thus require considerably wider signal bandwidths. Tone integration time cannot be significantly lengthened due to the necessity to acquire and process each user response in 0.5 sec.

6.7 RANGING EXPERIMENT CONCLUSIONS

The flight test performance of two distinct ranging techniques has been determined over a 6-month test program. Type I tests were performed with operational-class aircraft antennas. Type II tests measured performance on the multipath channel by inducing various multipath levels with a second antenna.

Results of the TSC ranging test showed that rms range error was typically 100 m at 43 dB-Hz carrier-to-noise density ratio in the narrowband mode (19.53-kHz clock). In the wideband mode (156.25-kHz clock), the rms error was reduced to roughly 30 m at the same condition. These results are generally larger than corresponding laboratory measurements, particularly so for the wideband mode. Possible reasons for this discrepancy are offered in section 6.5.

NASA ranging tests exhibited a typical rms error of 276 m in the 42 to 44 dB-Hz region, a performance measure in reasonable agreement with theoretical expections.

The NASA modem exhibited a rather high frequency of blunder error, perhaps due to incorrect ambiguity resolution. This was also observed to a lesser degree with the TSC modem when the modem was operated in a mode forcing reacquisition of the code on each measurement.

---

[2]The current AEROSAT system ranging performance specification was not applicable during the design phase of this modem.

7. MULTIPATH CHARACTERISTICS OF OCEANIC CHANNEL

The flight test measurement program has provided the data necessary to validate analytical and computer models for the channel multipath. The measured channel parameters can therefore be used to evaluate the degree of system performance degradation due to multipath over the range of expected operational conditions. This topic is addressed in the following discussion which relates to performance degradation for data communications and range measured in position-location systems.

7.1 SUMMARY CHARACTERISTICS OF OCEANIC CHANNEL

Based on the data analysis (vol. V) for the oceanic channel, it can be assumed that the channel consists of a direct propagation path between the satellite and aircraft, in parallel with the complex Gaussian wide-sense stationary uncorrelated scattering (WSSUS) channel with associated mean delays and Doppler shifts (ref. 7-1).

To simplify notation, the direct-path signal is normalized to unity gain, zero delay, and zero Doppler shift. Naturally, Doppler shifts will be present on this path, but here it is assumed that they are accounted for by an appropriate tracking loop.

Figure 7-1 depicts the assumed mathematical model of the channel relating input and output complex envelopes. Shown is a nonfading channel, corresponding to the direct path in parallel with a fading dispersive channel in which differential path delay τ_s, path gain G_s, and Doppler shift ω_s have been explicitly indicated by separate operations. The time-variant fading channel is thus defined to have a spectrum centered at ω_s and a delay power spectrum centered at τ_s, i.e., for a time-varying transfer function $T(f,t)$ and impulse response $g(t,\tau)$ representing the scattering channel as shown in figure 7-1, it is assumed that

$$\int_{-\infty}^{\infty} \tau\, Q(\tau)\, d\tau = 0$$

and

$$\int_{-\infty}^{\infty} \omega\, D(\omega)\, d\omega = 0 \ .$$

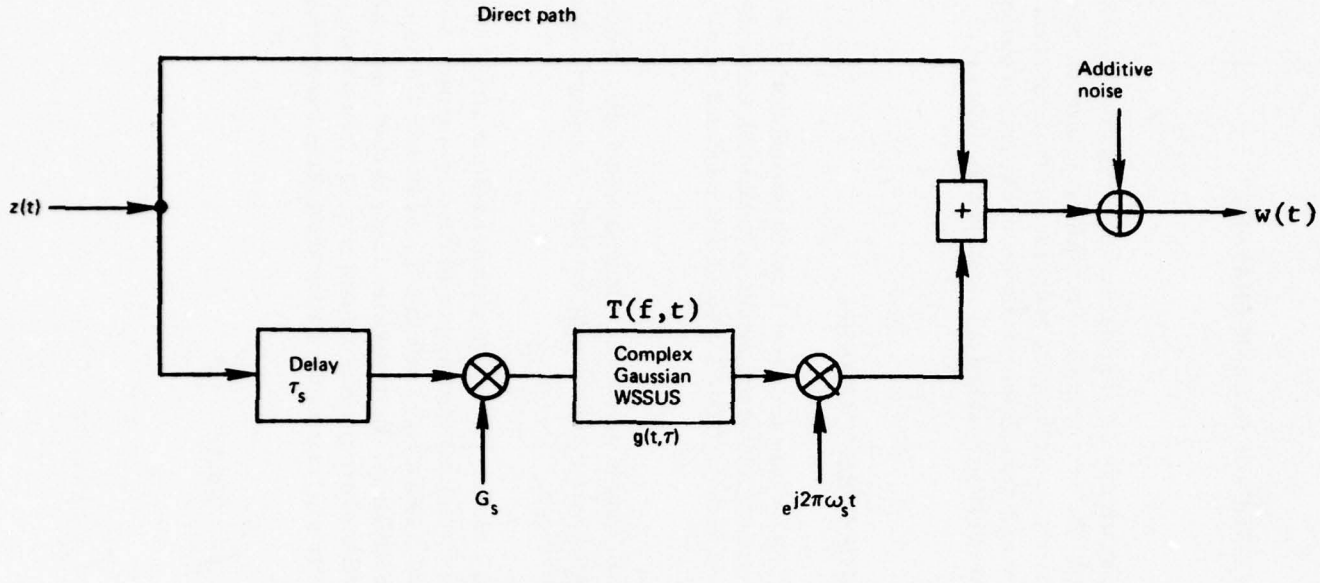

Figure 7-1. Channel Model

where $Q(\tau)$ and $D(\omega)$ are the delay power spectrum and Doppler spectrum, respectively (ref. 7-1). Note that in this discussion D and Q are not normalized to have unity area.

Discussion of performance degradation resulting from multipath can be carried out in terms of the following parameters and functions:

S/I Ratio:

$$S/I = \frac{\text{Direct path power}}{\text{Total indirect path power}}$$

$$= \frac{1}{|G_S|^2 \int_{-\infty}^{\infty}\int_{-\infty}^{\infty} S(\tau,\omega)\, d\tau\, d\omega}$$

$$= \gamma_S . \qquad (7\text{-}1)$$

Differential Delay and Doppler Shifts: τ_S, ω_S.

Scattering Function: $S(\tau,\omega)$.

Performance calculations may require knowledge of the shape of $S(\tau,\omega)$, margin functions such as $Q(\tau)$ and $D(\omega)$, Fourier transformations of $S(\tau,\omega)$ (ref. 7-1), or simple gross parameters such as Doppler spread.

Table 7-1 summarizes differential delay, Doppler, and the corresponding spreads as determined from the channel measurement program at various grazing angles. These pertain to the horizontal component of the reflected signal and are for cross-plane flights, i.e. perpendicular to a radial to the subsatellite point. Parameters shown may be considered typical of other conditions as well.

Before pursuing the performance on the oceanic channel, a few comments on antenna effects are in order. The S/I achieved at the receiver terminals is the ratio of direct path signal to total indirect signal. The latter depends on the coupling of the antenna's complex polarization response with the polarization properties of the scattered signal. Thus, the orientation and sense of the polarization ellipse is crucial as well as the gain difference between direct and indirect path angles.

It is also noted that at low grazing angles, the polarization of the aircraft antenna becomes predominantly vertical due to boundary conditions implied by the airframe. The scattered signal energy, however, resides primarily in the horizontal components. These facts, plus the sense-reversal phenomenon (vol. V), generally increase S/I beyond that predicted by gain difference considerations.

TABLE 7-1. TYPICAL SCATTER SIGNAL PARAMETERS FOR THE AERONAUTICAL CHANNEL

Altitude: 10 km; Velocity: 200 m/sec; Frequency: 1600 MHz

Grazing angle, deg	RMS scatter coefficients, dB		Differential delay, μsec	3-dB delay spread, μsec	3-dB Doppler spread, horizontal polarization, Hz[a]	
	Vertical	Horizontal			In-plane	Cross-plane
5	-14.0	-4.0	5.3	0.35	2.5	40
10	-10.5	-2.5	11.3	0.60	6.5	75
15	- 8.0	-2.0	17.1	0.75	15	125
20	- 6.0	-1.8	22.6	0.83	65	150

[a]For in-plane geometries, there is a differential Doppler of approximately 3.5 Hz.

Thus, the proper approach is to map the response of a *specific* operational antenna onto the scattering characteristics of the surface using the respective complex polarization vectors at various azimuths and elevations. This procedure is detailed in appendix A, volume VII. Surface integration can then provide the total scattered signal seen at the receiver, as well as its delay-Doppler character if necessary. An approach that usually suffices and avoids time-consuming numerical integration is to use the antenna response in the direction of the specular point. The assumption is that response does not vary significantly over the effective scattering region.

7.2 NARROWBAND DATA TRANSMISSION PERFORMANCE

The channel characteristics developed and summarized in section 7.1 will now be applied to a performance evaluation of narrowband data transmission through the satellite aeronautical channels. The discussion will be restricted to 1200- and 2400-bps transmission rates and, based on earlier channel characterization efforts, the channel will be assumed to be flat fading with complex Gaussian statistics. This implies specular delay and delay spread are both small relative to a bit interval. With these assumptions, communication performance is determined primarily by signal-to-noise ratio, signal-to-multipath ratio (S/I), and the bandwidth of the Doppler spectrum. Other effects causing degradation, such as nonideal satellite transponder characteristics, are not included in this discussion.

7.2.1 Candidate Modulation Schemes

Attention has been restricted to two different modulation/demodulation schemes:

Frequency-Shift Keying (FSK): Demodulation is assumed incoherent.

Differential Phase-Shift Keying (DPSK): Demodulation is achieved by comparison of the current and previous bit phase angles.

Coherent Phase-Shift Keying (CPSK): Demodulation is achieved with a Costas loop coherent reference, plus integrate-and-dump detection. Data may be differentially encoded and decoded to eliminate phase-lock ambiguity (DECPSK)

Communication performance for each of these schemes will be related to the measured channel characteristics in the following two sections.

7.2.1.1 Frequency-Shift Keying – The first mode of communication, incoherent FSK, is immune to the effects of multipath except for performance degradation resulting from slow fading of the data signal. Because of the orthogonal signal structure, FSK is generally 3 dB worse in performance than the other methods. Phase decorrelation and tracking noise effects may arise in DPSK and DECPSK and reduce their advantage over FSK. Full discussion of performance for this type of modulation can be found in references 5-4, 7-2 (pp. 4-3 and 4-6), and 7-3.

7.2.1.2 Differential Phase-Shift Keying – In the DPSK phase-modulation technique, the binary data is detected by comparing the carrier phase of a received bit with the carrier phase of the preceding bit. The receiver, therefore, takes advantage of the differential phase coherence of successive bits to detect a phase change without requiring knowledge of absolute carrier phase. The channel parameters affecting performance are known to be signal-to-noise and the correlation function of the time-varying channel multiplicative gain. With Gaussian channel statistics, this gain introduces two effects: Ricean fading of the signal with consequent error-rate degradation and decorrelation of phase between bits, which can further degrade performance. As fading becomes very rapid, improvement is actually observed since the energy is outside the effective data filter bandwidth (ref. 7-4).

The performance of a DPSK modulation scheme in the absence of bit-to-bit decorrelation is well known (refs. 7-3 and 7-5). The appropriate error probability is identical to FSK except for a 3-dB signal-to-noise advantage. The error probability may be written as

$$P_e = \tfrac{1}{2}\left[1 + \frac{E_b/N_o}{S/I}\right]^{-1} \cdot \exp\left[\frac{E_b/N_o}{1 + (E_b/N_o)/(S/I)}\right].$$

The consequences of bit-to-bit decorrelation, resulting from multipath phenomena, have been discussed at length in reference 7-6 and presented in a concise form relevant to the aeronautical channel in reference 7-2. Performance loss can be related to a single parameter, rms Doppler bandwidth, when the total Doppler spectrum is symmetrical about the direct-path frequency. An error probability plot for typical fading bandwidths is found in section 5.6.

For in-plane flights, the form of the Doppler spectrum has been shown to be asymmetrical and it is of interest to examine the consequences of the asymmetry. For narrowband communication, the signal bit duration will be small compared with the fading time constant, and the complete channel Doppler spectrum description can again be suppressed in favor of a simplified two-parameter

description. The received signal consists of a direct-path component and a weaker multipath return. Bit-to-bit correlation is determined by the properties of the composite signal. If it is assumed that direct-path Doppler shifts are tracked out by the receiver, then the direct-path frequency represents the origin in a discussion of spectral characteristics. The multipath spectrum will not be centered around this origin because of differential Doppler shifts and the asymmetrical spectrum shape. It can be shown, however, that the only important parameters are mean Doppler shift (centroid of multipath Doppler spectrum) relative to the direct-path frequency and the rms spread of the Doppler spectrum.[1]

The multipath component enters into performance calculations in two different ways:

a. The centroid of the Doppler spectrum (relative to the direct path) introduces a rotation of the signal decision vector, the amount of rotation being given by the relative magnitudes of S/I and the first moment of the spectrum. At the rates considered here, however, this rotation is less than 1^{o} and can be ignored.

b. The spectral width of the scattered component introduces an equivalent noise component, determined by the S/I ratio and the second moment of the spectrum around the direct-path Doppler frequency. Thus the analysis of reference 7-6 applies, with substitution of appropriate in-plane Doppler spreads.

7.2.1.3 Coherent Phase Shift Keying – The final approach requires that the receiver acquires knowledge of the transmitted carrier phase. This is achieved either by transmitting a residual carrier or by implementing suppressed carrier tracking loop (squaring or Costas loop). The phase reference derived from the tracking loop is used to coherently demodulate the data signal and, thus, performance is affected by properties of the phase reference. This latter quantity is determined by the instantaneous direct and indirect path gains and their relative phase.

If the tracking loop recovers the composite signal phase perfectly on an instantaneous basis, bit error performance is dependent only on the amplitude statistics in relation to the noise. Invocation of a slow fading assumption (i.e., amplitude nearly constant over a bit duration) allows calculation of error probability. Details are found in reference 7-7.

Perfect tracking implies a loop bandwidth large relative to the fading bandwidth. This is often practically unacceptable due to loop noise threshold effects, thus a more complex dependence on loop bandwidth enters. Reference 7-8 analyzes the DECPSK situation where B_L is on the order of the Doppler spread and provides some supplementary simulation. At low E_b/N_o and S/I, bit error rate is quite insensitive to B_L, while at higher S/I and E_b/N_o the dependence is more definite.

It is shown in reference 7-8 that, ignoring the increasing noise jitter in the loop, the error probability is minimized by having B_L greater than the fading bandwidth. Also, over the region of interest for AEROSAT, $B_L = 3\ B_F$ gives essentially the perfect phase knowledge case. Since the analyses of reference 7-8 ignore cycle-slipping effects, the existence of an optimum loop bandwidth versus S/I, E_b/N_o, and Doppler spread is inferred.

[1] Peter Alexander, "DPSK Performance Calculations With Asymmetrical Doppler Spectra," CNR, Inc., internal memorandum, September 1975.

Figures 5-11 through 5-14 provide theoretical prediction for DECPSK when $B_L \simeq 3$ times the fading bandwidth, or $B_L = 150$ Hz typically. Again, it is noted that cycle-slipping events, if any, are ignored.

As a final thought we note that attainment of 10^{-5} BER at 43 dB-Hz, as currently specified for the AEROSAT system, implies S/I = 15 to 16 dB, theoretically, for DPSK (this assumes no coding or other techniques for combating errors). When allowance is made for implementation losses, the required S/I is probably nearer 17 dB.

7.3 *WIDEBAND DATA TRANSMISSION PERFORMANCE*

In this context, wideband implies signal durations that are comparable with the inverse channel bandwidth. Because a complete analysis of bit-error performance depends on the details of the communications scheme, such as modulation type and receiver structure, no attempt will be made to cover the complete range of wideband configurations. Instead, a particular example will be presented: 38.4 kbps data transmission using coherent quadriphase modulation techniques. This signal is compatible with the 40-kHz (1-dB) bandwidth of the AEROSAT communication channel.

It is assumed that an ideal phase reference locked to the direct path can be obtained by means of a suitable tracking loop. We note, however, that the quadriphase error rate is more sensitive to carrier phase tracking error than is the error rate of binary PSK.

Implicit in the expressions presented here[2] *is the assumption of slow fading*; i.e., for analytical purposes the channel impulse response is time-invariant over the bit duration. Bit-error performance then depends primarily on thermal noise and selective fading phenomena, which are manifest as intersymbol interference. Error probability on any bit will be a function of the transmitted symbol on that time interval as well as the relative phase of the preceding symbol; i.e., there are three error probabilities to consider. The channel parameters that determine conditional error probabilities are:

$$E(1) = \int_0^T Q(\tau)\, d\tau \tag{7-2}$$

$$E(-1) = \int_0^T Q(\tau) \left[1 - \frac{2\tau}{T}\right]^2 d\tau \tag{7-3}$$

$$E(\pm j) = \int_0^T Q(\tau) \left[1 - \frac{2\tau}{T} + 2\left(\frac{\tau}{T}\right)^2\right] d\tau\,, \tag{7-4}$$

[2]Derived from P. A. Bello, "Effect of Multipath on QPSK Data Transmission Over the AEROSAT Channel," CNR, Inc., internal memorandum, October 20, 1975.

where:

T = bit duration

$Q(\tau)$ = multipath delay power spectrum referenced to the direct path.

The symbols in parentheses indicate the type of phase transition between adjacent bits. For example, $\pm j$ symbolizes a $\pm 90^{o}$ phase transition between the current bit and its predecessor. The conditional error probabilities can be expressed in terms of these parameters:

$$\text{Prob (error}|1) = \phi\left(\sqrt{\frac{a^2}{\int_o^T Q(\tau)\, d\tau + \frac{2N_o}{T}}}\right)$$

$$= \phi\left(\sqrt{\frac{1}{\frac{I}{S} + \frac{1}{\rho}}}\right) . \qquad (7\text{-}5)$$

$$\text{Prob (error}|{-1}) = \phi\left\{\left[\frac{I}{S}\frac{\int_o^T Q(\tau)\left(1 - 2\frac{\tau}{T}\right)^2 d\tau}{\int_o^T Q(\tau)\, d\tau} + \frac{1}{\rho}\right]^{-1/2}\right\}$$

$$= \phi\left\{\sqrt{\frac{1}{\frac{I}{S}\frac{E(-1)}{E(1)} + \frac{1}{\rho}}}\right\} . \qquad (7\text{-}6)$$

$$\text{Prob (error}|\pm j) = \phi\left\{\left[\frac{I}{S}\frac{\int_o^T Q(\tau)\left(1 - \frac{2\tau}{T}\right)^2 d\tau}{\int_o^T Q(\tau)\, d\tau} + \frac{1}{\rho}\right]^{-1/2}\right\}$$

$$= \phi\left\{\sqrt{\frac{1}{\left(\frac{I}{S}\right)\left[\frac{E(\pm j)}{E(1)}\right] + \frac{1}{\rho}}}\right\} , \qquad (7\text{-}7)$$

where:

$$\phi(x) = \int_x^\infty \frac{1}{\sqrt{2\pi}} \exp(-y^2)\, dy$$

$$= \text{erfc}(x) \,, \qquad (7\text{-}8)$$

and

α^2 = direct-path power

N_o = thermal noise power density

T = bit duration

$\frac{S}{I}$ = signal-to-multipath ratio = $\alpha 2/E(1)$

ρ = bit signal-to-noise ratio = $\alpha^2 T/2N_o = 2\,(E_b/N_o)$.

The conditional error probabilities can now be combined to form an expression for the total error probability; i.e.,

$$\text{Prob (error)} = \frac{1}{4}\,\text{Prob (error}|1) + \frac{1}{4}\,\text{Prob (error}|{-1}) + \frac{1}{2}\,\text{Prob (error}|\pm j). \qquad (7\text{-}9)$$

The multipath data for March 31, 1975, has been processed to yield the parameters given by equations (7-2) through (7-4) and the error probabilities derived from equations (7-5), (7-6), (7-7), and (7-9). Performance was evaluated over a range of S/I and C/N_o values, and the results are illustrated in figure 7-2.

7.4 APPLICATION TO TONE RANGING SYSTEMS

A brief account of multipath effects is given below for two specific types of ranging systems: tone ranging and PN ranging. The analysis details may be found in references 7-2 and 7-9 (secs. 2 and 3).

7.4.1 Effects of Multipath on Tone Ranging Performance

The multipath signal has a disrupting influence on tone ranging systems in two distinct ways: (1) rms range error is increased and (2) ambiguity error probabilities are increased.

For the AEROSAT system it is evident that adequate signal-to-noise ratios (S/N) can be achieved only by filtering the received tones to a narrow bandwidth, typically on the order of 5 to 10 Hz. The requirements for acquisition of the carrier and the necessity of having several tones for adequate system resolution imposed significant restrictions on the way in which power can be allocated to the various tones. The typical result is that a large portion of the total power budget must remain in the carrier to provide adequate margin for acquisition, leaving the ranging tones at a relatively low level. Satisfactory tone signal-to-noise ratios are then obtained through the use of narrow detection bandwidths.

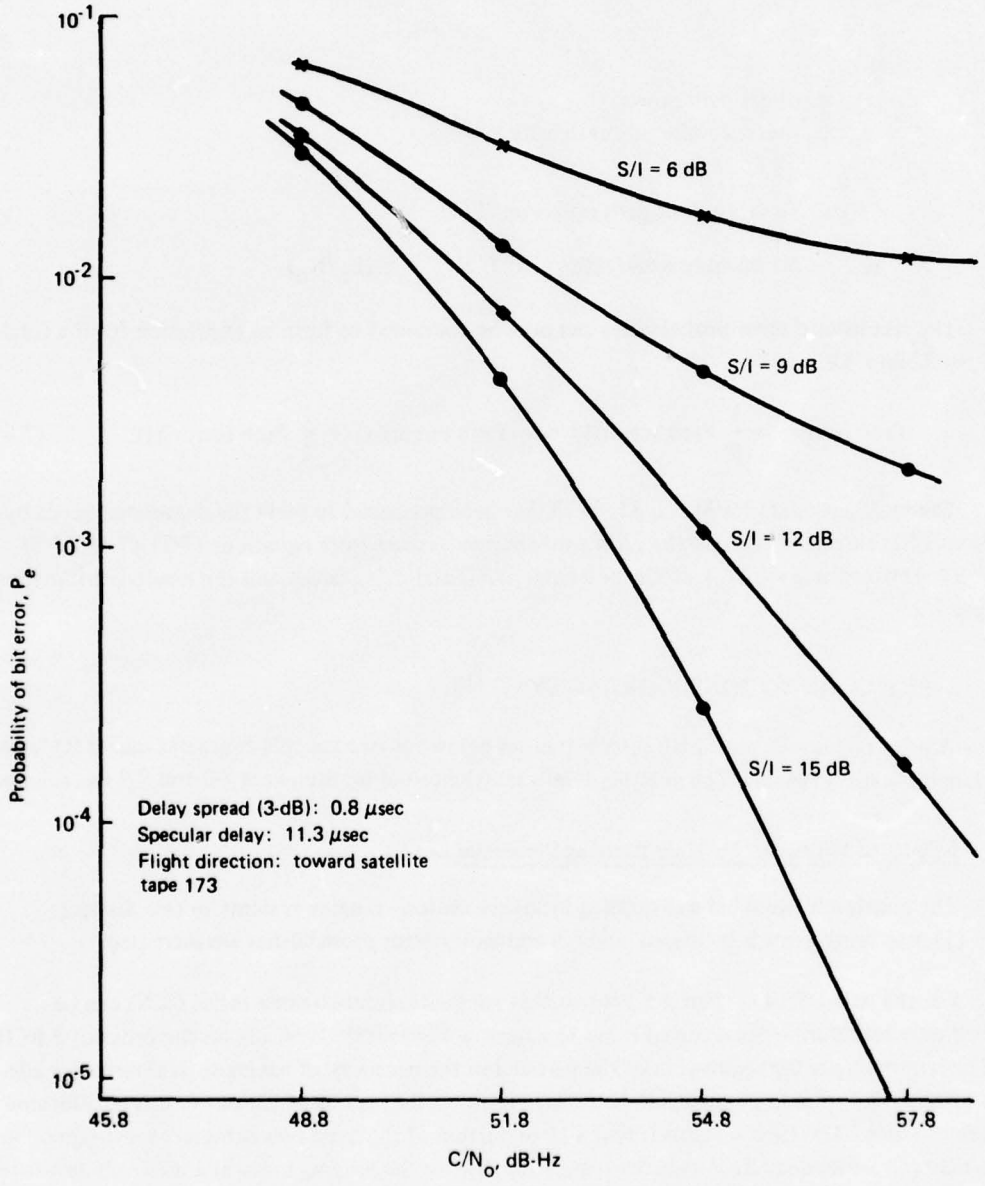

Figure 7-2. Error Probability, 38.4 kbps Quadriphase Shift Keying, March 31, 1975

7.4.2 RMS Tone Ranging Error

Calculation of ranging error requires knowledge of antenna characteristics along with measured channel parameters and functions. As explained in section 7.1, a simplified approach is used here that results in performance as a function of the S/I ratio, γ_S. In addition, representative channel behavior is obtained using the validated channel characteristics that would be obtained with an omnidirectional antenna.

In reference 7-2, single-sideband (SSB), one-way ranging errors are derived. These results are valid at all S/N, γ_S, and channel dispersive conditions. It is shown in section 2.7 of reference 7-2 that at S/N = ∞ and large γ_S, the ranging errors for a double-sideband system with tone frequency F will be very nearly the same as those for a single-sideband system with tone frequency 2F. For the range of S/N values expected at the tone filter outputs, this equivalence of performance will be valid. In the curves to be presented, we have used this approximate equivalence at all values of γ_S for an 8-kHz double-side and system. Thus, at low values of γ_S (< 10 dB), it should be understood that the rms error results are strictly correct only for a SSB system using 16-kHz tone frequency spacing.

Figure 7-3 presents calculated rms and bias one-way ranging errors as a function of multipath ratio γ_S for a 10° elevation angle, assuming an rms sea slope of 0.1 and an aircraft height of 30,000 ft. An 8-kHz ranging tone is assumed. The calculation for a different ranging tone frequency involves the multipath channel's frequency correlation function, as discussed in reference 7-9. No reduction in the strength of the multipath signal by the tone filter is assumed in the results. To approximately take account of such filtering, γ_S can be increased by the ratio of Doppler spread to tone filter bandwidth. With the Doppler spreads indicated in previous sections, it would appear that γ_S will be enhanced by approximately 6 to 10 dB, depending on the elevation angle and filter bandwidths.

The equations for tone ranging performance contained in reference 7-2 were applied to the multipath data acquired on March 31, 1975. The scattering function was obtained from an average of the tap spectra. After removal of the noise plateau, the scattering function was set to zero outside a bandwidth of 15 Hz, and the resulting function was integrated in frequency to form a modified delay power spectrum. This function was, in turn, Fourier-transformed to yield the modified frequency-correlation function.

Performance, in terms of rms ranging error, was then computed as a function of tone-separation frequency, S/I, and S/N. The results are illustrated in figures 7-4 and 7-5.

7.4.3 Ambiguity Error Considerations

In section 7.4.2, the rms ranging error was applied to the fine, but ambiguous, tone ranging estimate. To resolve these ambiguities, additional tones are used with sufficiently close spacing between tones so that the phase between these tones can resolve the ambiguities in the fine-ranging estimates. Due to the noise and multipath, there is a finite probability that this ambiguity will not be resolved correctly. This occurs when the coarse-ranging error exceeds one-half the inherent ambiguity

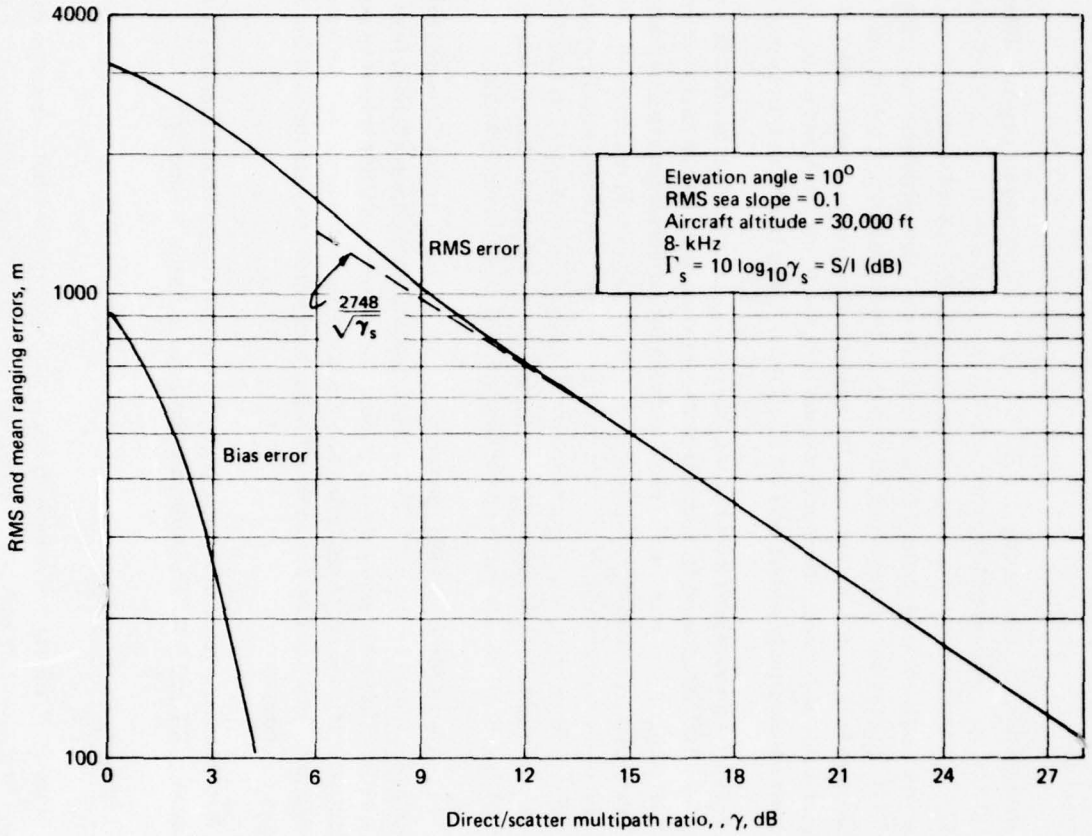

Figure 7-3. RMS and Bias Ranging Errors as a Function of Direct/Scatter Ratio for a Tone Ranging System

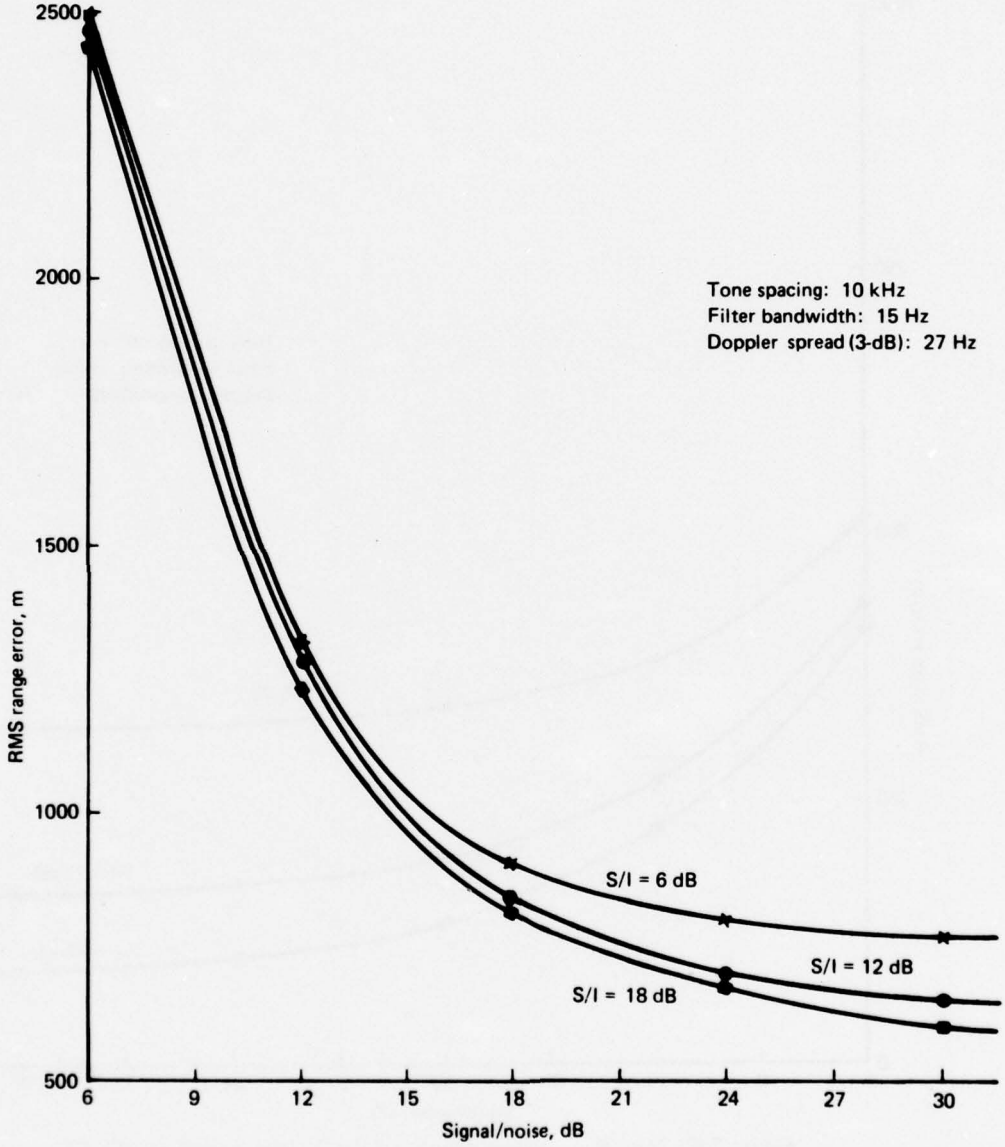

Figure 7-4. Tone Ranging Performance, Δf = 10 kHz, March 31, 1975

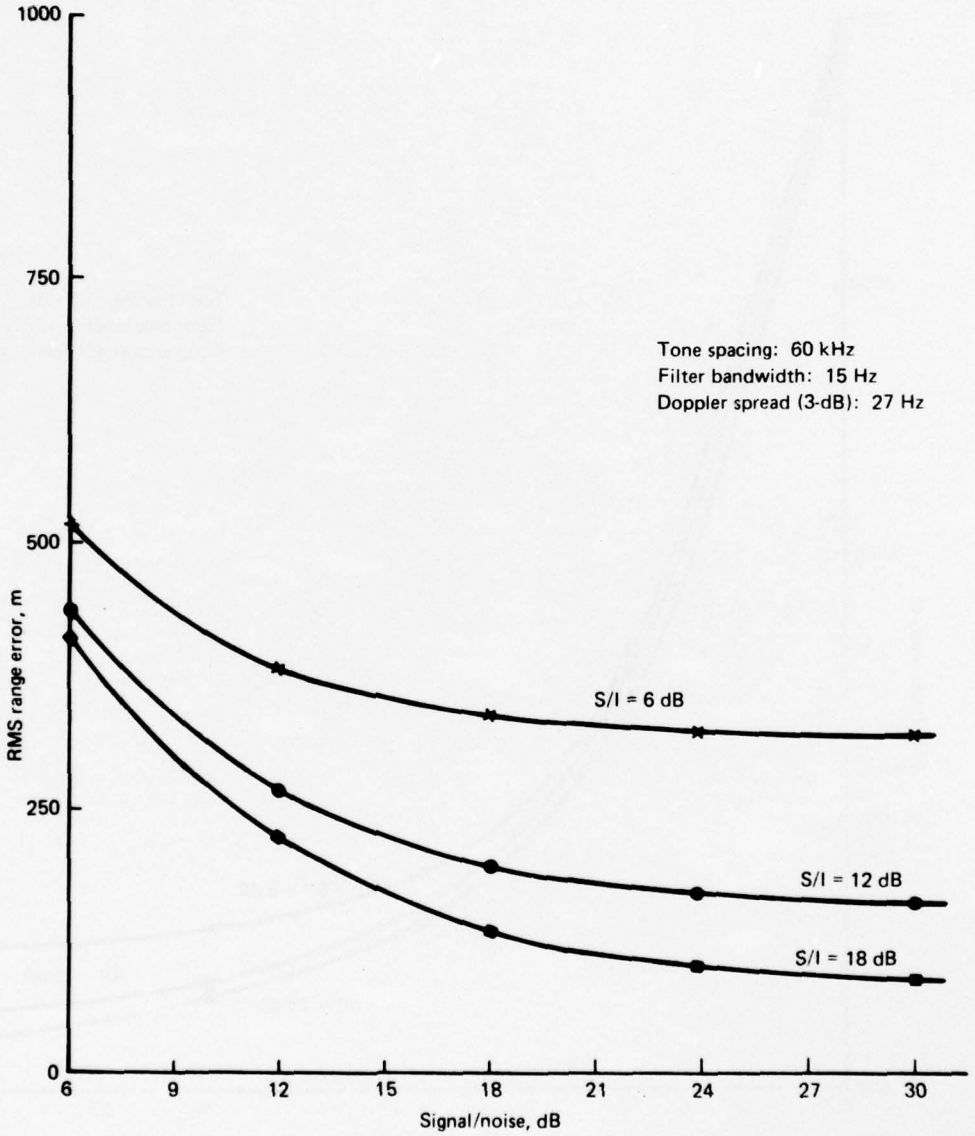

Figure 7-5. Tone Ranging Performance, Δf = 60 kHz, March 31, 1975

of the fine-ranging-tone pair. In fact, a series of range measurements may be made with increasing coarseness (larger ambiguity) to achieve the desired ambiguity resolution. Errors may occur at any step of this process when the error in the coarser range measurements exceeds one-half the ambiguity of the finer measurement. In a properly designed system, this event should occur with very low probability. Thus, we are led in this section to consider the "tails" of the ranging error probability distribution.

The results presented in reference 7-9 make it possible to calculate exact range error probability distributions for the single-sideband tone ranging system, and these may be integrated numerically to find the probability that any given range error is exceeded. As an example, we consider the same geometry and sea-state conditions assumed for figure 7-3. The same assumptions regarding the delay power spectrum and the complex Gaussian model for the diffuse multipath signal were made as in section 7.4.2. Figure 7-6 shows plots of the probability that the magnitude of the ranging error will exceed a specified multiple of the rms ranging error. Each curve is for a different direct/multipath ratio γ_s for a 30,000-ft altitude, 10^{o} elevation angle, and an rms sea slope of 0.1. The corresponding error probability curve is also shown for a Gaussian probability distribution of ranging error. It is noted that if extremely small probability of ambiguity resolution error is desired, use of a Gaussian distribution can give overly optimistic predictions. With the current AEROSAT system specification of 10^{-2} probability of error, the Gaussian approximation is reasonably accurate, however.

To illustrate the influence of ambiguity error on system design, we consider the following example. Suppose it was desired to upgrade the 16-kHz SSB system discussed in section 7.4.2, adding a higher frequency tone to improve fine-ranging accuracy and retaining the 16-kHz SSB tone to provide ambiguity resolution. Using figure 7-6, it is possible to calculate the maximum tone frequency that may be used while achieving a given probability of ambiguity errors; results are shown in table 7-2. In obtaining these results, a 7-dB improvement in direct-to-scatter ratio due to tone filtering is assumed. If, for example, a tone frequency of 70 kHz were required to achieve the fine-ranging requirements, an ambiguity error probability of approximately 10^{-3} would be achieved for an S/I of 7 dB, while an error probability of 10^{-7} would be achieved for an S/I of 12 dB.

TABLE 7-2. MAXIMUM FINE-RANGING FREQUENCY ALLOWED IN SSB TONE RANGING TO ACHIEVE LESS THAN A GIVEN AMBIGUITY ERROR PROBABILITY AT SPECIFIED S/I

Probability of ambiguity error	Frequency allowable to achieve given error probability, kHz	
	S/I = 12 dB	S/I = 7 dB
10^{-3}	132	68
10^{-5}	90	42
10^{-7}	70	32

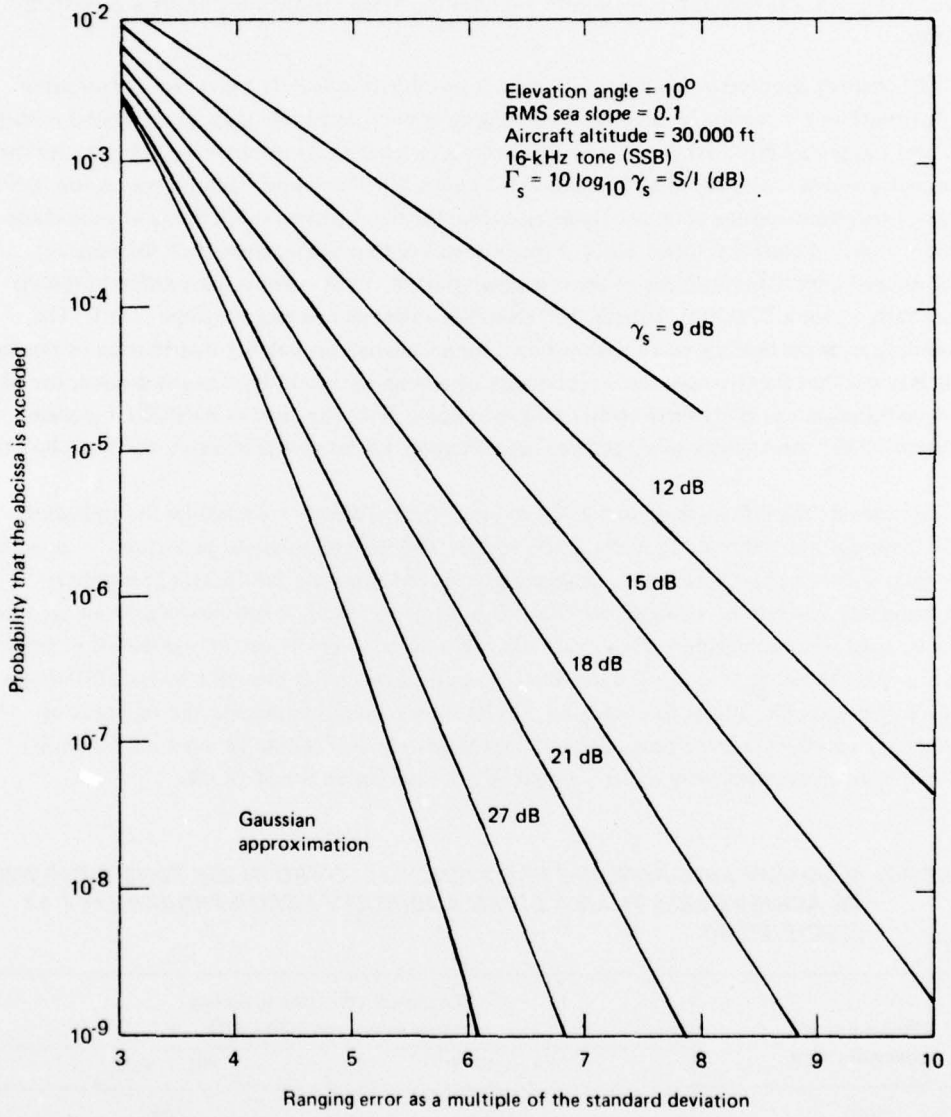

Figure 7-6. Probability of Exceeding a Given (Absolute) Ranging Error

7.5 EFFECT OF MULTIPATH ON A PSEUDO-NOISE RANGING MODEM

The analysis carried out in reference 7-2 allows prediction of pseudo-noise (PN) ranging modem performance under the same conditions assumed in section 7.4.1 for a tone ranging modem. In section 7.4.1, it was assumed initially that the tone filters do not reduce the strength of the multipath signal. In this section, we make the equivalent assumption that the loop filter of the receiver code tracking loop passes the multipath component without distortion.

The equations shown in reference 7-2 (p. 3-23) have been used to calculate the rms ranging errors shown in figure 7-7. The theory assumes a flat-fading channel again. The assumed elevation angle, sea slope, and aircraft height are the same as for figure 7-3. The reader is cautioned in extending this result to other geometries and chip rates; the dependence on these parameters is not simply a scaling relationship. Details of the PN receiver model may be found in reference 7-2; the receiver bandpass filter is assumed to be Gaussian with a 3-dB RF bandwidth equal to 1.5 times the PN pulse rate.

It is noted that the example presented is one in which the multipath return is only a small fraction of a chip delayed relative to the direct signal. Thus, the multipath signal is not decorrelated in the code tracking process as would be the case if the specular delay were equivalent to several code chips.

Also in figure 7-7, no additional improvement is assumed for narrowband filtering, which is usually implied by the code-tracking loop. The effective S/I gain is, as for tone ranging, the ratio of the effective filter bandwidth to effective Doppler bandwidth.

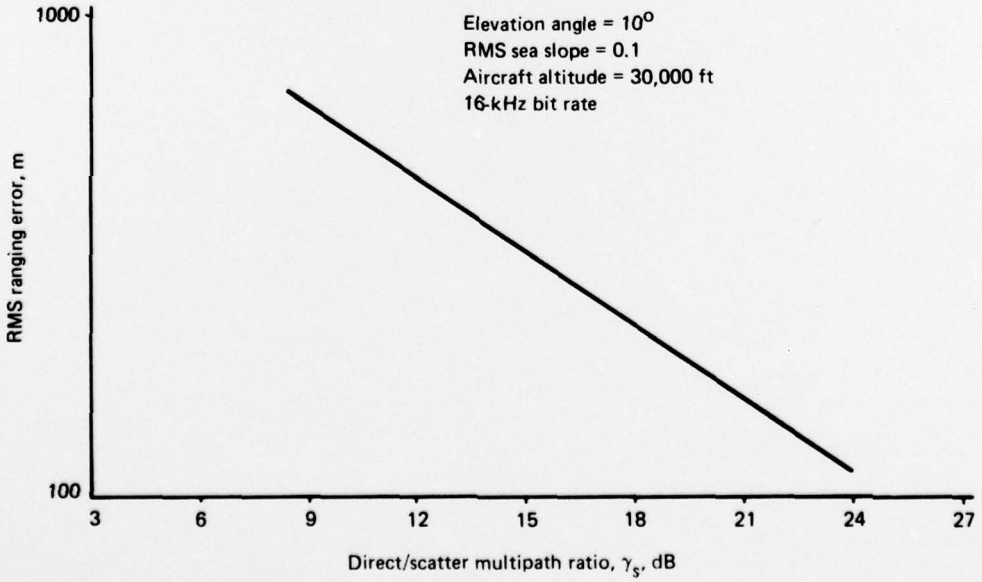

Figure 7-7. RMS Ranging Error as a Function of Direct Path/Scatter Ratio for Pseudo-Noise Ranging System

Ambiguity error resolution does not arise for PN ranging as it does for tone ranging. The range measurement is unambiguous over the code sequence length. For certain multipath conditions, however, additional stable tracking points can occur corresponding to the specular-point delay. For the normal S/I's encountered, one can easily detect whether the proper null point is being tracked by scanning delay cells corresponding to smaller time delays for the presence of the strong direct signal.

REFERENCES

1-1 "Integrated Test Plan for ATS-F L-Band Experiment," report TP-750-73-1, NASA/GSFC, September 1973.

3-1 "ATS-5 Multipath/Ranging/Digital Data L-Band Experimental Program, Volume III: Terminal Design," final report FAA-RD-73-57-III, Boeing Commercial Airplane Company, April 1973.

3-2 "ATS-5 Multipath/Ranging/Digital Data L-Band Experimental Program, Volume V: Multipath/Ranging Analysis and Results," final report FAA-RD-73-57-V, Boeing Airplane Company, April 1973.

3-3 P. Milner and J. S. Golab, "Intelligibility of Voice Transmissions Through a Satellite Relay System," paper presented at the 89th Meeting of the Acoustical Society of America, University of Texas, April 1975.

4-1 M. Melnick, "Intelligibility Performance of Variable Slope Delta Modulation," Proc. IEEE Intl Conf. Communications, 1973, p. 46-5 and 46-7.

4-2 G. A. Miller and J. C. R. Licklider, "The Intelligibility of Interrupted Speech," JASA, vol. 22, no. 2, March 1950, p. 167-173.

5-1 "ATS-5 Multipath/Ranging/Ditial Data L-Band Experimental Program, Phase IVD, Volume 1: Satellite/Aircraft L-Band Data Communication Tests," final report FAA-RD-73-57-IVD, Boeing Commercial Airplane Company, April 1973.

5-2 H. C. Salwen and C. B. Duncombe, "Performance Evaluation of Data Modems for The Aeronutical Satellite Channel," IEEE Trans. on Communications, July 1975, p. 695-705.

5-3 W. C. Lindsey and M. K. Simon, TELECOMMUNICATION SYSTEMS ENGINEERING, Prentice-Hall, Englewood Cliffs, New Jersey, 1973, p. 246-248.

5-4 L. A. Frasco and H. D. Goldfein, "Signal Design for Aeronautical Channels," IEEE Trans. on Communications, May 1973, p. 534-547.

5-5 W. C. Lindsey, "Error Probabilities for Coherent Receivers in Specular and Random Channels," IEEE Trans. on Information Theory, January 1968, p. 147-150.

REFERENCES (Continued)

5-6 J. J. Bisaga, H. A. Blank, and A. J. Brown, "Access Control and Processing Studies for Ground-Satellite Mobile Communications/Surveillance Systems," Dept. of Transportation report FAA-RD-74-106, June 1974, p. 4-8 and 4-10.

5-7 J. C. Blair and J. F. Balcewicz, "Results of an Experimental Study of Coherent PSK in a Multipath Environment," EASCON '68 Record, p. 607-614.

5-8 Bell Aerospace Company, PLACE Final Report," report 6225-950002, June 1970.

5-9 E. H. Schroeder et al., "U.S. Aeronautical L-Band Satellite Technology Test Program – Interim Test Results," interim report FAA-RD-75-111, June 1975.

5-10 J. Salz and B. R. Saltzberg, "Double Error Rates in Differentially Coherent Phase Systems," IEEE Trans. on Communication Systems, June 1964, p. 202-295.

6-1 J. J. Stiffler, THEORY OF SYNCHRONOUS COMMUNICATION, Prentice Hall, Englewood Cliffs, N. J., 1971, p. 184-191.

7-1 P. A. Bello, "Aeronautical Channel Characterization," IEEE Trans. on Communications, vol. COM-21, no. 5, May 1973, p. 548-563.

7-2 P. A. Bello et al., "Impact of Satellite Aeronautical Channel on Modem Specifications, Phase I," report FAA-RD-74-54, March 1974.

7-3 J. J. Jones, "Multichannel FSK and DPSK Reception with Three Component Multipath," IEEE Trans. on Communication Tech., vol. COM-16, no. 6, December 1968, p. 801-821.

7-4 H. Salwen, "Differential Phase Shaft Keying Performance Under Time-Selective Multipath," IEEE Trans. on Communications, vol. COM-23, no. 3, March 1975, p. 383-385.

7-5 H. B. Voelcker, "Phase Shift Keying in Fading Channels," Proc. IEE, part B, vol. 107, January 1960, p. 31-38.

7-6 P. A. Bello and D. B. Nelin, "The Influence of Fading Spectrum on the Binary Error Probabilities of Incoherent and Differentially Coherent Matched Filter Receivers," IRE Communication Systems, vol. CS-10, June 1962, p. 160-168.

REFERENCES (Concluded)

7-7 W. C. Lindsey, "Error Probabilities for Rician Fading Multichannel Reception of Binary and N-ary Signals," IEEE Trans. on Information Theory, vol. IT-10, October 1964, p. 339-350.

7-8 J. C. Blair and J. F. Balcewicz, "Results of an Experimental Study of Coherent PSK in a Multipath Environment," EASCON '68 Record, p. 607-614.

7-9 P. A. Bello and C. J. Boardman, "Effect of Multipath on Ranging Error for an Airplane-Satellite Link," IEEE Trans. on Communications vol. COM-21, no. 5, May 1973, p. 564-576.

A-1 K. D. Kryter and J. H. Ball, "SCIM – A Meter for Measuring the Performance of Speech Communication Systems," interim report, ESD-TDR-64-674, contract AF 19 (628)-2453, Bolt Beranek and Newman, Inc., October 1964.

A-2 N. R. French and J. C. Steinberg, "Factors Governing the Intelligibility of Speech Sounds, JASA, vol. 19, no. 1, January 1947, p. 90-118.

B-1 A. J. Viterbi, PRINCIPLES OF COHERENT COMMUNICATION, McGraw-Hill, New York, 1966, p. 29.

B-2 J. J. Stiffler, THEORY OF SYNCHRONOUS COMMUNICATION, Prentice-Hall, Englewood Cliffs, N.J., 1971.

APPENDIX A

RESULTS OF SCIM MEASUREMENTS FOR VOICE MODEMS

One method developed for evaluating voice channel performance has been the speech communication index meter (SCIM) (ref. A-1). The technique is based on the articulation index (AI) concept, as described in reference A-2, and uses synthetic speechlike signals to measure the signal-to-noise ratio at the end of the channel at various audio frequencies. This ensemble of signal-to-noise ratio measurements is then used to calculate the articulation index, a value ranging between 0 and 1. Somewhat implicit in the AI concept is the notion that the AI can be related to other psychometric measures of speech performance, e.g., PB word intelligibility, and thus that an automated SCIM scoring approach could eliminate the need for listener panel evaluations.

SCIM signal transmissions were recorded for each modem following transmission of the word lists. The November test data was transcribed and evaluated at NASA/GSFC using a computerized version of earlier hardware analyzers. AI scores provided by NASA were then collated with the PB word intelligibility scores derived at CBS Laboratories during the same test interval; the resultant plot is shown in figure A-1.

The curves of figure A-1 are from reference A-1 and indicate a universal relationship between AI and various intelligibility measures. For the 400-word lists used here, a curve somewhere between the 256- and 1000-word relationships should presumably be used.

It is observed from the data that the results, in total, straddle such an interpolated curve. However, a definite modem dependency seems to exist. For example, a given articulation index for ANBFM corresponds in general to a much lower word intelligibility than that for the Hybrid No. 1 and 2 modems. Thus, this data refutes a universal relationship between AI (as estimated by SCIM) and word intelligibility.

If in the future it is desired to use the SCIM technique for meaningful evaluations of speech modem performance, a minimum requirement appears to be that the AI (as estimated by SCIM) versus intelligibility curve be calibrated accurately for each modem under test.

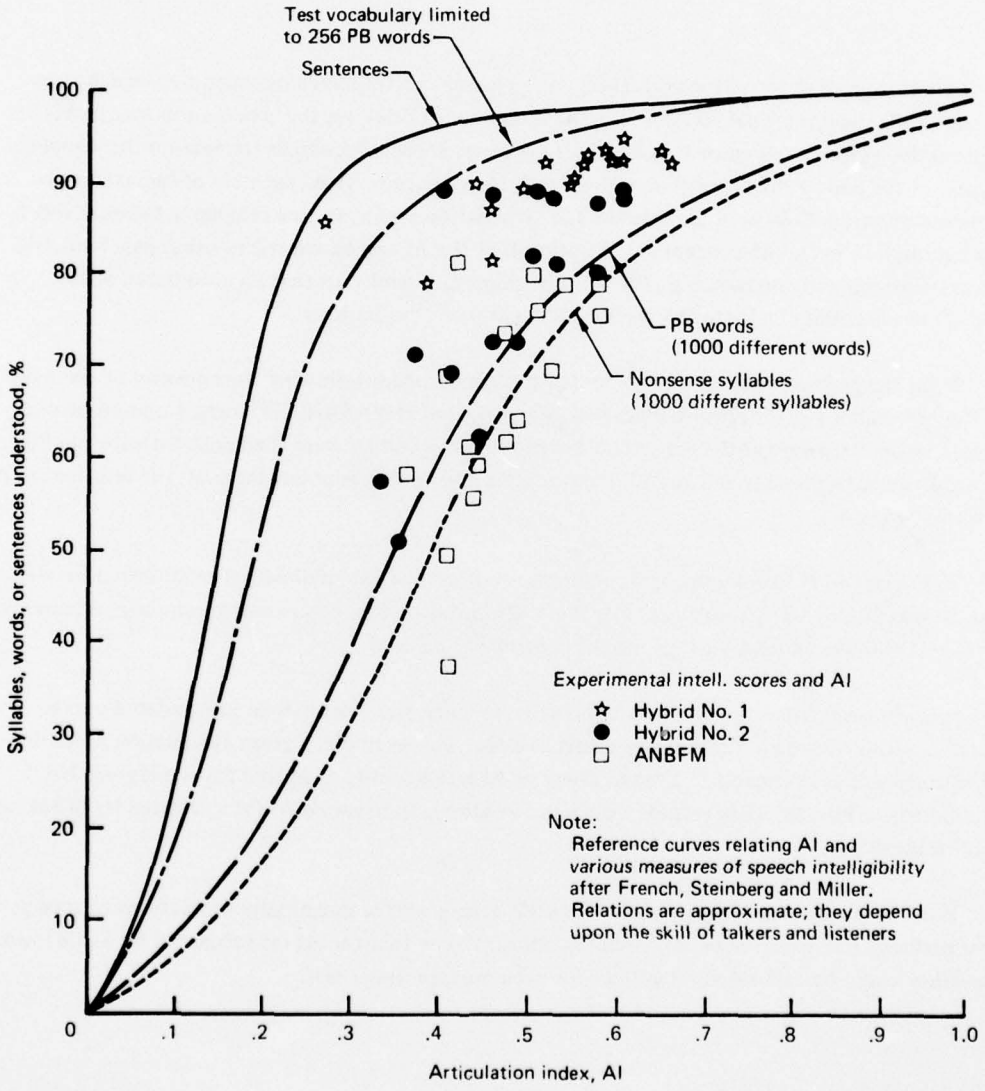

Figure A-1. Voice Modem Intelligibility Scores (400 PB Words) Versus Articulation Index Determined From SCIM Measurements

APPENDIX B

PERFORMANCE ANALYSIS OF TSC RANGING MODEM[1]

A performance analysis for the TSC ranging modem in the additive-noise environment is given in this appendix. The calculations provide a standard of comparison for laboratory and flight test measurements.

The transmitted signal is

$$s(t) = \cos [\omega_c \tau + \beta d(t)] \tag{B-1}$$

where:

β = peak phase deviation
$d(t)$ = a ± 1 range code

$d(t)$ is synthesized by majority voting on square waves that are binary subharmonics of a clock frequency, $f_{c\ell}$. The total number of component frequencies in the code is n. Using narrowband signal representation, the received signal is

$$r(t) = (2C)^{1/2} \cos [\omega_c t + \beta d(t)] + n(t) \tag{B-2}$$

Letting the noise power density (single-sided) of $n(t)$ be a constant N_o (in W/Hz) over the signal bandwidth, we implicitly define a white Gaussian noise channel with carrier-to-noise density ratio of C/N_o (in dB-Hz).

Since $n(t)$ is a narrowband waveform, $r(t)$ may be rewritten as

$$r(t) = (2C)^{1/2} \cos [\omega_c t + \beta d(t)] + n_c(t) \cos \omega_c t + n_s(t) \sin \omega_c t , \tag{B-3}$$

where $n_c(t)$, $n_s(t)$ are independent, zero-mean Gaussian processes each having single-sided, low-pass spectral density $2N_o$ (in W/Hz) (ref. B-1).

---

[1] Data were provided for the analysis by TSC personnel P. Engels and P. Mauro.

The receiver coherently demodulates the received signal with an estimate of the carrier phase. We assume this phase estimate is perfect and denote the reference signal as

$$a(t) = 2^{1/2} \sin(\omega_c t) .$$

The demodulator output (low-pass components only) is

$$\begin{aligned} e(t) &= LP\,[r(t)\,a(t)] \\ &= C^{1/2} \sin \beta d(t) + \frac{n_c(t)}{2^{1/2}} \\ &= C^{1/2} \sin \beta d(t) + n_c'(t) , \end{aligned} \qquad \text{(B-4)}$$

where n_c' is defined to have single-sided power density N_o.

The problem is thus converted to that of tracking a digital code of amplitude $C^{1/2} \sin \beta$ in additive noise. Reference B-2 pursues the analysis from this point and concludes that the phase error variance is

$$\sigma_\phi = \left(\frac{\pi}{2}\right)^2 \frac{N_o B_L}{C \sin^2 \beta\, \rho_{c\ell}^2} . \qquad \text{(B-5)}$$

Here, B_L is the equivalent one-sided noise bandwidth of the clock-tracking loop and $\rho_{c\ell}$ is the correlation between the clock component and the composite code. Following reference 6-1:

$$\rho_{c\ell} = \frac{2A - N}{N},$$

with

$$N = 2^n$$

and

$$= 2 \sum_{i=0}^{[(n-1+a)/2]} \binom{n-1}{i} .$$

In this summation limit, a is the weighting of the clock compoent relative to other components of the code.

To convert to range error, we simply scale according to the clock wavelength. Thus

$$\sigma_R = \frac{c\,\sigma_\phi}{2\pi f_{c\ell}}$$

$$= \frac{c}{4\rho_{c\ell} \sin\beta\, f_{c\ell}} \left(\frac{N_o B_L}{C}\right)^{1/2}. \qquad \text{(B-6)}$$

This result has also been independently derived by TSC and was included in data furnished to Boeing.

To evaluate the above expression, we note that

β = 1.2 radians
$\sin\beta$ = 0.93
$f_{c\ell}$ = 156.250 kHz (wideband mode)
= 19.53125 kHz (narrowband mode)
B_L = 1.25 Hz (wideband mode)
= 1.125 Hz (narrowband mode).

Also, in the narrowband mode, format 3, n = 9, a = 3, so

$$A = 2\sum_{i=0}^{5} \binom{8}{i} = 438$$

$$\rho_{c\ell} = \frac{2A - 2^n}{2^n} = 0.711.$$

For the wideband mode, format 4, n = 12, a = 4, so

$$A = 2\sum_{i=0}^{7} \binom{11}{i} = 3632$$

$$\rho_{c\ell} = \frac{2A - 2^n}{2^n} = 0.773.$$

This allows calculation of the rms additive-noise error for both modes via equation (B-6). In addition, the receiver possesses two quantization noise sources: the digital PLL that tracks the clock and the 40-MHz range measurement clock.

The digital PLL has a phase-correction interval of 1/12B of a clock tone cycle in either mode. Assuming the true phase is uniformly distributed on this interval, the rms error induced by the digital PLL is

$$\sigma_{PLL} = \left(\frac{1}{128}\right)\left(\frac{c}{f_{c\ell}}\right)\left(\frac{1}{2\sqrt{3}}\right), \text{ meters.}$$

At $f_{c\ell} = 156.250$ kHz, σ_{PLL} is 4.33 m, and with $f_{c\ell} = 19.53125$ kHz, σ_{PLL} is 34.64 m.

Range measurements are performed by counting a 40-MHz clock between epochs of the incoming and reference codes. Again assuming the actual range is equally likely over the interval, the rms error due to clock precision

$$\sigma_{c\ell} = \left(\frac{c}{40 \times 10^6}\right)\left(\frac{1}{2\sqrt{3}}\right)$$

$$= 2.165 \text{ m}.$$

These various error sources may be treated as independent, so that the rms error of all sources is the root-sum square of the individual components. Figure B-1 provides the net rms error for wideband and narrowband modes as a function of C/N_O.

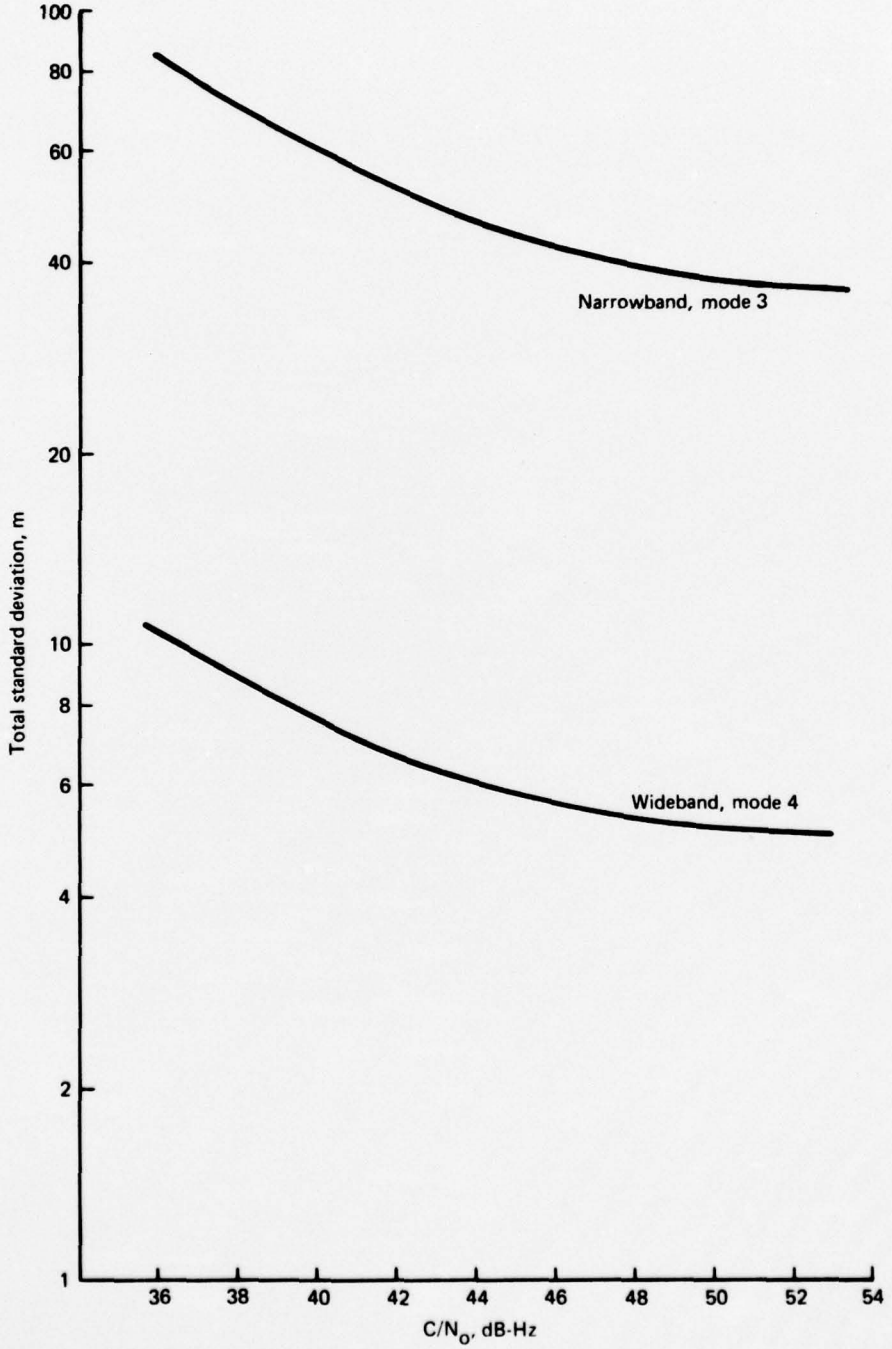

Figure B-1. Theoretical RMS Range Error, TSC Ranging Modem, Additive Gaussian Noise Channel

*U.S. GOVERNMENT PRINTING OFFICE: 1976—700-696/124